As partial fulfilment of the requirements for the degree of Ph.D.

An Analytical Mathematical Theoretical Study of Single-Well Push-Pull "Echo" Tests

Sverre Gullikstad Johnsen

2003-2007

Norwegian University of Science and Technology
Faculty of Engineering Science and Technology
Department of Petroleum Technology and Applied Geophysics

ISBN 82-471-8090-1 (printed)
ISBN 82-471-8089-8 (electronic version)
ISSN ????
Doctoral theses at NTNU, 2007:???

Imagination is more important than knowledge.

- Albert Einstein

To my mentors.

Abstract

Analysis of stream-line-based formulations is exercised to develop a stream-line based semi-analytical model for the single-well push-pull test, taking into account natural ground-water drift. The model is employed to calculate the time of breakthrough for clean water and the end-time of tracer production in addition to the overall producing tracer concentration vs. time.

Contradictory to traditional approaches to the problem, natural ground-water drift is considered important and physical dispersion of the injectant front is considered negligible.

As a main topic we study injection/production in unconfined homogeneously stratified aquifers of infinite areal extent, subject to natural groundwater drift. Injectant and in situ groundwater are assumed to be miscible, incompressible fluids with identical fluid properties. Only macroscopic flow is considered, and flow is assumed to experience no in situ fluid mixing (physical dispersion) so fluid interfaces remain sharp.

Analytically obtained results are compared to field study data provided by Pickens and Grisak, finite difference numerical simulation data obtained by Coats *et al.*, and stream-line based simulation data from Streamsim Inc.'s 3DSL. The excellent match to experimental data and close agreement with simulation data validate the physical dispersion-free method proposed. It is concluded that the semi-analytical stream-line based solution gives the theoretically true production profile, and that any disagreement with simulation data is due to numerical dispersion and/or a poorly built model, on the simulator side.

Making use of the stream-line based semi-analytical model, it is shown that, for a given set of boundary values and test-parameters, there exists a theoretical maximum injection phase duration giving conservative tracer production. The model is employed to study the tracer production profiles as the injection phase duration is extended to values larger than this limit. The applicability of the one-dimensional convection-dispersion equation on calculating apparent dispersivity Peclet numbers is studied, as the injection phase duration is increased, and it is shown how it fails to predict the volume of recoverable tracer and how it fails to fit the measured data. It is also shown how a strongly scale depending apparent

dispersivity may occur in a model, with no physical dispersion, due to natural drift only.

Stream-line patterns for a two-well transmission test in a naturally flowing aquifer is created, and studied as a function of natural ground-water drift direction. It has been indicated how the natural ground-water drift may have an even bigger impact on the two-well transmission test than on the single-well push-pull test.

Acknowledgements

I would especially like to thank professor Curtis H. Whitson for supervising me through my work and directing me towards the topic of this thesis. He did not put too much restraint on my research, letting my imagination roam free. I would also like to express my gratitude to him for introducing me to parts of his network of highly adept colleagues and associates of science.

I would like to congratulate dr. Keith Coats at Coats Engineering Inc. for, together with my supervisor and L.K. Thomas, presenting the well-formulated and path-breaking SPE 90390 paper, "Modelling Conformance as Dispersion". Furthermore I want to thank dr. Coats for his help on my building of SENSOR models and reviewing of my work.

Dr. Mohammad Faizul Hoda at PERA a/s was also of great assistance, helping me out with access to simulator soft- and hard-ware.

I would like to express my gratitude and relief that there exist thorough authors and scientists, like John F. Pickens and Gerald E. Grisak. A huge part of my work is based on their classic *Water Resources Research* paper "Scale-Dependent Dispersion in a Stratified Granular Aquifer". The work here presented can, to a great extent, be appreciated because of their sense of detail and integrity.

Dr. Marco Thiele at Streamsim Inc. has contributed with invaluable assistance with my modelling in 3DSL. He has commented upon and reviewed my models as well as my final results, giving constructive comments and advice.

Professor Michael Golan has assisted in getting the papers published, and he has also contributed with interesting discussions and a generally nice atmosphere at the department. For this I owe him my thanks.

I would like to thank dr. Bjørn Åge Bergsjordet for helping out with LaTeX issues.

The staff at the Department of Petroleum Technology and Applied Geophysics, has been of tremendous help, taking care of all the administrative aspects of my Ph.D. study, which is not little. They deserve my cordial thanks for their persistence.

My fellow Ph.D. student colleagues and friends over the years, dr. Øyvind Kvam, dr. Alf S. Lackner, dr. Nan Cheng, André Strupstad, dr. Thomas Røste,

Tor-Erik Rabben, Sissel Ø. Martinsen, Isac Olalemi, Arif Kuntadi, Christian Crescente, Olve Rasmussen, Håvard Sjøvoll, Milana Ayzenberg, Ørjan Pedersen, Janniche Nordskag, Reynir Fjalar Reynisson, Kenneth Duffaut, Andreas Evensen, have contributed with keeping up spirits every day, and I would like to thank them out of my heart for on- and off-topic, interesting and inspiring discussions.

I would also like to thank dr. Hans Herfjord for his never-ending good mood and friendly presence at the Department of Petroleum Technology and Applied Geophysics.

I really appreciated the hospitability of dr. Wei Yan, dr. Erling Stenby and the staff at Institut for Kemiteknik, at the Technical University of Denmark, during my stay there the autumn of 2004. I pass my greetings and my thanks to you.

The staff at Petrell a/s, my current employer, has shown flexibility and patience and has granted me the time and opportunity to finish my doctoral thesis. For this, I am grateful.

My good friend and brother, Magnar Gullikstad Johnsen, has been of great help proof reading and helping with the texts of the thesis. How can one expect someone from another field of study to work their way through this many pages of mathematical formula and field-specific terminology? Thank you for your patience and persistence, your constructive remarks and criticism.

Thanks also goes to Ronny Kjelsberg, for contributed to the editing process, by proof reading and giving constructive remarks.

I would like to reward my close friend and partner, Marie E. J. Vo, for her patience and for always being there, reminding me of the better things in life, with a huge thanks.

Finally, the opportunity to undertake and perform the study presented in this thesis has been possible because of the financial support from the Gas Technology Center NTNU-SINTEF. I am really grateful for getting this opportunity.

Sverre Gullikstad Johnsen
Trondheim, April 2007

Preface

This thesis is presented to the Department of Petroleum Technology and Applied Geophysics at the Faculty of Engineering Science & Technology, the Norwegian University of Science and Technology, Trondheim, as partial fulfilment of the requirements for the degree of Philosophiæ Doctor, Ph.D.

The work presented here is mainly based on the extensive experimental work presented in the classic *Water Resources Research* paper "Scale-Dependent Dispersion in a Stratified Granular Aquifer" of August 1981, by John F. Pickens and Gerald E. Grisak, and the natural ground-water drift considerations and corresponding numerical simulations presented in the *SPE 90390* paper "Modelling Conformance as Dispersion" of September 2004, by K.H. Coats, C.H. Whitson and L.K Thomas.

The thesis is built upon three papers prepared for and submitted to the Springer Verlag journal *Transport in Porous Media*. The papers, as shown in the List of Papers below, are attached at the back of the thesis. All three papers are on the topic "Analytical Treatment of a Push-Pull "Echo" Test", but they all treat different aspects of the test and the interpretation of the test.

In Paper I, the general method of the stream-line based "source/sink in a uniform stream" approach to the single-well test is described. Mathematical expressions are derived, and a method to trace individual stream-lines and generating a production profile is outlined. It is, furthermore, shown how neglecting physical dispersion, introducing natural drift, may give an excellent match to experimental data, applying the method on a simplified single-layer homogeneous aquifer.

In Paper II, the effects of varying injection/production phase durations are studied, using the methodology described in Paper I. The applicability of the, traditionally applied, one-dimensional convection-dispersion equation (1D CD-EQ) on calculating apparent dispersivities is studied.

In Paper III, the methodology of Paper I is extended to apply to homogeneously stratified aquifers. It is shown how an exact match to experimental data can be achieved, emphasising that the physical dispersion is negligible.

The main body of the thesis consists of three parts and an appendix.

The first part, "Analytical Treatment of a Push-Pull Echo Test", gives an introduction to the terminology and concepts of the push-pull test as well as the one-

dimensional convection-dispersion equation and the field experiments performed by Pickens and Grisak, in Chapter 1. In Chapter 2 a summary of the methodology developed in Paper I is given. In addition, Chapter 2 contains comments regarding approximations, in Section 2.4, required number of stream-lines, in Section 2.5, and the asymptotic recoverable area, in Section 2.6. These are subjects not mentioned in the papers, but relevant to the stream-line based analytical model developed therein.

The second part, "Finite Difference and Stream-line Simulation of a Push-Pull "Echo" Test", gives a brief summary of the relevant results obtained by Coats *et al.*, as well as a report from building an input-deck for the stream-line based simulator 3DSL, developed by StreamSim Technologies Inc., to model the single-well push-pull test.

The third part, "Two-Well Transmission Tests", contains an overview of what to expect from a stream-line based solution approach to the two-well transmission test, closely related to the single-well push-pull test, but mathematically more complex.

Just after Part III, a suggestive list of "things to do" is given along with the conclusions of the thesis.

In Appendix A the Coats *et al.* SW2 SENSOR input deck is listed, the final input deck to 3DSL is cited in Appendix B, the MatLab source code developed to perform the stream-line based calculations of the thesis is quoted in Appendix C, and in Appendix D the documentation of the compact disc created to go with the thesis is presented.

List of Papers

TABLE OF CONTENTS

LIST OF TABLES

LIST OF FIGURES

Paper II

Paper III

LIST OF SYMBOLS

A	Area , $[m^2]$.
A_j	$= 2\pi r_w h_j$,$[m^2]$.
A_{rec}	Asymptotic recoverable injectant area, intersecting area of the injection phase and the production phase Rankine half-bodies,$[m^2]$.
b	Total height of the reservoir ,$[m]$.
b_j	Height of layer j ,$[m]$.
$\mathscr{C}$	Integration constant, dimensions according to context .
$\mathscr{C}_j$	$= \frac{\phi_A}{\phi_j}\frac{k_j}{k_A}$, scaling factor to account for layerwise heterogeneity.
$\mathscr{C}_j^*$	$= \mathscr{C}_j \cdot f$.
C	Producing normalised fractional concentration of tracer as a function of time, t_p or dimensionless volume produced, Q_D .
C_{CD}	Producing fractional concentration of clean water, in a single-well test, as predicted by the Convenction-Dispersion equation .
C_{N^*}	Normalised sum of rates from all stream-lines with $T_{BT,\psi_{p,n}} \geq t_p$.
f	$= \frac{\Sigma(C_j h_j)}{h}$.
g	Gravity ,$[m/s^2]$.

h Hydraulic head,$[m]$.

h_u Hydraulic head due to the uniform natural gradient,$[m]$.

h_w Hydraulic head due to injection/production,$[m]$.

K Hydraulic conductivity,$[10^{-2}{}^{cm}/_{s}]$.

k Permeability,$[darcy]$.

K_A Arithmetic average hydraulic conductivity ,$[10^{-2}{}^{cm}/_{s}]$.

k_A Arithmetic average permeability ,$[darcy]$.

K_j Hydraulic conductivity in layer j ,$[10^{-2}{}^{cm}/_{s}]$.

k_j Layer j permeability,$[darcy]$.

K_{anal} Hydraulic conductivities calculated from the analytical stream-line approach ,$[10^{-2}{}^{cm}/_{s}]$.

K_{Thiem} Hydraulic conductivities calculated from the Thiem equation ,$[10^{-2}{}^{cm}/_{s}]$.

L Length travelled,$[m]$.

L_m $= \sqrt{2Q_i \cdot T_i + r_w^2} - r_w$, mean maximal radial tracer front distance from the well ,$[m]$.

M Total number of layers.

$\vec{n}$ $= \hat{\boldsymbol{x}}\frac{dy}{ds} - \hat{\boldsymbol{y}}\frac{dx}{ds}$, normal vector to the curve s at any point (x,y) on s,$[m]$.

N Total number of stream-lines traced.

N^* Total numbers of stream-lines with $T_{BT,\psi_{p,n}} \geq t_p$ at any given time, t_p, during the production phase.

N_{Pe} Peclet number .

P Pressure,$[Pa]$.

PV_{inj} Pore-volumes injected .

Q $= \frac{q}{2\pi\phi}$,$[{}^{m^2}/_{day}]$.

q 2-dimensional flow rate ,$[{}^{m^2}/_{day}]$.

Q_D $= \frac{|Q_p|t_p}{Q_i T_i}$, dimensionless volume produced .

Q_i $= \frac{q_i}{2\pi\phi}$,$[m^2/day]$.

q_i 2-dimensional injection phase flow rate ,$[m^2/day]$.

Q_j $= \frac{q_j}{2\pi\phi_j}$,$[m^2/day]$.

q_j $= \frac{q_{3D,j}}{h_j}$, 2-dimensional flow rate in layer j,$[m^2/day]$.

Q_p $= \frac{q_p}{2\pi\phi}$,$[m^2/day]$.

q_p 2-dimensional production phase flow rate,$[m^2/day]$.

$q_{3D,j}$ Volumetric rate into/out of layer j ,$[m^3/day]$.

q_{3D} Volumetric well rate,$[m^3/day]$.

$Q_{p,n,j}$ Reformulated 2-dimensional rate from production phase stream-line n in layer j,$[m^2/day]$.

$Q_{p,n}$ Reformulated2-dimensionalrate associated with theproduction phase stream-line n ,$[m^2/day]$.

$q_{p,n}$ 2-dimensionalrate associated with theproduction phase stream-line n ,$[m^2/day]$.

$\hat{\boldsymbol{r}}$ Vector of unit length pointing in the positive r-direction,$[m]$.

r Polar coordinate, radial distance from Origo,$[m]$.

r_b Polar coordinate, radial distance from Origo, of the point of intersection of the injection phase and production phase boundary stream-lines,$[m]$.

r_w Well radius ,$[m]$.

$r_{max,\psi_{i,n}}$ $= r_{\psi_{i,n}}(t = T_i)$, maximum radial tracer advancement for the spesific injection phase stream-line no. n,$[m]$.

r_{max} $= r(t = T_i)$, maximum radial tracer advancement.May refer to overall tracer advancement, i.e. for $\theta = 0$, or along some specific stream-line ,$[m]$.

r_{msp} Polar radius coordinate of the multi-level sampling points,$[m]$.

s Integration path.

t Absolute time, since the injection phase started.During the injection phase $t \equiv t_i$ and during the production phase $t = T_i + t_p$.

T_c Critical time; Injection phase duration limit to for conservative tracer production ,$[days]$.

T_i Total duration of the injection phase ,$[days]$.

t_i Time since the injection phase started,$[days]$.

T_p Duration of tracer production,$[days]$.

t_p Time since the production phase started ,$[days]$.

$t_{0.5}$ Time at which the tracer concentration reaches 0.5 at some measurement distance ,$[days]$.

$T_{BT,\psi_{p,n}}$ Time of breakthrough for the production phase stream-line with index n,$[days]$.

$T_{BT,max}$ Theoretical maximum for the overall T_{BT}, i.e. the time needed to travel from the injection phase stagnation point to the well-bore during the production phase .

T_{BT} Time, since the production phase started, of breakthrough, may refer to overall production or production from a specific stream-line ,$[days]$.

$\vec{u}$ $= U_r \cdot \hat{\boldsymbol{r}} + U_\theta \cdot \hat{\boldsymbol{\theta}} = U_x \cdot \hat{\boldsymbol{x}} + U_y \cdot \hat{\mathbf{y}}$, velocity vector at a given space coordinate,$[m/day]$.

$\vec{u}_i$ Velocity vector at a given space coordinate during the injection phase,$[m/day]$.

$\vec{u}_p$ Velocity vector at a given space coordinate during the production phase ,$[m/day]$.

u $= \frac{v}{\phi}$, macroscopic fluid particle velocity,$[m/day]$.

U_θ $= r \cdot \frac{d\theta}{dt}$, tangential velocity,$[m \cdot rad/day]$.

u_j Fluid particle velocity in layer j,$[m/day]$.

U_r $= \frac{dr}{dt}$, radial velocity ,$[m/day]$.

U_u Natural, uniform ground-water velocity in the positive x-direction,$[m/day]$.

U_x $= \frac{dx}{dt}$, velocity in the x direction,$[m/day]$.

U_y $= \frac{dy}{dt}$, velocity in the y direction ,$[m/day]$.

v	Darcy velocity , $[^{m}/_{day}]$.
$V_t(t_p)$	Volume of tracer recoverable in the time intercal $(t_p, t_p + dt_p)$,$[m^3]$.
$V_{t,tot}$	Total volume of recoverable tracer,$[m^3]$.
$\hat{\boldsymbol{x}}$	Vector of unit length pointing in the positive x-direction,$[m]$.
x	Cartesian coordinate in the x-direction ,$[m]$.
$\hat{\boldsymbol{y}}$	Vector of unit length pointing in the positive y-direction,$[m]$.
y	Cartesian coordinate in the y-direction ,$[m]$.
z	Depth ,$[m]$.

Greek Symbols

α_a	Apparent dispersivity ,$[m]$.
$\hat{\boldsymbol{\theta}}$	Vector of unit length pointing in the positive θ-direction ,$[rad]$.
θ	Polar coordinate, angle to the positive x-axis,$[rad]$.
θ_b	Polar coordinate, angle to the positive x axis, of the point of intersection of the injection phase and production phase boundary stream-lines,$[m]$.
θ_{msp}	Polar angle coordinate of the multi-level sampling points ,$[rad]$.
μ	Viscosity ,$[cp]$.
∇P	Pressure gradient ,$[^{Pa}/_{m}]$.
ρ_w	Density of water,$[^{kg}/_{m^3}]$.
ϕ	Fractional porosity .
ϕ_A	Arithmetic average porosity .
ϕ_j	Layer j fractional porosity .
ψ	Stream-line number.
ψ_i	Injection phase stream-line number.
ψ_p	Production phase stream-line number .

$\psi_{i.n}$ Injection phase stream-line no. n .

$\psi_{p.n}$ Production phase stream-line no. n.

Subscripts

i Denoting injection phase variables and parameters.

j Index to denote layer number, $j \in [1,M]$.

j^* New layer indexing to gather several layers of equal properties .

m_1, m_2 $\in [1,N]$; all layers $j \in [m_1,m_2]$ have identical properties.

n Accounting index to denote individual stream-lines, $n \in [1,N].n = 1$ denotes the stream-line with constant $\theta = 0$, and $n = N$ denotes the stream-line with constant $\theta = \pi$.

p Denoting production phase variables and parameters.

Part I

Analytical Treatment of a Push-Pull "Echo" Test

CHAPTER 1

Introduction

Single-well push-pull "echo" tests are run literally hundreds of times a year, all over the world. The tests are used to assess, quantitatively, a variety of physical, chemical and microbiological reservoir/aquifer properties, [6], ranging from residual oil saturation, [10], to microbial activity, [5], to regional natural flow, [7], to mention a few.
Here is given a short introduction to the concept of the push-pull test as well as what should be of concern regarding the current way of treating natural groundwater drift and the application of the one-dimensional convection-dispersion equation to calculate dispersivity.

1.1 The Push-Pull "Echo" Test

The push-pull test is an example of one of the most typical ground-water field tests conducted hundreds of times a year all over the world, and correct understanding and interpretation of the concentration profiles are, of course, essential to making use of the obtained data. Searching the Internet, for the phrase "push pull test", reveals a vast amount of literature on the topic.

Push-pull "echo" tests, also known as single-well injection-withdrawal tests, consist of a controlled injection phase where a prepared test solution is being "pushed" into an aquifer, and thereafter a production phase where the test solution/in situ fluid mixture is "pulled" from the same location/well. **Figure 1.1** displays a schematic of the push-pull test. It can be seen how, during the injection phase, (a), the injectant is "pushed" into the test-well and flows away from the well in a roughly cylindrical fashion. The hydraulic head, as a function of the radius, will behave approximately as $\ln|r|$. During the production phase, (b), fluids are flowing towards the well and are "pulled" out.

The test solution consists of water containing one or more tracers/solutes. The type, combination and amount/concentration of tracer/solutes are selected depending on which aquifer characteristics are monitored.

Usually tracers are added to the injectant in relatively small concentrations to obtain near ideal tracer behaviour. An ideal tracer is chemically and physically stable, not interacting with in situ fluids or solids and not naturally present in the aquifer. Throughout this thesis the notions injectant and tracer will be used equivalently about the fluid being injected. In situ water containing no tracer will be referred to as clean water.

The produced mixture injectant concentration will be in the range $[0,1]$, and the tracer/injectant concentration at time, t, is accordingly the ratio of injectant volume to the total volume produced in the infinitesimal time interval $(t, t+dt)$.

During the injection phase the injectant flows away from the test well, and it is assumed, in this thesis, that the interface between the injectant and the in situ

water remains sharp, i.e. there is no physical dispersion. During the production phase, the well flow is reversed and the concentration of tracer, solutes and possible reaction products are measured as a function of time. Injectant concentration in the produced mixture is calculated. In this work, it is assumed that the tracer is ideal, so that the fractional relationship between tracer and injectant in the produced mixture is constant.

1.2 Natural Drift

Traditionally it has been assumed that the presence of natural drift in the aquifer is of no concern, since the natural drift velocity most often is small compared to the injection/production induced velocity field. This is, however, only true close to the test well, and hence, the assumption is only valid for short time-scale experiments. This assumption was criticised by Coats *et al.*, [3]. It has been shown, in this thesis, how the natural drift may affect the producing injectant vs. time profile even though the drift velocity is small. In this thesis, the assumptions are turned upside down; the physical dispersion is assumed to be zero or negligible and the natural ground-water drift is taken into account.

1.3 The One-Dimensional Convection-Dispersion Equation

A common way of interpreting the producing injectant profile is to assume the natural ground-water drift is negligible and to fit the one-dimensional convection-

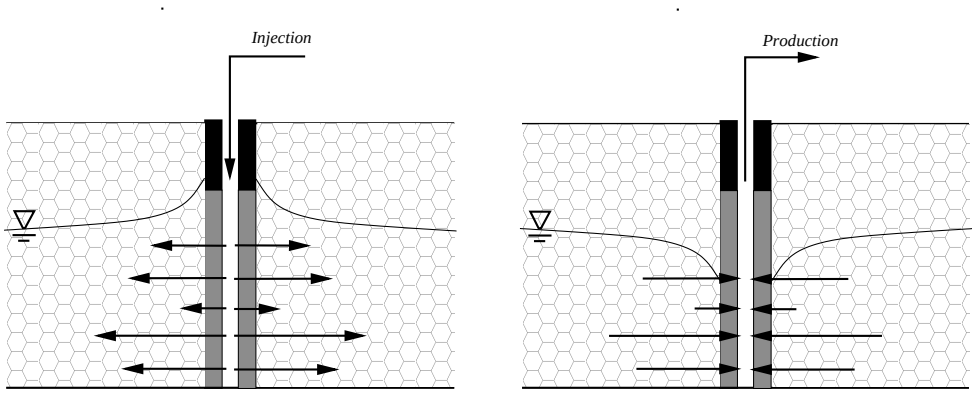

(a) Injection phase (b) Production phase

Figure 1.1: Schematic of the push-pull “echo” test, injection and production phases.

dispersion equation (1D CD-EQ), [1], [2], [8], [9]. Obvious flaws of this way of interpretation is the fact that the ground-water velocity might not be negligible, and the fact that the 1D CD-EQ was developed for constant-velocity one-dimensional flow through a stream-tube. Even if the natural drift is neglected, the radial flow pattern from the test well is two dimensional indeed, and the injectant velocity decreases as $1/r$ rather than being constant. A well known problem typically being the result of such interpretations, is the scale-dependency of the apparent dispersion several orders of magnitude higher than corresponding laboratory measurements of the physical dispersion. Coats *et al.*, [3], remind us that the physical dispersion is a rock property, and that no laboratory results show scale dependency of the physical dispersion.

The Gelhar-Collins, [4], analytical approach applied by Pickens and Grisak is equivalent to the one-term approximation to the Aronofsky equation, [1], [3].

1.4 The Pickens-Grisak Field Scale Experiment

As an example, we study two push-pull tests performed by Pickens and Grisak, [9], in 1982. The test wells were not the same, but in the vicinity of each other. Resulting dispersions, applying the Gelhar-Collins analytical solution, [4], were $3.0cm$ and $9.0cm$ from their two single-well field experiments, SW1 and SW2, respectively, while laboratory experiments on core-samples from the same area gave approximately $0.035cm$.

References

[1] J.S. Aronofsky and J.P. Heller. A diffusion model to explain mixing of flowing miscible fluids in porous media. *Trans AIME*, 210:345–349, 1957.

[2] A. Arya, T.A. Hewett, R.G. Larson, and L.W. Lake. Dispersion and reservoir heterogeneity. *SPERE*, 3:139–148, 1988. SPE 14364.

[3] K. H. Coats, C.H. Whitson, and L.K. Thomas. Modelling conformance as dispersion. SPE Annual Technical Conference and Exhibition, 26-29 September, Houston, Texas, September 2004. SPE 90390.

[4] L.W. Gelhar and M.A. Collins. General analysis of longitudinal dispersion in nonuniform flow. *Water Resources Research*, 7(6):1511–1521, 1971.

[5] J. Istok, M. Humphrey, M. Schroth, and K. O'reilly. Single well "push-pull" test for in situ determination of microbial activities. *Ground Water*, 35(4), 1997.

[6] Young Kim, Mohammad Azizian, Jonathan Istok, and Lewis Semprini. *Field Push-Pull Test Protocoll for Environmental Security Technology Certification Program*. Oregon State University, Civil, Construction, and Environmental Engineering Department, Corvallis, OR 97331, April 2005.

[7] D. Leap and P. Kaplan. A single-well tracing method for estimating regional advective velocity in a confined aquifer: Theory and preliminary laboratory verification. *Water Resources Research*, 24(7), 1988.

[8] J. Mahadevan, L.W. Lake, and R.T. Johns. Estimation of true dispersivity in field scale permeable media. SPE/DOE Improved Oil recovery Symposium, Tulsa, Oklahoma, USA, April 2002. SPE 75247.

[9] J.F. Pickens and G.E. Grisak. Scale-dependent dispersion in a stratified granular aquifer. *Water Resources Research*, 17(4):1191–1211, 1981.

[10] J. Tomich, R.L. Dalton, H. Deans, and L. Shallenberger. Single-well tracer method to measure resiudal oil saturation. *JPT*, pages 211–218, February 1973.

CHAPTER 2

Source/Sink in a Uniform Stream Approach

In this chapter, a brief introduction to the stream-line method, described in the three papers attached at the back of the thesis, Paper I, Paper II, Paper III, is given. In addition, a few concepts not discussed in the papers are presented; approximations, convergence depending on the number of stream-lines used, the asymptotic recoverable area.

2.1 Introduction

Stream-lines are steady-state particle flow-paths, i.e. the traces a "fluid particle" would leave if monitored as it moved through a domain. The stream-line is a line everywhere tangent to the velocity vector at a given instant, and stream-lines are also the geometrical interpretation of the stream function, ψ, [6]. That is, a stream-line is a constant ψ contour.
The stream function idea only works if the four terms of the continuity equation,

$$\frac{\partial \rho}{\partial t} + \frac{\partial}{\partial x}(\rho U_x) + \frac{\partial}{\partial y}(\rho U_y) + \frac{\partial}{\partial z}(\rho U_z) = 0 \,, \tag{2.1}$$

can be reduced to two terms. A common approach is to assume incompressible two-dimensional flow in the xy-plane[1], which has been assumed throughout this thesis;

$$\frac{\partial U_x}{\partial x} + \frac{\partial U_y}{\partial y} = 0 \,. \tag{2.2}$$

This equation is satisfied identically if there exists a function, $\psi(x,y)$, such that

$$U_x = \frac{\partial \psi}{\partial y} \quad \wedge \quad U_y = -\frac{\partial \psi}{\partial x} \,, \tag{2.3}$$

which becomes, in polar coordinates,

$$U_r = \frac{1}{r}\frac{\partial \psi}{\partial \theta} \quad \wedge \quad U_\theta = -\frac{\partial \psi}{\partial r} \,. \tag{2.4}$$

There is also a physical interpretation that relates ψ to volume flow. The two-dimensional rate between two stream-lines, ψ_1 and ψ_2, are found by integrating along some path, s, as seen in **Figure 2.1**,

$$q = \int_s dq \,, \tag{2.5}$$

[1] It is also possible to assume compressible flow, but this will demand redefining of the stream function.

where dq is given by

$$dq = (\vec{u} \cdot \vec{n})\, ds \; . \tag{2.6}$$

The normal vector, $\vec{n}$, to the line segment ds is given by

$$\vec{n} = \hat{\boldsymbol{x}} \frac{dy}{ds} - \hat{\boldsymbol{y}} \frac{dx}{ds} \; . \tag{2.7}$$

Applying Equation 2.3 , Equation 2.6 and Equation 2.7 to Equation 2.5 we get

$$q \;\; = \;\; \int_s (U_x dy - U_y dx) = \int_{\psi_1}^{\psi_2} d\psi = \psi_2 - \psi_1 \; . \tag{2.8}$$

Hence, the numerical stream-line number difference between two arbitrary stream-lines is a measure of the two-dimensional rate flowing between them. Furthermore, the direction of the flow can be ascertained by noting whether ψ increases or decreases.

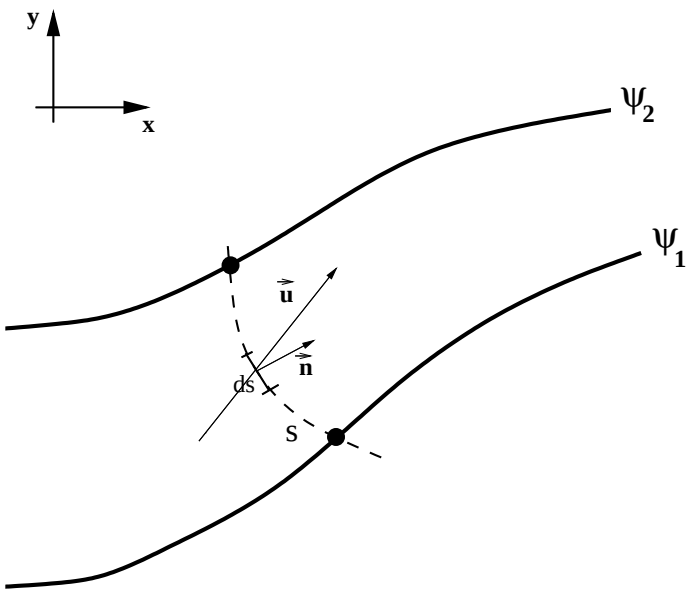

Figure 2.1: Geometrical interpretation of the stream function; volume flow between two stream-lines.

2.1.1 Uniform Stream

In a uniform stream, the particle velocity (direction and magnitude) is the same for all spatial coordinates. For the single-well push-pull test it has been assumed,

in this thesis, that the uniform stream is in the direction of the positive x-axis,

$$\vec{u}_u = U_u \cdot \hat{\boldsymbol{x}} \, . \tag{2.9}$$

The velocity field satisfies continuity since Equation 2.2 holds, and a stream function exists. The stream function of the uniform stream is simply

$$\psi_{uniform} = U_u y \, . \tag{2.10}$$

2.1.2 Source/Sink

A point source/sink in a two-dimensional space or a line source/sink in a three-dimensional space is treated in the same way, i.e. it is assumed uniform radial outflow along the length of the line source. Throughout the thesis, test wells are viewed as vertical, i.e. strictly z directional, line sources/sinks, and the aquifer has been considered to be flat, i.e. in the xy-plane. We see that for a homogeneous three-dimensional reservoir, the flow from a source or to a sink is reduced to a two-dimensional problem.

The "strength" of the source/sink is defined as

$$Q \equiv \frac{q}{2\pi\phi} = \frac{q_{3D}}{2\pi\phi h} \, . \tag{2.11}$$

Q is, per definition, positive for injection and negative for production. Assuming the point source/sink is located in Origo, the velocity field, in polar coordinates, is given by

$$U_r = \frac{Q}{r} \quad \wedge \quad U_\theta = 0 \, , \tag{2.12}$$

and, in Cartesian coordinates,

$$U_x = \frac{Qx}{x^2+y^2} \quad \wedge \quad U_y = \frac{Qy}{x^2+y^2} \, , \tag{2.13}$$

which satisfies the continuity equation, so a stream function exists;

$$\psi_{source/sink} = Q \cdot \theta = Q \arccos\left(\frac{x}{\sqrt{x^2+y^2}}\right) \, . \tag{2.14}$$

It is also possible to formulate the stream function using the other trigonometric functions, but using the arccos function has proved, for the push-pull test, to give the simplest calculations.

2.1.3 Source/Sink in a Uniform Stream

A superposition of the two previously described solutions, uniform stream and source/sink, is also a valid stream function solution[2], [6]. In this thesis the single-well push-pull test is viewed as a superposition of an alternating source/sink in a uniform stream, and the composite stream function of the problem is simply

$$\begin{aligned} \psi &= \psi_{uniform} + \psi_{source/sink} \\ &= U_u \cdot r \sin\theta + Q \cdot \theta \qquad (2.15a) \\ &= U_u y + Q \cdot \arccos\left(\frac{x}{\sqrt{x^2+y^2}}\right) . \qquad (2.15b) \end{aligned}$$

The velocity field is of course also a superposition of the two velocity fields.

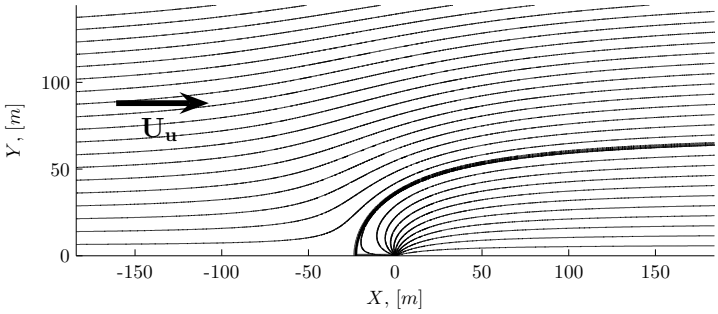

(a) Source

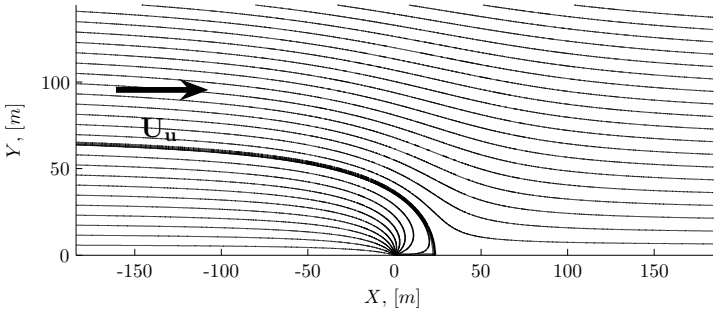

(b) Sink

Figure 2.2: Source(injection phase)(a) and sink (production phase) (b) in a uniform stream streamlines.

[2]For irrotational flow, i.e. $\nabla \times \vec{u} = 0$, the stream function is a solution to the linear partial differential equation $\nabla^2 \psi = 0$, and all superpositions of valid solutions are also valid solutions.

In **Figure 2.2** it can be seen what the upper half-plane stream-lines look like for a source and a sink in a uniform stream in a) and b), respectively. The stream-line pattern is symmetric about the x-axis, and the weighted lines, which are no cross-flow boundaries and separate injected fluid from in situ fluids (a) and produced fluid from escaped fluid (b), forms the Rankine half-body.

2.2 Push-Pull "Echo" Test in a Naturally Flowing Aquifer

Treating the push-pull test as a source/sink in a uniform stream gives the possibility of tracing the injectant front as it advances outward during the injection phase, and similarly back during the production phase. Knowing the particle velocity at all points in space and the flow-paths of a particle leaving the well-bore at a given radius and angle, it is possible to develop an analytical expression for the injectant front position, at a specific stream-line, as a function of time.

Likewise, knowing the injectant front position at a given injection phase stream-line at the end of the injection phase, it is possible to calculate the time of arrival, at the well-bore, for the injectant particle located at the injectant front. A particle flow path, back to the producer, is uniquely identified from the particle coordinate at $t_p = 0$, as is illustrated in **Figure 2.3**.

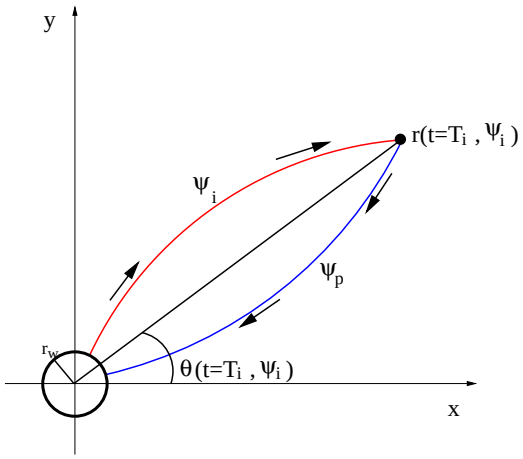

Figure 2.3: General view of the trace of a fluid particle leaving the wellbore at the radius r_w at the time $t = 0$. The trace is described by the injection phase stream-line ψ_i until the particle reaches it's maximum radial advancement r_{max} at the time $t = T_i$ and thereafter by the production phase stream-line ψ_p until it is back at the well-bore radius r_w.

2.2.1 Methodology

Due to the symmetry about the x-axis, a solution is found for the upper half-plane, only. Basically, three problems are solved, for each phase, for polar angles, θ, equals π, 0 and all angles in-between. Mathematically, the problem is formulated as three differential equations for each phase.
For the injection phase;

$$\frac{dr}{dt} = \left(U_u + \frac{Q_i}{r}\right)\hat{r} \quad \text{for } \theta = \pi \,, \tag{2.16a}$$

$$\frac{dr}{dt} = \left(-U_u + \frac{Q_i}{r}\right)\hat{r} \quad \text{for } \theta = 0 \,, \tag{2.16b}$$

$$\frac{d\theta}{dt} = -\frac{(U_u \sin\theta)^2}{\psi - Q_i\theta} \quad \text{for } \theta \in (0,\pi) \,. \tag{2.16c}$$

For the production phase;

$$\frac{dr}{dt} = \left(U_u - \frac{|Q_p|}{r}\right)\hat{r} \quad \text{for } \theta = \pi \,, \tag{2.17a}$$

$$\frac{dr}{dt} = \left(-U_u - \frac{|Q_p|}{r}\right)\hat{r} \quad \text{for } \theta = 0 \,, \tag{2.17b}$$

$$\frac{d\theta}{dt} = -\frac{(U_u \sin\theta)^2}{\psi + |Q_p|\theta} \quad \text{for } \theta \in (0,\pi) \,. \tag{2.17c}$$

The radial position is related to the angular position through the stream function,

$$r = \frac{\psi - Q\theta}{U_u \sin\theta} \,. \tag{2.18}$$

Appropriate boundary conditions should be picked for the injection phase, and boundary conditions for the production phase are coordinates at $t = T_i$ from the injection phase.

Solving these equations is relatively easy, however, we get implicit solutions for the tracer front position, (r,θ), as a function of time, so a numerical method is needed to find the position at the end of the injection phase, $t = T_i$. For the injection phase we find $r_{max} = r(t = T_i)$ by solving the equations:

$$U_u\,(r - r_w) + Q_i \ln\left|\frac{Q_i - U_u \cdot r}{Q_i - U_u \cdot r_w}\right| = -U_u^2 \cdot t \,, \tag{2.19a}$$

for the stream-line with constant $\theta = \pi$,

$$U_u\,(r - r_w) - Q_i \ln\left(\frac{Q_i + U_u r}{Q_i + U_u r_w}\right) = U_u^2 t \,, \tag{2.19b}$$

for the stream-line with constant $\theta = 0$, and

$$r(t = T_i, \psi_i) = \left. \frac{\psi_i - Q_i \theta}{U_u \sin\theta} \right|_{\theta = \theta(t = T_i, \psi_i)} , \tag{2.19c}$$

where θ is given by

$$(Q_i \theta - \psi_i) \cot\theta - Q_i \ln|\sin\theta| = -U_u^2 t + \mathscr{C}(\psi_i) , \tag{2.20a}$$

and

$$\mathscr{C}(\psi_i) = \left. -U_u r_w \cos\theta - Q_i \ln|\sin\theta| \right|_{\theta = \theta(t=0, \psi_i)} , \tag{2.20b}$$

for the stream-lines with $\theta \in (0, \pi)$.

Knowing the maximum radial advancement, r_{max,ψ_i}, for the injectant front along each injection phase stream-line, it is easy to find the time of break-through along each production phase stream-line. We find the time of breakthrough, T_{BT,ψ_p}, along each production phase stream-line by inserting the $r_{max} = r(t = T_i)$, found by solving the equations above, and $r = r_w$ for r into the equations we get from solving the differential equations 2.17,

$$U_u (r - r_{max}) - |Q_p| \ln \left| \frac{|Q_p| + U_u \cdot r}{|Q_p| + U_u \cdot r_{max}} \right| = -U_u^2 \cdot t , \tag{2.21a}$$

for the stream-line with constant $\theta = \pi$,

$$U_u (r - r_{max}) + |Q_p| \ln \left(\frac{|Q_p| - U_u r}{|Q_p| - U_u r_{max}} \right) = U_u^2 t , \tag{2.21b}$$

for the stream-line with constant $\theta = 0$, and

$$-U_u^2 t + \mathscr{C}(\psi_p) = -(|Q_p|\theta + \psi_p) \cot\theta + |Q_p| \ln|\sin\theta| , \tag{2.21c}$$

where

$$\mathscr{C}(\psi_p) = \left. -U_u r_{max} \cos\theta + |Q_p| \ln|\sin\theta| \right|_{\theta = \theta(t = T_i, \psi_i)} , \tag{2.22a}$$

for the angles between 0 and π.
$\theta(r_w, \psi_p)$ is found from

$$r = \frac{\psi_p + |Q_p|\theta}{U_u \sin\theta} , \tag{2.22b}$$

and the production phase stream-line numbers are given by

$$\psi_p = \psi_i - (|Q_p| + Q_i)\theta , \tag{2.22c}$$

The injectant flowing along the $\theta = \pi$ stream-line has zero angular velocity and is always located at this angle. This stream-line will be the first to provide the well-stream with clean water and define the over-all time of break-through, T_{BT}. The $\theta = 0$ stream-line tracer-front will be the last one to arrive at the well-bore and define the end-time of injectant production.

Associating an inflow rate to each stream-line, for instance by using the relation Equation 2.8 , it is now possible to generate a producing injectant concentration profile. The fundamental assumption is that a production phase stream-line will provide the producing test well with injectant until the time of break-through is reached, for that particular stream-line, and thereafter feed the well-stream with in situ/clean water, only. Thus, each production phase stream-line provides a fraction of the well-stream, so by subtracting the fraction of each stream-line, ψ, with time of break-through, $T_{BT,\psi}$, smaller than the current time, t_p, it is possible to generate the production profile. By stepping along the time axis, a histogram can be generated, and by using enough stream-lines a smooth production profile is obtained. The calculations are programmed, using MatLab, [5], and the source code is shown in Appendix C.

2.3 The Shape of the Injectant Covered Area

Following the method prescribed by Bear, on the pages 532 and 533 in chapter 9.5.4 *Horizontal Interface Displacement* in [2], we can derive a formula for the shape of the injectant covered area. Solving Equation 2.16c and Equation 2.17c , we get

$$(Q\theta - \psi)\cot\theta - Q\ln|\sin\theta| = -U_u^2 t + \mathscr{C} \ , \tag{2.23}$$

where $Q = Q_i$ or $Q = -|Q_p|$, and $\mathscr{C}$ must be independent of θ. Putting in, for ψ, Equation 2.15a , we get

$$r\cos\theta + \frac{Q}{U_u}\ln|\sin\theta| = U_u t + \mathscr{C} \ , \tag{2.24}$$

which is equivalent to

$$x + \frac{Q}{U_u}\ln\left|\frac{y}{\sqrt{x^2+y^2}}\right| = U_u t + \mathscr{C} \ . \tag{2.25}$$

If doing as Bear, assuming $x = y = 0$ for $t_i = 0$, we get $\mathscr{C} \equiv 0$, and the analytical expression for the advancing injectant front, during the injection phase, becomes

$$\sqrt{1 + \frac{x^2}{y^2}} = \exp\left[-\frac{U_u}{Q_i}(U_u t_i + x)\right] \ . \tag{2.26}$$

Requiring $r = r_w$ for $t_i = 0$, however, yields

$$\mathscr{C} = x + \frac{Q_i}{U_u}\sqrt{1 - \frac{x^2}{r_w^2}}\ , \tag{2.27}$$

which has no solution, since the right hand side is not constant with respect to θ, and an analytical expression for the advancing injectant front cannot be found.

For $t_p = 0$, the production phase injectant covered area takes the shape

$$r_{max}\cos\theta - \frac{|Q_p|}{U_u}\ln|\sin\theta| = \mathscr{C}\ , \tag{2.28}$$

where r_{max} can be expressed by putting in $t_i = T_i$ in Equation 2.26 , if we accept that $r_w \simeq 0$,

$$r_{max}\cos\theta + \frac{Q_i}{U_u}\ln|\sin\theta| = U_u T_i\ . \tag{2.29}$$

We now get

$$\mathscr{C} = U_u T_i - \frac{Q_i + |Q_p|}{U_u}\ln|\sin\theta|\ . \tag{2.30}$$

Since the right hand side is not constant, with respect to θ, it is not possible to find an analytical expression for the shape of the withdrawing injectant front.

2.4 Approximations

As in any physical system, there are sources of error in the conduction of and the measuring of the single-well push-pull test, and test results may be uncertain to higher or lower degrees. Developing the mathematical expressions, in this thesis, a series of simplifying assumptions and approximations have been done, e.g. assuming homogeneity, assuming zero viscosity, assuming the injectant to be an ideal tracer, assuming zero dispersivity, etc. Due to these facts, it may be argued that model results are already so uncertain, that the positive effects of more simplification may overshadow the added uncertainty. Here are proposed and studied two ways of simplifying the mathematical expressions developed for the single-well push-pull test, which may if applied correctly speed up calculations significantly.

2.4.1 Neglecting the Natural Drift

As shown in Paper I, the no-drift radial advancement, as a function of time, is given by

$$r(t \leq T_i) = \sqrt{r_w^2 + 2Q_i t_i}\,, \tag{2.31a}$$

$$r(T_i < t \leq T_i + T_p) = \sqrt{r_{max}^2 - 2|Q_p| t_p}\,. \tag{2.31b}$$

From Equation 2.31 , it is obvious that a free-of-physical-dispersion production curve should drop from one to zero instantaneously, as there is angular symmetry around the test well, and all stream-lines should obtain break-through at the same time. The traditional assumtion is that the natural drift is negligible, and that any smearing of the step function production profile is due to physical dispersion of the injectant front. In a zero-dispersivity system we see, in **Figure 2.4**, that only for a very short injection phase can the no-drift assumtion be expected to predict the up-gradient tracer front position within an acceptable uncertainty. In Figure 2.4 the theoretical no-drift injection phase $r(t)$ is compared to the with-drift up-gradient injectant front $r(t)$.

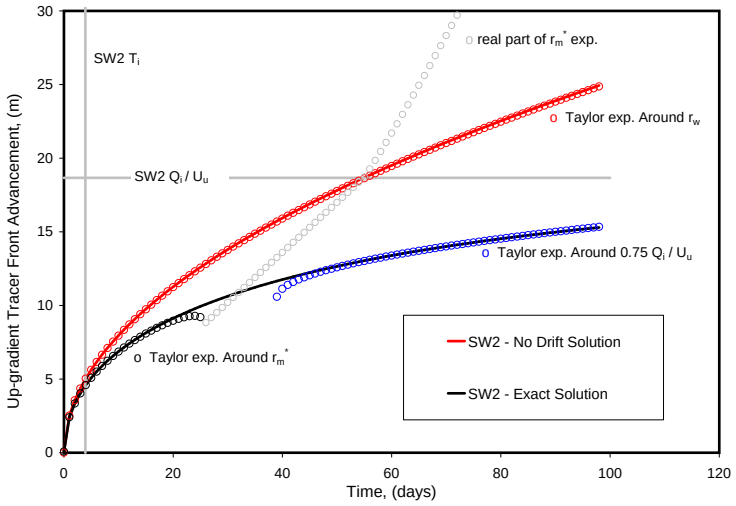

Figure 2.4: Comparison of the exact maximum up-gradient radial advancement vs. time, from the analytical model, with the no drift radial advancement and Taylor expansion results. Test parameters from the Pickens-Grisak SW2 field test were used, [3].

2.4.2 Taylor Expansions

The expressions developed for the maximum up-stream radial advancement, Equation 2.19a , and the maximum down-stream radial advancement, Equation 2.19b

, are implicit expressions for $r(t)$, and considerable effort may be required to find $r(t)$, depending on the other variables and parameters. Substituting the left-hand side of the equations with their corresponding Taylor expansions, [1], will give implicit polynomial expressions for $r(t)$.
Choosing a second-order polynomial, the expressions may be inverted and explicit expressions for the approximated $r(t)$, can be found, however, picking the points around which the expressions are expanded, should be given careful consideration, since these will significantly affect the accuracy of the approximations.

As an example, the expansion of the up-stream expression, Equation 2.19a , around $r = r_w$ becomes

$$\begin{aligned} r(t \leq T_i) &\simeq \frac{U_u r_w^2 + \sqrt{U_u^2 r_w^4 + 2tQ_i^3 - 4tQ_i^2 U_u r_w + Q_i^2 r_w^2 - 2Q_i U_u r_w^3 + 2Q_i U_u^2 r_w^2}}{Q_i} \\ &= \frac{U_u r_w^2 + \sqrt{(Q_i - r_w U_u)^2 (r_w^2 + 2Q_i t)}}{Q_i} , \end{aligned} \tag{2.32}$$

which for dominating injection rates, $U_u r_w << Q_i$, becomes

$$\begin{aligned} r(t \leq T_i) &\simeq r_w \cdot \mathscr{O}\left(\frac{U_u r_w}{Q_i}\right) + \sqrt{r_w^2 \left[1 + \mathscr{O}\left(\frac{U_u r_w}{Q_i}\right)\right] + 2Q_i t \left[1 + \mathscr{O}\left(\frac{U_u r_w}{Q_i}\right)\right]} \\ &\simeq \sqrt{r_w^2 + 2Q_i t} , \end{aligned} \tag{2.33}$$

which is exactly the no-drift solution. That is, for dominating injection rates, the no-drift solution is equivalent to the second-order Taylor expansion around r_w. As can be seen in Figure 2.4 , this is the case for the Pickens-Grisak SW2 field test parameters,[3].
This statement does also imply that the no-drift approximation, even for dominating injection rates, is only valid for small radial advancements/injection phase durations.

Expanding around the no-drift $r_{max} \simeq r_m^* \equiv \sqrt{2Q_i T_i}$ may give a more accurate approximation for larger values of r;

$$r(t \leq T_i) = \frac{r_m^{*\,2} + \sqrt{\left[2r_m^{*\,2} U_u^2 + 2U_u Q_i (r_m^* - r_w) + 2Q_i^2 \ln\left(1 - \frac{U_u r_m^*}{Q_i}\right)\right](-Q_i + U_u r_m^*)^2}}{Q_i U_u} , \tag{2.34}$$

but at some point, $r(t)$ becomes a complex number, and the real part of the $r(t)$ becomes irrelevant, as can be seen in Figure 2.4 . In this case, another point should

be chosen. In Figure 2.4 an expansion around the point $0.75 \cdot Q_i/U_u$[3] is shown, also.

2.5 Number of Stream-lines Convergence Study

2.5.1 SW2 Test Parameters

To study the effect of varying the number of stream-lines traced in the developed MatLab code, the model was run with N=10 000, 1000, 50, 10 and 3 stream-lines. The resulting injectant production profiles, using single-layer SW2 test parameters, can be seen in **Figure 2.5**.

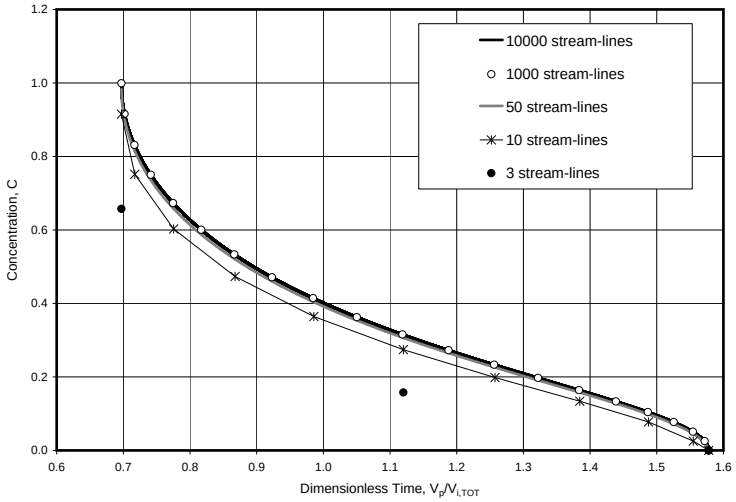

Figure 2.5: Resulting SW2 injectant production profiles from the analytical stream-line based model, tracing 10 000, 1000, 50, 10 and 3 stream-lines.

There is no visible difference between the 10 000 and the 1000 stream-line profiles, so it can be concluded that a 1000 stream-lines is sufficient to model the SW2 test.
The 50 stream-line production profile is a good approximation to the converged curves, so a lower number than 1000 might also be sufficient. This could, however change if more demanding experimental set-ups were employed, for instance if the injection phase duration was extended beyond the critical time, T_c. When injecting for a period of time longer than T_c, some stream-lines will transport injectant beyond the production phase no cross-flow boundary, as seen in Figure 2.2 , and the MatLab code deals with this simply by discarding these stream-lines, and the total number of stream-lines decrease.

[3] $(x,y) = (-Q_i/U_u, 0)$ is the injection phase stagnation point, the theoretical absolute maximum up-gradient radial advancement.

The 10 and 3 stream-line production profiles are too far from the converged curves to be considered as good approximations. It should be noted, however, that the 3 stream-line model time outputs are of some value.
Three stream-lines is the minimum number the model will allow, and the n=1 streamline is the down-gradient stream-line with constant $\theta = 0$ and the n=3 stream-line is the up-gradient stream-line with constant $\theta = \pi$. These two individual stream-lines' break-through times are the over-all end-time of injectant production and the time of clean water break-through, respectively. Hence, running the model with three stream-lines, only, is a "quick and dirty" way of getting these two points in time, although the corresponding producing injectant concentrations are of no value. The end-time of injectant production, can of course only be found when $T_i < T_c$.

2.6 The Asymptotic Recoverable Area

For an infinite injection phase duration, the Rankine half-body of the "source/sink in a uniform stream" problem will be completely covered with injectant. Just a finite fraction, however, of the total amount of injectant is recoverable. The recoverable injectant is found in the intersection area of the injection phase and the production phase Rankine half-bodies, as can be seen in **Figure 2.6**. The point

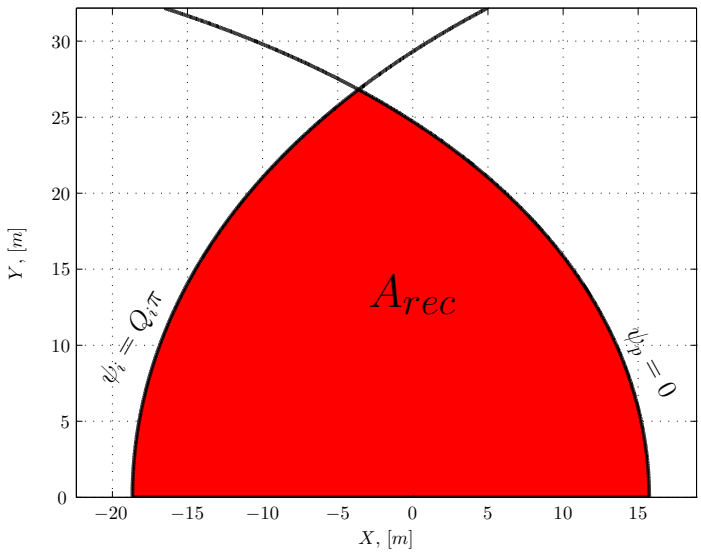

Figure 2.6: Recoverable area bound by the injection phase and the production phase Rankine half-bodies (upper half-plane only).

at which the two boundary stream-lines cross is given by the coordinates r_b and

θ_b, and

$$\psi_i = \quad Q_i\pi \quad = U_u r_b \sin\theta_b + Q_i\theta_b \ , \tag{2.35}$$

$$\psi_p = \quad 0 \quad = U_u r_b \sin\theta_b - |Q_p|\theta_b \ . \tag{2.36}$$

The area A_{rec}, can now be calculated by integration.

$$A_{rec} = -\int_{\pi}^{\theta_b} \frac{1}{2} r^2(\theta, \psi_i = Q_i\pi) d\theta + \int_{0}^{\theta_b} \frac{1}{2} r^2(\theta, \psi_p = 0) d\theta \ . \tag{2.37}$$

Inserting for, $r = \frac{\psi - Q\theta}{U_u \sin\theta}$, we get the integral of r^2,

$$\int r^2(\theta,\psi) d\theta = \int \left(\frac{\psi - Q\theta}{U_u \sin\theta}\right)^2 d\theta = \int \frac{\psi^2 - 2\psi Q\theta + Q^2\theta^2}{U_u^2 \sin^2\theta} d\theta$$

$$= \frac{1}{U_u^2}\left[-\psi^2 \cot\theta + \mathscr{C}_1 + 2\psi Q\big(\theta\cot\theta - \ln|\mathscr{C}_2 \sin\theta|\big) + \int \frac{Q^2\theta^2}{\sin^2\theta} d\theta\right] \ , \tag{2.38}$$

where $\mathscr{C}_1$ and $\mathscr{C}_2$ are arbitrary integration constants. Since this is a half-plane calculation, the A_{rec} has to be multiplied by two to get the total recoverable injectant covered area. The area may be calculated using for instance Maplesoft's Maple, [4], as seen in Subsection 2.6.1. Notice also that A_{rec} is an asymptotic injectant covered area, being the limit as $T_i \to \infty$.

2.6.1 Maple Worksheet

This subsection shows a Maple worksheet used to calculate and plot the recoverable area as a function of $f = q_{i,3D}/|q_{p,3D}|$, using the SW2 $q_{i,3D} = 62.12 m^3/day$. The θ_b is also calculated and plotted as a function of $f = q_{i,3D}/|q_{p,3D}|$. The output data generated is not shown, except for the figures. The figures show how the recoverable area and the angle of intersection, between the injection phase and production phase no-flow boundaries, vary as functions of the ratio Q_p/Q_i, respectively.

```
> with(plots);
```

Number of data points

```
> N:=100;
```

Define arrays

```
> f:=array(1..N);
> thetabmat:=array(1..N);
> A:=array(1..N);
```

Define variables

```
> for i from 1 to N do
> f[i]:=i*0.05;
> end do;

> Qi:=62.12;
> Uu:=0.17;
```

Start loop, calculate the Area for each instance of f

```
> for i from 1 by 1 to N do
```

Production rate

```
> Qp:=-f[i]*Qi;
```

Polar angle coordinate of intersection point

```
> thetab:=evalf(Qi*Pi/(Qi+abs(Qp)));
```

Calculate areas

```
> A1:=-Qi^2/(2*Uu^2)*int(((Pi-theta)/(sin(theta)))^2,
> theta=Pi..thetab);
> A2:=Qp^2/(2*Uu^2)*int(((theta)/(sin(theta)))^2, theta=0..thetab);
> Arec:=A1+A2;
> thetabmat[i]:=[f[i],thetab];
> A[i]:=[f[i],2*Re(Arec)];
> end do;

> plot(A, labels=["f=-Qp/Qi","Recoverable Area"]);
```

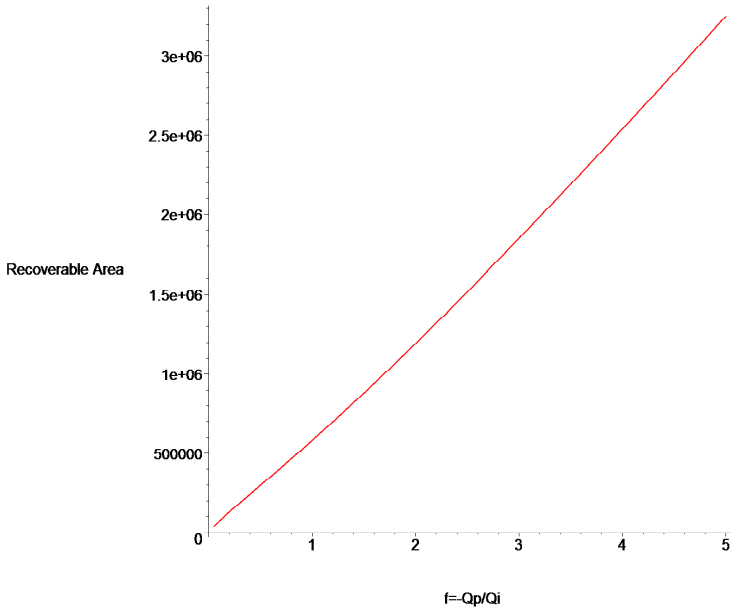


```
> plot(thetabmat,labels=["f=-Qp/Qi","thetab"]);
```

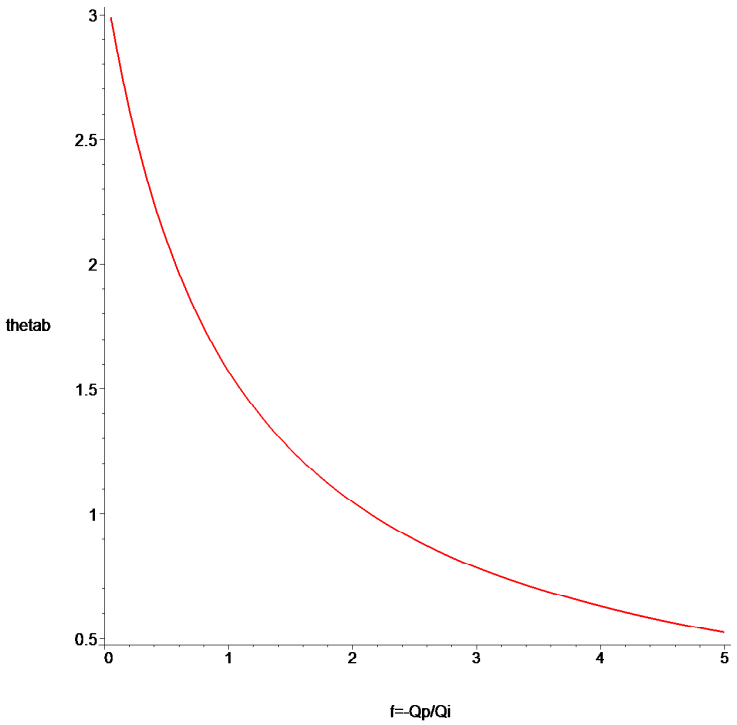

References

[1] M. Abramowitz and I.A. Stegun, editors. *Handbook of Mathematical Functions*. Dover Publications, inc., 1964.

[2] Jacob Bear. *Dynamics of Fluids in Porous Media*. American Elsevier Publishing Company, Inc., 1972. Reprint by Dover Publications, Inc.

[3] J.F. Pickens and G.E. Grisak. Scale-dependent dispersion in a stratified granular aquifer. *Water Resources Research*, 17(4):1191–1211, 1981.

[4] The Maplesoft web page. http://www.maplesoft.com, 2006.

[5] The MathWorks web page. http://www.mathworks.com, 2006.

[6] F.M. White. *Fluid Mechanics*. McGraw - Hill, New York, USA, 5th edition, 2003.

Part II

Finite Difference and Stream-line Simulation of a Push-Pull "Echo" Test

CHAPTER 3

Finite Difference Simulation in SENSOR

3.1 Introduction

In 2004, at the SPE annual technical conference and exhibition in Houston, USA, the paper *Modelling Conformance as Dispersion*, SPE 90390 by Coats, Whitson and Thomas, [2], was presented by dr. Keith Coats. In the paper they presented a single-layer radial $1000x25$ $r-\theta$ SENSOR model, where the radial spacing was 999 equal-volume blocks from $r = r_w = 0.17ft$ to $r = 20ft$ and one block from $r = 20ft$ to $r = 1405ft$. Angular spacing was uniform with $\Delta\theta = 7.2^\circ$. Injection and production wells on BHP contstraint were put in cells (1000,25) and (1000,1), respectively, to give a nearly uniform constant pressure gradient of $\sim 0.0023 psi/ft$ within the 40 ft diameter of the test well region. The test well was located in the centre of the grid. Employing the presented SENSOR model, simulations were run putting in the Pickens-Grisak, [4], field test parameters. It was shown that the model was free of grid-related numerical dispersion, as grids $500x25$ and $1000x50$ gave identical results. In Appendix A the SENSOR input file of Coats *et al.* is cited.

3.2 The Coats *et al.* Simulation Results

The Coats *et al.* SW1 and SW2 results are shown in **Figure 3.1** a and b, respectively, along with the Pickens-Grisak field test data and theoretical data from the semi-analytical stream-line based model. The results obtained from SENSOR must be considered strong evidence that the natural ground-water drift has significant impact on the tracer flow-back behaviour. It "stretches" the the injectant plume and the injectant production profile, implying a non-physically large effective dispersivity, that cannot be explained from the rock properties. Coats *et al.* also showed that the apparent dispersivity is strongly affected by the test parameters.

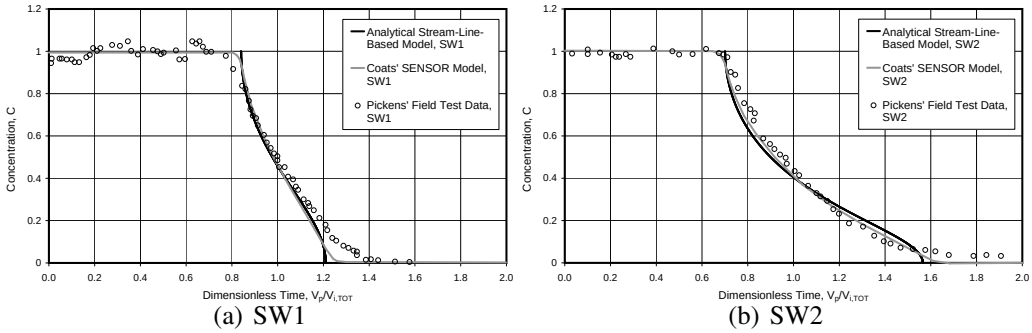

(a) SW1 (b) SW2

Figure 3.1: Coats *et al.* SENSOR results compared to the Pickens-Grisak field data and the semi-analytical solution.

In the litterature, [1], [3], the apparent dispersivity is commonly reported to be dependent of the length travelled. Coats *et al.* showed that their SENSOR model apparent dispersivity is not only a function of the length travelled, but also the injection/production rates and the time scale of the experiment, comparing two simulation runs with equal travel lengths, 3 days at SW1-rate and 6 days at half-SW1-rate.

References

[1] A. Arya, T.A. Hewett, R.G. Larson, and L.W. Lake. Dispersion and reservoir heterogeneity. *SPERE*, 3:139–148, 1988. SPE 14364.

[2] K. H. Coats, C.H. Whitson, and L.K. Thomas. Modelling conformance as dispersion. SPE Annual Technical Conference and Exhibition, 26-29 September, Houston, Texas, September 2004. SPE 90390.

[3] J. Mahadevan, L.W. Lake, and R.T. Johns. Estimation of true dispersivity in field scale permeable media. SPE/DOE Improved Oil recovery Symposium, Tulsa, Oklahoma, USA, April 2002. SPE 75247.

[4] J.F. Pickens and G.E. Grisak. Scale-dependent dispersion in a stratified granular aquifer. *Water Resources Research*, 17(4):1191–1211, 1981.

CHAPTER 4

3DSL Simulations of “A quarter of a 5-spot”

4.1 Introduction

"3DSL is a three-dimensional black-oil reservoir simulator that uses a stream-line grid to transport fluids along. The methodology is similiar to a conventional IMPES-type code, except that fluids are moved along stream-lines, rather than between discrete grid blocks. 3DSL extends the basic stream-line formulation to three-phase, compressible black-oil models." (Chapter 2.1 in the 3DSL User Manual -Version 2.30, [4])

"Streamline simulation is a novel approach particularly suitable for simulating large, heterogeneous reservoirs." (Preface of the 3DSL User Manual -Version 2.30, [4]). 3DSL has previously proved itself to be an extremely effective and accurate tool for particular simulation tasks, especially where high grid resolution is needed, [7]. Simulation run-times an order of magnitude less than the run-time of equivalent finite difference models, have been demonstrated, [2], and for the quarter of a 5-spot problem an exact match to the Morel-Seytoux analytical solution, [3], has been shown, [5].
For details on the 3DSL formalism and terminology see the 3DSL user manual, [4].

4.2 A Quarter of a 5-spot

The 5-spot pattern is a repeating pattern of injectors surrounded by four producers, similiar to the number 5 on a dice. In a homogeneous reservoir, there will exist no-flow boundaries sectioning the 5-spot pattern into identical squares with an injector and a producer located in the opposite diagonal corners. Since all the squares are identical, assuming homogeneity, it suffices to study one of these squares to get an understanding of the reservoir productivity. Morel-Seytoux developed an analytical expression for the injectant production profile as a function of time, for a 5-spot, [3].

Provided from Streamsim, [5], at their Internet web page, there are several example input decks to their stream-line based simulator 3DSL. One of these is a $50x50$ grid-block single-layer "quarter of a 5-spot" model, "q5spt". Each grid-block is $2x2x1m^3$ of size and the total model dimensions are $100x100x1m^3$. The porosity is set to a 100% and the permeability to a $100mD$. The 3DSL TRACER type model was used[1].

The injector is located in grid-block $(i, j, k) = (1, 1, 1)$ and the producer is

[1] "The model is implemented as a three-phase immiscible system with each phase having identical PVT properties of the oil phase. All phases have straight-line relative permeabilities with no residual saturations. The tracer model can be viewed as a limiting case of the more general, immiscible, three-phase problem",[4]

located in grid-block $(i, j, k) = (50, 50, 1)$. The injector is operated at a constant injection rate of $20^{m^3}/_{day}$ for a total of a $1000 days$ using 27 time-steps of equal size, and the producer is operated at a constant bottom-hole pressure of $2500 psi$. The time-steps from the start until $340 days$ were calculated by 3DSL from the restraint DPVMAX=0.10, meaning that no more than 0.10 pore-volumes can be injected per time-step. The remaining $660 days$ were split into 20 equal steps.

From the Morel-Seytoux solution, injectant break-through at about 0.7 pore-volumes injected is expected, corresponding to 350 days of injection.

As can be seen in **Figure 4.1**, the 3DSL simulation injectant production profile matches perfectly the analytical solution by Morel-Seytoux, although lack of detailed data around the injectant time of break-through hides any dispersed break-through behaviour[2].

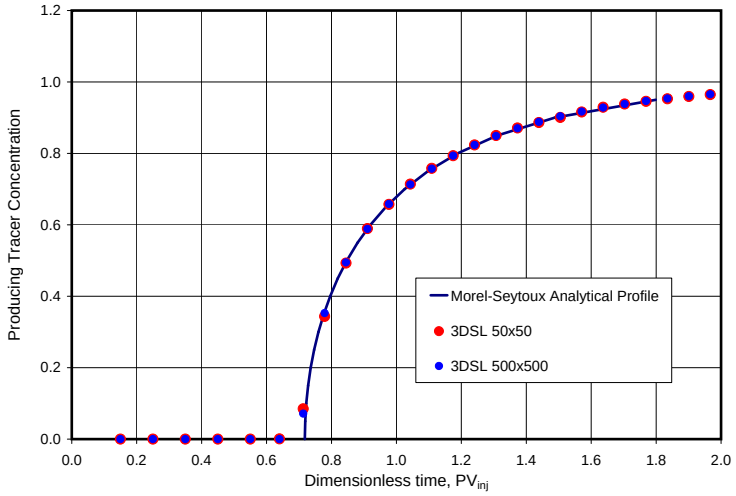

Figure 4.1: 3DSL quarter of a 5-spot 50x50x1 and 500x500x1 grid simulation runs, using 27 time-steps, compared to the Morel-Seytoux's analytical solution.

To assess the effect of refining the simulation grid, the Streamsim example was refined to a $500x500x1$ grid-block model, changing no other model parameters, except the grid-block dimensions. The grid-block size was now, $0.2x0.2x1m^3$. Although, as can be seen in **Figure 4.2**, the dispersion of the injectant front, at 0.7 pore volumes injected, was significantly reduced in the refined model, the refinement did not, however, affect the production profile much, as can be seen in Figure 4.1 .

To get a more detailed view of the production profile at the time of break-through, better time-step resolution was introduced. Both the $50x50x1$ and the

[2]Note that the 3DSL rate data written out at the end of a time-step is really the average over that time-step. To compare with the analytical solution, the 3DSL data are plotted with a time-shift of $-\frac{\Delta T}{2}$, where ΔT is the length of the time-step, which may vary from time-step to time-step, [6].

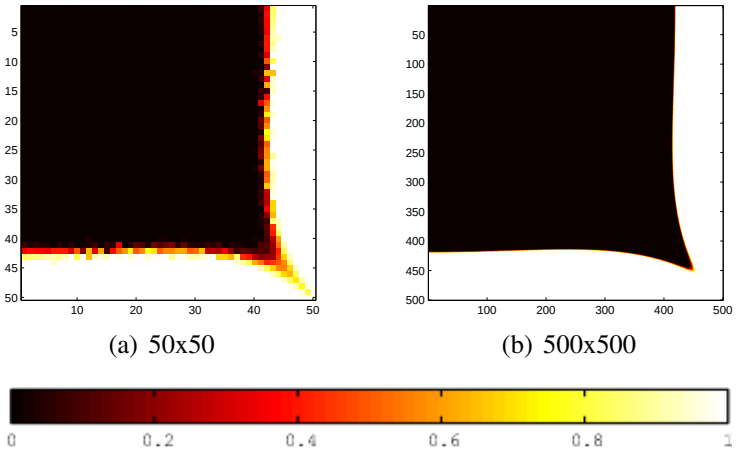

(a) 50x50 (b) 500x500

Figure 4.2: 3DSL quarter of a 5-spot in situ fluid saturation profile for 27 time-steps 50x50x1 and 500x500x1 models, respectively, at 0.7 PV injected.

$500x500x1$ models were run using a 107 time-steps. The same approach as in the original model was used, the time interval from 340 days to 1000 days was split into a 100 equal steps.

It has to be kept in mind that, using stream-line based simulators, identical models, using different numbers of time-steps, are not automatically comparable, since increasing the number of time-steps means increasing the numerical dispersion. This is due to the mapping back and forth, from the stream-lines to the underlying grid, which happens for every time-step. Every time fluids are mapped from a stream-line to a grid-block, artificial mixing may occur. Either because one fluid is transported to a grid-block originally containing another fluid, because two stream-lines, carrying different kinds of fluids, deliver to the same grid-block or because of a combination of the two.

In **Figure 4.3** it can be seen that the 107 time-step simulations both gave excellent matches to the theoretical Morel-Seytoux profile. We see that the coarse model give a less accurate description of the production profile around the time of break-through than the refined model. Note that the numerical dispersion around the time of break-through should be about the same in the 27 time-step models and the 107 time-steps models, as the number of time-steps done prior to the time of break-through is approximately the same.

4.3 Conclusions

It has been seen that the grid refinement may play an important role regarding the injectant front dispersion. However, even in the coarse model, the injectant

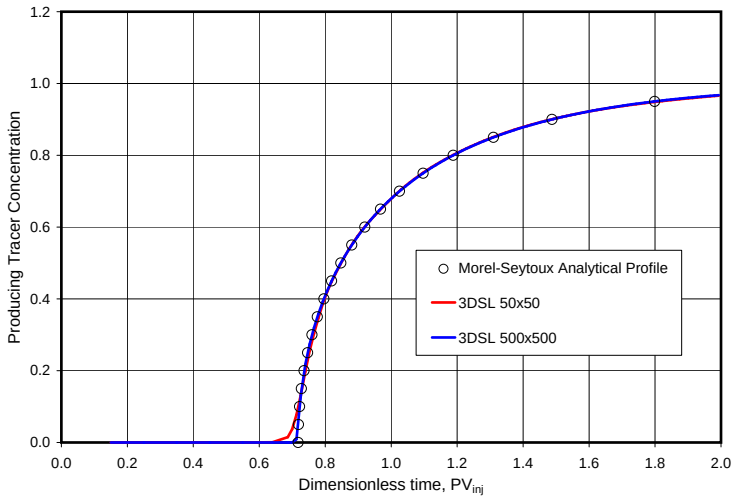

Figure 4.3: 3DSL quarter of a 5-spot 50x50x1 and 500x500x1 grid simulation runs, using a 107 time-steps, compared to the Morel-Seytoux's analytical solution.

front remains sharp compared to what one would expect from conventional finite difference simulators such as Eclipse, [1].
For the particular case of generating injectant production profiles for a quarter of a 5-spot, the grid refinement is not that important. Both the coarse and the refined model reproduced the Morel-Seytoux analytical solution accurately, except around the time of break-through, where the coarse model performed worse than the refined one.
Even though a higher degree of numerical dispersion was expected for the high-number-of-time-steps models, this was not observed.

References

[1] Roderick Panko Batycky. *A Three-Dimensional Two-Phase Field Scale Streamline Simulator*. PhD thesis, Stanford University, January 1997.

[2] W. Huang, G. Di Donato, and M.J. Blunt. Comparison of streamline-based and grid-based dual porosity simulation. *Journal of Petroleum Science and Engineering*, 43:129–137, 2004.

[3] H.J. Morel-Seytoux. Analytical numerical method in waterflooding predictions. *SPEJ*, pages 247–258, September 1965.

[4] Streamsim Technologies, Inc. *3DSL User Manual - ver. 2.30*, December 2005. Available at:
http://www.streamsim.com.

[5] The Streamsim web page.
http://www.streamsim.com, 2006.

[6] Marco Thiele. Fwd: RE: 3DSL Quarter Five Spot vs Analytical solution. E-mail correspondance between M. Thiele and C.H. Whitson, July 2004.

[7] M.R. Thiele. Streamline simulation. Presented at the 6th International Forum on Reservoir Simulation, Schloss Fuschl, Austria, September 2001.

CHAPTER 5

3DSL Simulations of Push-Pull Tests

5.1 Introduction

When conducting the study of this thesis, Coats *et al.* had allready shown how their SENSOR model, [2], performed and was able to reproduce experimental data from the Pickens-Grisak field tests, SW1 and SW2, [3], quite accurately. As the good results from the stream-line based semi-analytical model were obtained, the idea occurred, to set up a model for a commercial stream-line based simulator. It would be interesting to see how such a model would compare to the Coats *et al.* model as well as the semi-analytical model described in Chapter 2 and Paper I. Since it was allready shown how the stream-line based semi-analytical model outperformed a finite difference approach, it was quite natural to assume that this would also be the case for a commercial stream-line based simulator. Limiting the study to the use of one simulator only, Streamsim's 3DSL, [6], was chosen to represent the class of available commercial stream-line based simulators.
In Appendix B, the final 3DSL input deck is printed, and in this chapter a description of the building process of the model and of the the final model itself is given. In addition some general considerations and conclusions to the 3DSL modelling, are presented.
For details on the 3DSL formalism and terminology see the 3DSL user manual, [5].

5.2 Building the Model

5.2.1 Base-Case

To create a 3DSL model as accurate as possible, a coarse model. expected to perform poorly, was picked as a starting point. The base-case model was a regular (I,J,K) 201x201x1 active grid cell model with cell dimensions $4.6x4.6x8.2m^3$, approximating the model dimensions of the Coats *et al.* model, [2]. The cell height, $8,2m$, was taken from the Pickens-Grisak test site description, [3], as was the permeability and fractional porosity, $14.8darcy$ and 0.38, respectively. The 3DSL TRACER functionality was applied, so that the three possible phases, gas, oil and water, were miscible, yet all phases had the same properties as the oil phase. Hence, the only difference between the phases are their names, and it is possible to model tracer injection, keeping track of amounts and saturations of each phase. The reservoir model was initiated with "water" as the in situ fluid, and the test well injected "oil". Generating production profiles, the injectant concentration in the producing fluid was simply the rate of "oil" to the total rate produced.
Since it was desired to model the effect of naturally flowing ground-water, on the push-pull test injectant production profile, horizontal wells in the columns I=1

and I=201, were set to a constant BHP of 173.92kPa and 126.08kPa, respectively. Thus, the mean reservoir pressure of 150kPa was maintained[1] and a natural, uniform, pressure gradient of 0.052$^{kPa}/_{m}$, was established.
The test well was located in the middle of the model, at (I,J,K)=(101,101,1). The Pickens-Grisak SW2 field test data were put into the model, injection at a rate of 62.12$^{m^3}/_{day}$ for a period of 3.93 days and thereafter producing at a rate of 52.36$^{m^3}/_{day}$ for a period of 14 days.
Due to the coarse gridding, and the extreme smearing of the injectant saturation profile, as can be seen in **Figure 5.1**, it is not surprising that the base-case production profile, as shown in **Figure 5.2**, is a poor approximation to the theoretical analytical dispersion free profile. Comparing the injection phase base-case stream-line pattern with the theoretical "source in a uniform stream" stream-lines, as can be seen in **Figure 5.3**, it can be seen that despite some disagreement, the base-case stream-line pattern is not that far off.

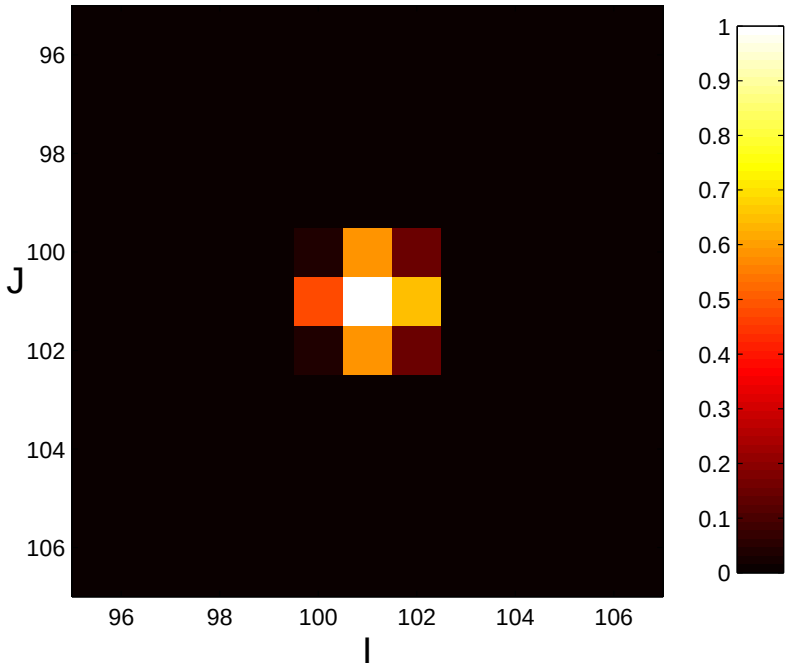

Figure 5.1: 3DSL Base case injectant saturation profile at the end of the injection phase.

[1] 150kPa is approximately one and a half atmospheric pressure, being the assumed pressure at five metres depth of water.

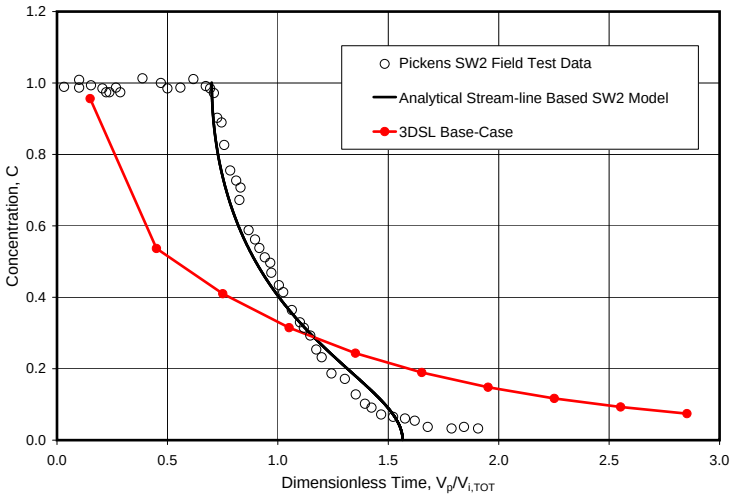

Figure 5.2: Comparing the 3DSL Base case production profile with the Pickens-Grisak SW2 field test result and the theoretical dispersion-free model result.

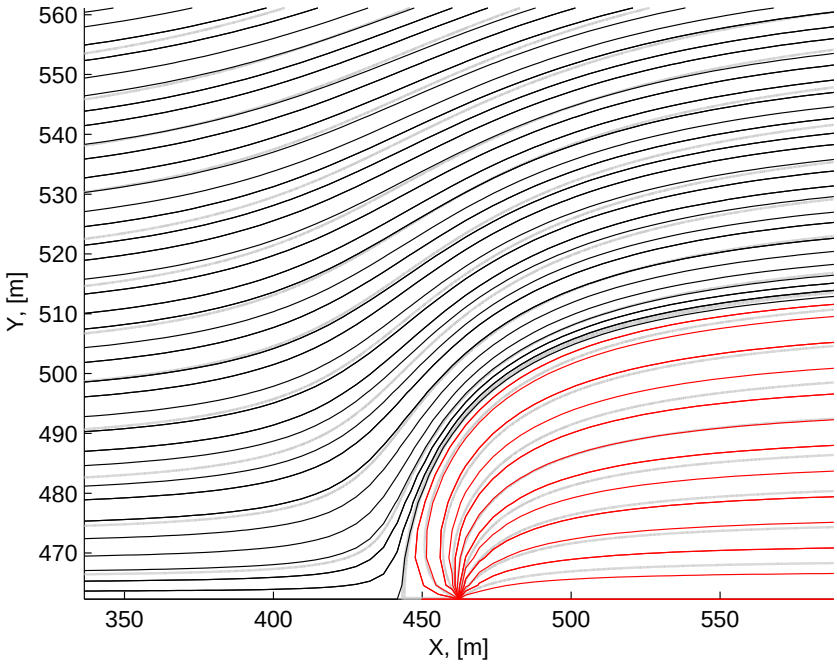

Figure 5.3: Comparing SW2 theoretical injection-phase stream-lines (grey) with the 3DSL Base case stream-lines (black from the natural ground water flow and red from the injection well).

5.2.2 Global Grid Refinement

Realising the need for grid refinement, due to the highly dispersed injectant front seen in Figure 5.1 , a global refinement of the grid was attempted. Four different refinement schemes were investigated, 401x401x1, 801x801x1, 1201x1201x1, 1501x1501x1. The reservoir scale was maintained, such that the grid cell size of the 401x401x1 model was one fourth of the base-case grid cell size. It can be seen in **Figure 5.4**, how the production profile approaches some limit, as the grid gets finer. The profiles seems to come close to the theoretical profile, but the lack of data points generated make it impossible to assess the details of the production profile, especially at the time of break-through. There are, however, enough points to make out that the end-time-of tracer production is not matched very well, even by the very refined 1501x1501x1 model.
In **Figure 5.5** it can be seen how the injectant saturation front at the end of the injection phase gets less dispersed as the grid gets finer.

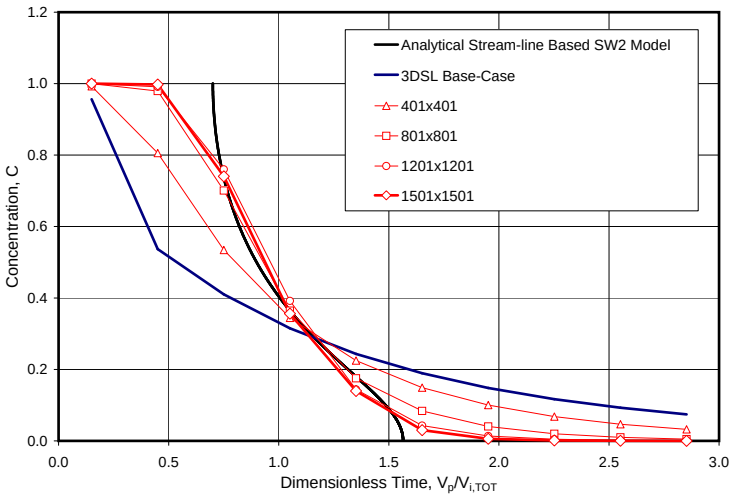

Figure 5.4: Comparing the theoretical dispersion-free model data and the 3DSL Base case with globally refined grid simulations. The grid cells are down-scaled as the number of grid cells is increased, such that the overall model dimensions are kept constant.

5.2.3 Local Grid Refinement

Although, the 1501x1501x1 grid contains more than two million grid cells, it is still no problem to run the simulation in a fairly short time on a common desktop computer, even if it would take long time with a traditional finite difference simulator. Simulation cost, measured in time, however, should always be minimised, and there is evidence that the refinement of the 1501x1501x1 model is not even enough. It might be more efficient and more clever to locally refine the model,

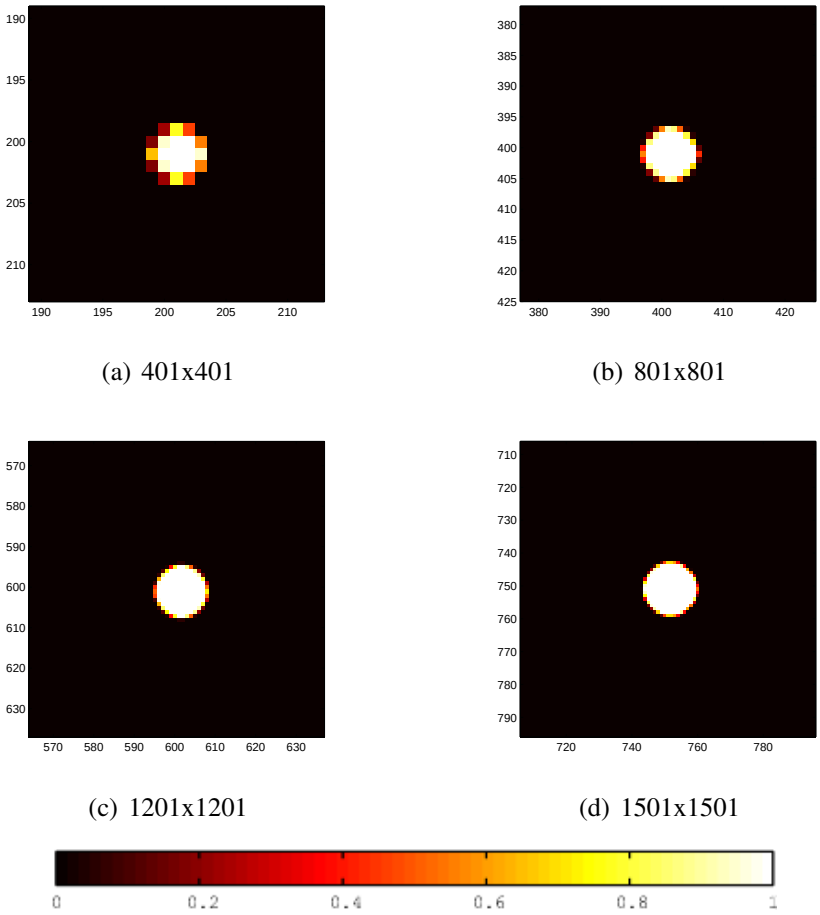

(a) 401x401 (b) 801x801

(c) 1201x1201 (d) 1501x1501

Figure 5.5: 3DSL injectant saturation profiles, at the end of the injection phase, for the various globally refined models.

around the test well.

Refinement is important where sharp fluid fronts are important and where the stream-line curvatures are strong, where the linearly varying velocity assumption is far from the truth[2]. Thus, it suffices to refine the grid around the test well, since there are no fluid fronts of particular interest far from the well and that the stream-lines far from the test well are close to linear.

By trial and error, it was found that the stagnation points of the source/sink in a uniform stream problem should be inside the refined area, so for the SW2 test parameters, an area of $40 \times 40m^2$ around the test well was refined. That is, 9 rows and columns in the base-case model were refined.

[2]"The underlying assumption is that the velocity field in each coordinate direction varies linearly and is independent of the velocities in the other directions", [1](Chapter 3.5), [4].

Two different local refinement models were investigated, 401x401x1 and 601x601x1, where for instance the 401x401x1 model consisted of 192 cells of width $4.6m$ and 209 cells of width $\frac{9 \cdot 4.6m}{209} = 0.198m$, in the I direction, and similarly in the J direction .

In **Figure 5.6** it can be seen how the locally refined models perform just as well as the globally refined 1501x1501x1 model. Using local grid refinement, it is possible to get an even finer grid ($0.1 \times 0.1 \times 8.2m^3$ cell sizes in the 601x601x1 model), and sharper fluid fronts, than in the 1501x1501x1 globally refined grid ($0.6 \times 0.6 \times 8.2m^3$ cell sizes), in the relevant study area, as well as a much lower simulation run-time.

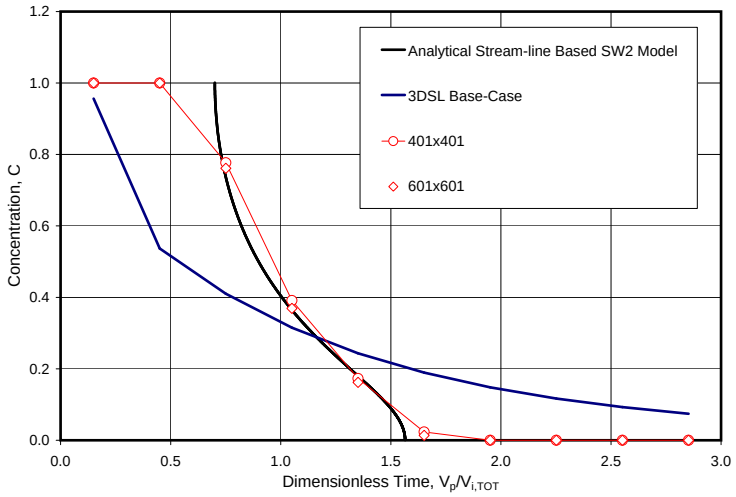

Figure 5.6: $40x40m^2$ local grid refinement around the test well injectant production profiles.

5.2.4 Grid Dimensions

It has been assumed that the reservoir model should be wide and long to avoid the model boundaries affecting the stream-line pattern in a non-physical way. In the semi-analytical model, the reservoir has been assumed to be of infinite areal extent. It was assumed, for the base-case model, that the Coats *et al.* model dimensions were sufficiently large.

Investigating the effect of shrinking the model, however, does not give conclusive proof that the width is of great importance, although it is obvious that extremely narrow models, for instance narrower than the Rankine half-body, will affect the model stream-lines in very non-physical ways. Keeping the cell sizes constant, the number of grid-cells in the 401x401x1 ($2.3 \times 2.3 \times 8.2m^3$ cell sizes) and the 801x801x1 ($1.15 \times 1.15 \times 8.2m^3$ cell sizes) globally refined models were altered, both decreased and increased. Dividing the number of grid cells by four

involved dividing the model area by four, as well. The pressure gradient was kept at $0.052^{kPa}/_{m}$ and the test well was kept in the middle of the grid.
As can be seen in **Figure 5.7** and **Figure 5.8**, even shrinking the model area greatly, by a factor 16 for the 401x401x1 model and a factor 64 for the 801x801x1 model, did not affect the production profiles much.

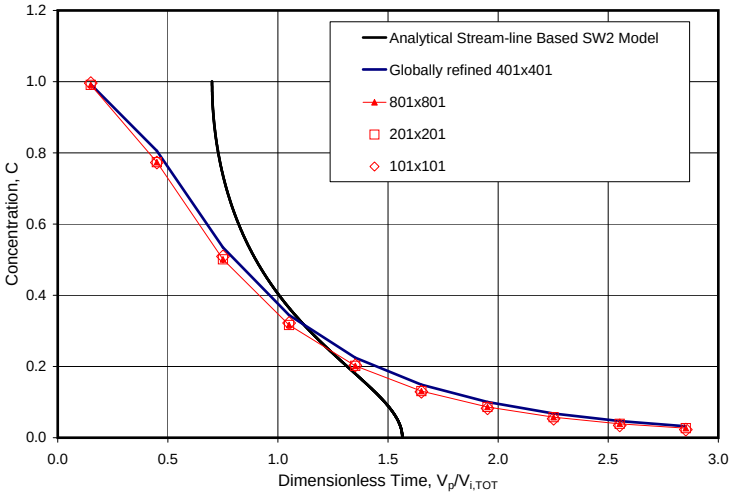

Figure 5.7: Injectant production profiles from $2.3x2.3m^2$ grid-block area models with different number of grid-blocks.

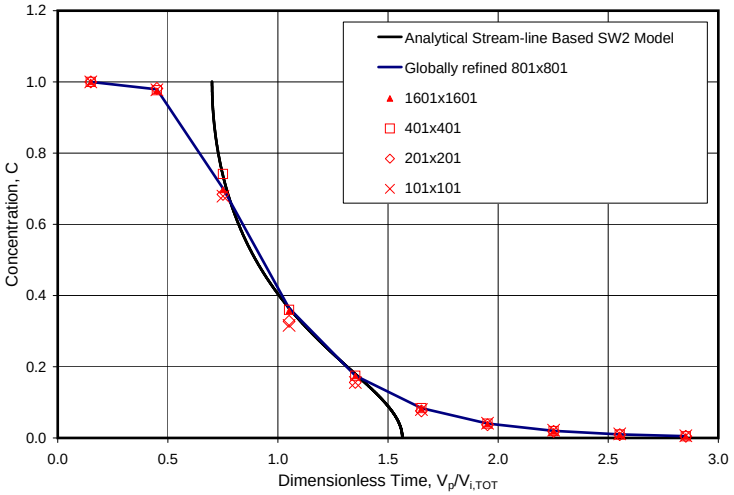

Figure 5.8: Injectant production profiles from $1.15x1.15m^2$ grid-block area models with different number of grid-blocks.

5.2.5 3DSL Model Boundaries

One of the features of 3DSL is the BOUNDARIES section, [5], where *open-flow boundaries* may be defined.
"Open boundaries are useful for incompressible problems where total field production/injection volume will typically not be equal throughout the field life. Boundaries can also be used to model constant pressure aquifers", [5].
Open-flow boundaries are similiar to the *boundary wells* that can be defined in the RECURRENT section along with injection and production wells, but where the boundary wells can only be perforated in one cell each, the open-flow boundaries can span multiple cells. The open-flow boundary cell pressures are set to the initial pressure defined in the cell, and is assumed fixed throughout the simulation run. The boundary cell will act as an injector/producer depending on the pressure of the neighbouring cells. When injecting, the boundary cell will inject fluids as specified in the input deck.
A study was done to evaluate the use of open-flow boundaries, longitudinally, compared to the natural drift direction, to avoid no-flow boundaries affecting the stream-line pattern, and transversally to ensure the natural pressure gradient (instead of the horizontal wells of the base-case model). For the longitudinal open-flow boundaries, there was no significant effect on the production profile, but simulation run-time was affected negatively. For transversal open-flow boundaries, there was a negative effect on the production profile, resulting in a more dispersed curve.
Due to these observations, the BOUNDARIES feature of 3DSL was not made use of in the final model presented here.

5.3 Problems to be Considered

Here is listed the main concerns and problems experienced during the model building:

1. One of the assets of 3DSL is that there is no limit to the length of time-steps, in principle. Contradictory to the intuition developed through traditional finite difference simulation, the numerical dispersion of 3DSL actually increases as the number of time-steps is increased. This is due to the mapping and re-mapping of fluid saturations to the underlying grid. Every time output data are generated and a new time-step is begun, the saturation data in the underlying grid is updated, and artificial mixing may occur. Hence, generating as little output data as possible is desired. In **Figure 5.9** saturation profiles at a selection of points in time are compared, for the 401x401x1 locally refined model using 11 and 51 time-steps. It can clearly be seen how

the saturation profile is (1) the more dispersed the later in the simulation we get and (2) more dispersed for the 51 time-step run than for the 11 time-step run.

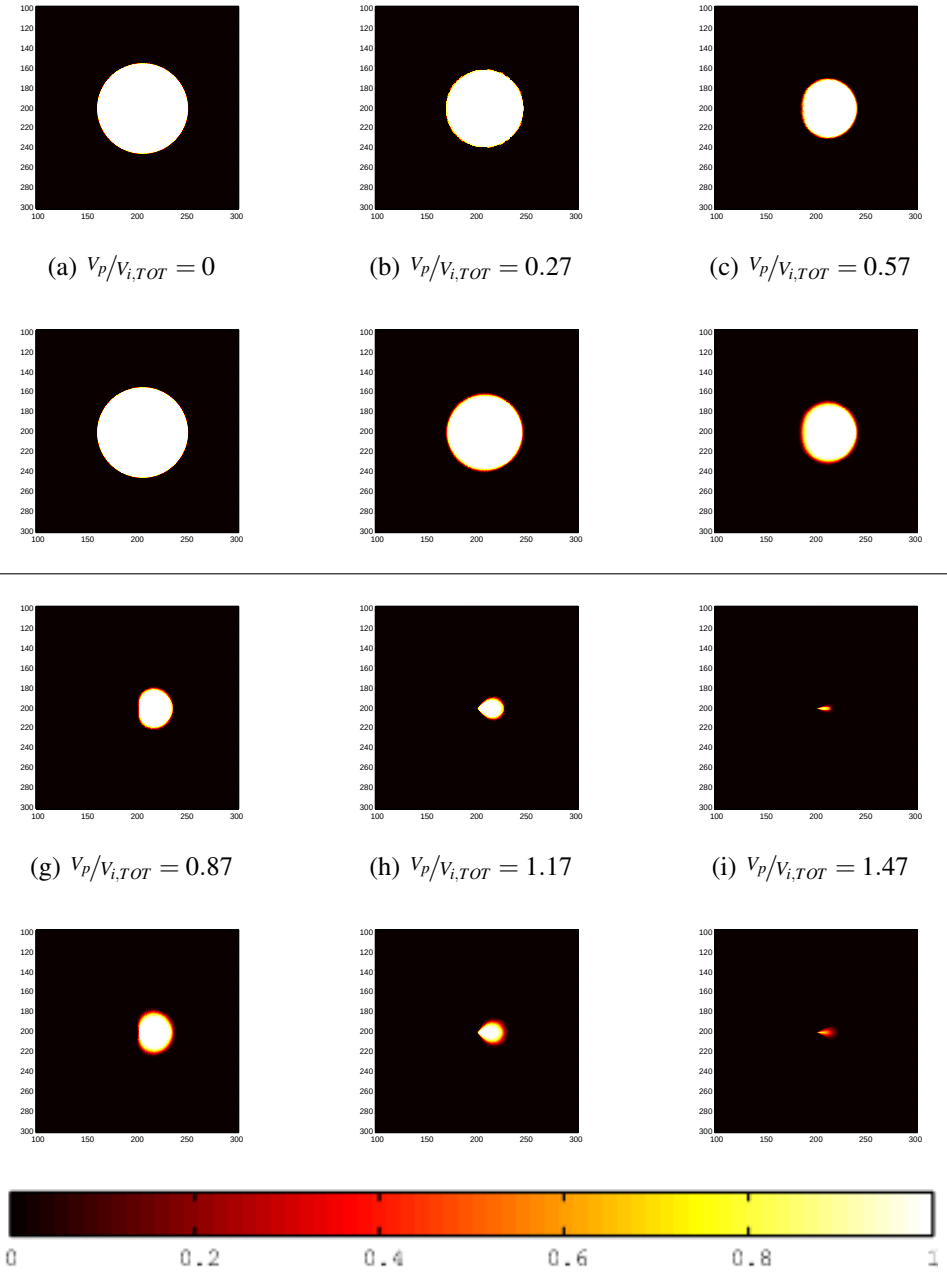

(a) $V_p/V_{i,TOT} = 0$ (b) $V_p/V_{i,TOT} = 0.27$ (c) $V_p/V_{i,TOT} = 0.57$

(g) $V_p/V_{i,TOT} = 0.87$ (h) $V_p/V_{i,TOT} = 1.17$ (i) $V_p/V_{i,TOT} = 1.47$

Figure 5.9: 3DSL injectant saturation profiles at a selection of points in time, for the 401x401 locally refined model using 11 (first and third rows) and 51 (second and fourth rows) time-steps, respectively .

On the other hand, scarce output data gives poorly detailed production profiles, and the output rates are actually an average rate over the time-step, and they might be way off, if the time-step is long and the rate is varying. A balance must be found, between acceptable inaccuracy due to numerical dispersion, on one hand, and acceptable inaccuracy due to averaging and lack of detail on the other hand.
These arguments alone, is enough to realise that a dispersion-free, detailed, exact match to the theoretical production profile cannot generally be found.

2. Even though the solving of the flow equations, one-dimensionally, along the stream-lines can be very accurate, the finite difference aspect of the underlying grid is haunting the simulator. Both saturations and pressures are discretized and piecewise constant over each grid cell, and the velocity field inside each grid cell, used to find the stream-line patterns, is assumed to be piecewise linear, across the grid cells, [4]. Inter cell velocity fields are calculated from the grid cell interface Darcy velocities, [1]. Hence, a coarse grid is unfit for modelling velocity fields varying rapidly in space and for models where a sharp fluid front is crucial.

3. Both the Coats *et al.* model as well as the semi-analytical stream-line based model are concerned with the upper half-plane only, due to the symmetry of the problem. This saves, in both models, computation time, saving grid cells in the numerical model and saving stream-lines in the stream-line based model. An attempt was done, using 3DSL, also, to model the upper half-plane only. The results were not good. A good match to the expected values were obtained for time of break-through and end-time of tracer production, but the intermediate production profile gave a very poor match to the theoretical semi-analytical results.
No further study regarding this topic was done, but it is believed that the problem is related to the fact that the well is located at the centre of a grid-cell and that stream-lines will emerge from the well at all angles, not only for $\theta \in [0, \pi]$. This leads to an unnatural high density of "forced" stream-lines along the model boundary closest to the well.

5.4 The Best Model

Based on the study reported from and described in this chapter, the 601x601x1 locally refined model, using no-flow boundaries and horizontal wells to assure the natural pressure gradient has come to be regarded as the best model. The locally refined area includes both the injection phase and production phase stagnation points, and the full injectant plume.

No conclusion is drawn regarding the time-stepping question, except that the injection phase should be finished in one time-step only, and that one time-step only, should be taken from the end of the injection phase until the time of break-through. Other than that, the number of time-steps should be chosen to satisfy the demand for production profile detail and accuracy. In Appendix B the 3DSL input deck of the final model is cited.

As can be seen in **Figure 5.10** and **Figure 5.11**, 19 time-step solutions, using the final model, give very good intermediate matches to the theoretical dispersion-free

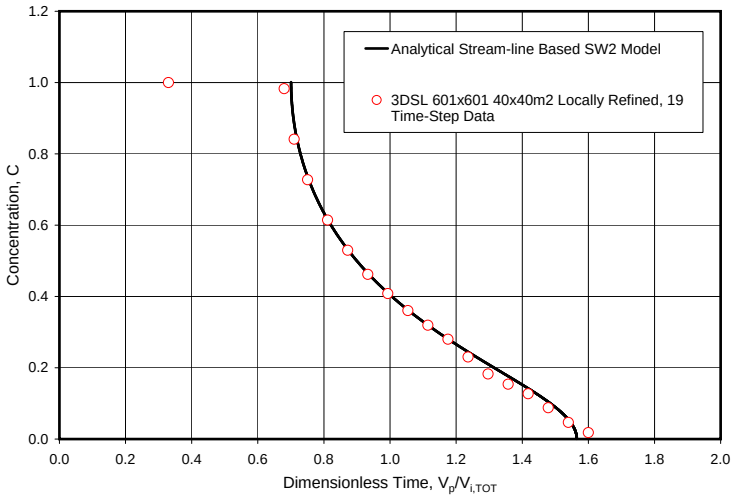

Figure 5.10: Comparing the 19 time-step $40x40m^2$ locally refined 601x601x1 grid block SW2 model with the theoretically expected SW2 injectant production profile.

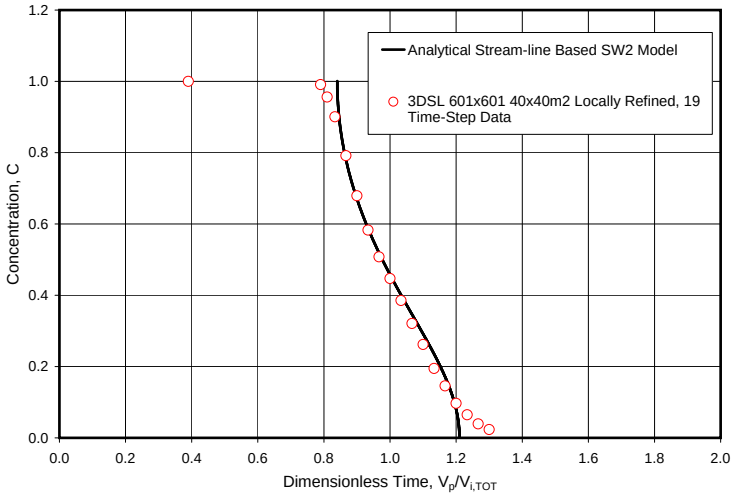

Figure 5.11: Comparing the 19 time-step $40x40m^2$ locally refined 601x601x1 grid block SW1 model with the theoretically expected SW1 injectant production profile.

production profiles, but pre-break-through and at the end of tracer production, the profile is smeared[3].

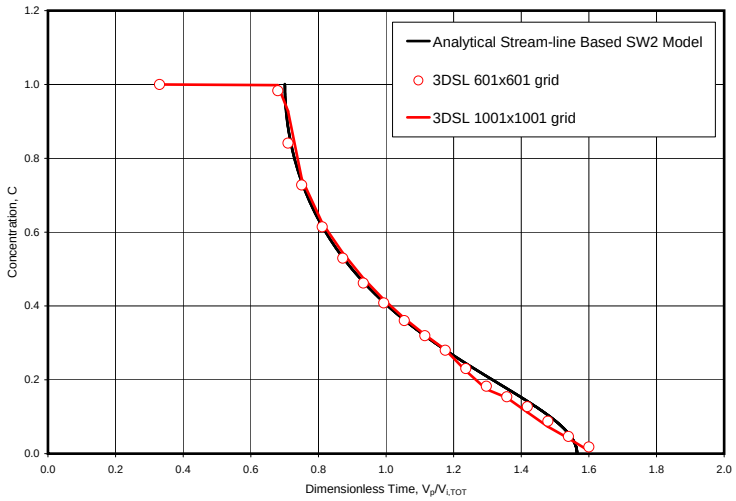

Figure 5.12: Comparing 19 time-step $40x40m^2$ locally refined 601x601x1 and 1001x1001x1 grid block SW2 models results with the theoretically dispersion-free solution.

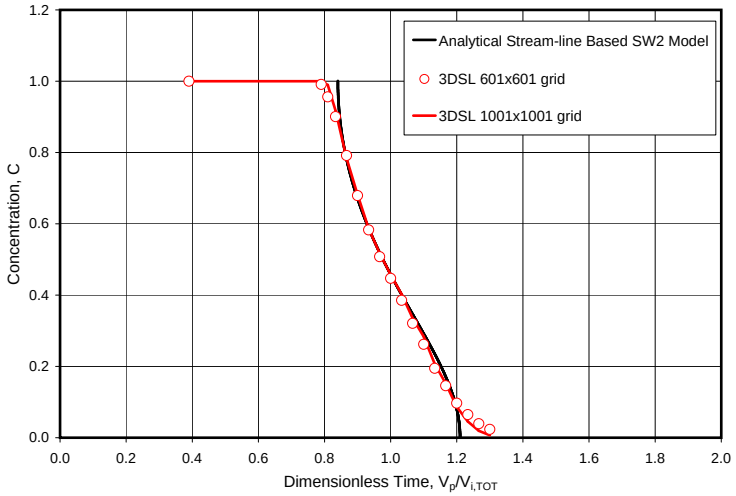

Figure 5.13: Comparing 19 time-step $40x40m^2$ locally refined 601x601x1 and 1001x1001x1 grid block SW1 models results with the theoretically dispersion-free solution.

[3]Note that if exchanging the SW2 test parameters in the Appendix B input deck with SW1 test parameters, the grid should also be changed so that the SW1 stagnation points are included in the refined ares, for instance by altering the grid dimensions $0.1m \rightarrow 0.12m$, to get the most accurate results.

To assess the degree of convergence of the 601x601x1 model, the model was refined even more, to a 1001x1001x1 model, where the locally refined grid-blocks were divided by four. As can be seen in **Figure 5.12** and **Figure 5.13**, there is no great difference between the 601x601x1 and the 1001x1001x1 model results, so it can be concluded; grid-related numerical dispersion has negligible effect on the 601x601x1 model results.

5.5 Conclusions

It has been seen through the 3DSL study, that the refinement of the grid is essential; the sharp fluid interfaces needed to model a dispersion-free push-pull test accurately, requires a fine grid. The solution is local refinement, and it has been shown that it suffices to refine an area around the test well, including the stagnation points, larger than the maximum injectant covered area.

Close attention should be paid to the number of time-steps taken, as this will affect the numerical dispersion as well as the accuracy and the detail of the production profile. A high level of detail will require a lot of time-steps, as output data, from 3DSL, is only generated at the end of a time-step, leading to an increase in the numerical dispersion. Vice versa, a small numerical dispersion will require few time-steps and will lead to a low level of production profile detail. In addition, the rate data output are averages over the time-steps and may be way off, for long time-steps and varying rates.

It has been seen that the 3DSL model developed here matches the production profile accuracy of the SENSOR model developed by Coats et al, but deviates somewhat from the theoretical dispersion-free model results. It is also worth noticing that the 3DSL simulations finished faster than the SENSOR simulations, run on the same computer.

Based on this study and correspondences with Marco Thiele at Streamsim Technologies Inc., [6], it has to be concluded that the stream-line based semi-analytical model developed in this thesis presently is the most accurate model and that available commercial simulators, finite difference or stream-line based, cannot readily be used to model push-pull tests accurately.

References

[1] Roderick Panko Batycky. *A Three-Dimensional Two-Phase Field Scale Streamline Simulator*. PhD thesis, Stanford University, January 1997.

[2] K. H. Coats, C.H. Whitson, and L.K. Thomas. Modelling conformance as dis-

persion. SPE Annual Technical Conference and Exhibition, 26-29 September, Houston, Texas, September 2004. SPE 90390.

[3] J.F. Pickens and G.E. Grisak. Scale-dependent dispersion in a stratified granular aquifer. *Water Resources Research*, 17(4):1191–1211, 1981.

[4] David W. Pollock. Semianalytical computation of path lines for finite-difference models. *Ground Water*, 26(6):743–750, November-December 1988.

[5] Streamsim Technologies, Inc. *3DSL User Manual - ver. 2.30*, December 2005. Available at:
http://www.streamsim.com.

[6] The Streamsim web page.
http://www.streamsim.com, 2006.

Part III

Two-Well Transmission Tests

CHAPTER 6

On the Stream-Line Based Solution to the Two-Well Transmission Test

6.1 Introduction

In addition to single-well tests, two-well tests are commonly run all over the world. The two-well test is closely related to the single-well push-pull test, but as the name implies, the test involves the use of two test wells some distance apart. One of the wells act as an injector and the other as a producer. As in the push-pull test, the injectant is a mixture of water and tracer/solutes, and the concentration versus time, of injectant, is calculated from the measured tracer/solute content in the produced fluid. The two wells may, in principle, inject/produce at different rates. In the paper by Pickens and Grisak, [2], where the single-well push-pull test data were collected, there is also reported from a two-well test, and in their paper from 2001 Coats *et al.*, [1], also report from a two-well transmission test simulation model, using SENSOR, [3].

6.2 Source Plus Sink in a Uniform Stream

In **Figure 6.1** a schematic of a general two-well transmission test setup can be seen. The two test wells are located, symmetrically on either side of the y-axis, on the x-axis, with an inter-well distance of $2a$. The natural, uniform stream flows at angle, α, to the positive x-axis. The reformulated two-dimensional injection and production rates are Q_i and Q_p, respectively, as for the push-pull test, and the production rate is per definition negative. The mathematical formulation of the "source plus sink in a uniform stream" is similar to that of the "sink/source in a uniform stream", which is treated in Chapter 2 and Paper I. The stream-line numbers, ψ, of the system is simply the super-position of the stream-line numbers from each component, the uniform stream, the source and the sink, [4];

$$\begin{aligned}\psi &= \psi_{uniform} + \psi_{source} + \psi_{sink} \\ &= U_u\,(-x\sin\alpha + y\cos\alpha) + Q_i \arctan\frac{y}{x+a} - |Q_p| \arctan\frac{y}{x-a}\,. \quad (6.1)\end{aligned}$$

Here, the arctan function has been used, but the arccos or the arcsin functions may also be chosen, adjusting the argument. Note that the choice of functions might ease or complicate the problem, mathematically and graphically. Transformations to other coordinate systems have not been studied.

In **Figure 6.2** it can be seen how the injection/production rate ratio affects the stream-line picture and also how the injection/production "strength" compared to the natural drift is of importance. The injector and the producer are denoted by I and P, respectively, and the natural drift velocity direction is indicated with an arrow. Test parameters from the Pickens-Grisak two-well transmission test, [2],

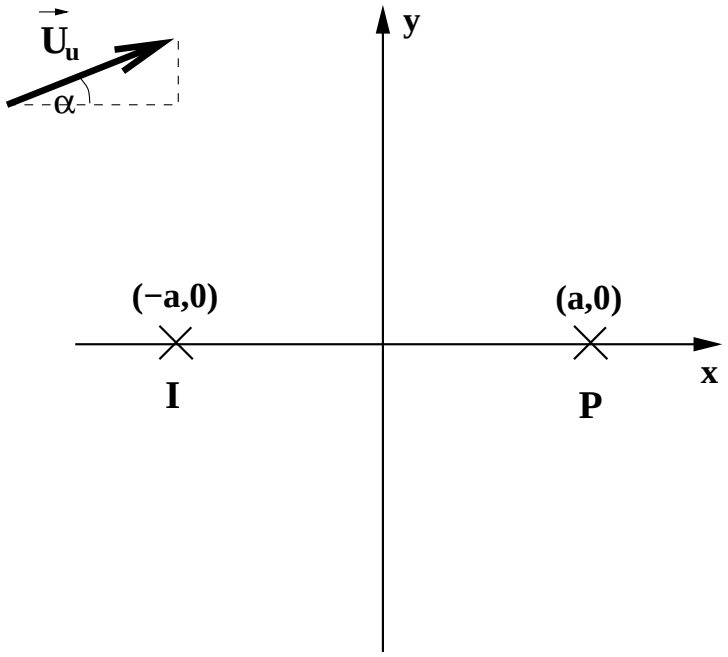

Figure 6.1: Schematic of a two-well transmission test setup in a uniform stream.

has been used as default; $Q_i = |Q_p| = 1.99^{m^2}/_s$, $a = 4m$, $U_u = 0.17^{m}/_{day}$.
Due to the formulation of the stream-line number, ψ, in Equation 6.1 , there are asymptotes in $x = -a$ and $x = a$. These asymptotes show up as y-directional lines in the stream-line plots, but represent, really, non-physical stream-line effects due to the mathematical formulation. The over-all picture, however, is correct. The problem may be mended by switching from arctan to arccos or arcsin, but other graphical artifacts will occur as the natural drift angle is varied.
In Figure 6.2 (a) and (b) the production rate is half and double the injection rate, respectively, and it can be seen, in a), that injectant easily escapes the production well while, in b), the production well "swallows" all the injectant and in addition some in situ water.
In Figure 6.2 (c) the injection and production rates are equal, but both rates have been reduced by 90 % from the Pickens-Grisak values. In addition the natural drift direction is set to $\alpha = \pi/4$. As can be seen, the two wells are connected by very few stream-lines, hence, the communication between the test wells is poor. Monitoring the pressure in the wells, will reveal the presence of the other well, but no or very little injectant can be recovered. Hence, without a good understanding of the natural drift regime, unfortunate test set-ups may be designed, where the two test wells do not communicate.

In **Figure 6.3** it can be seen how the direction of the natural drift affects the

stream-line picture, maintaining the Pickens-Grisak test parameters, varying the natural drift direction, α, only. Although it is not emphasised, we can see how the Rankine oval, [4], separates injected fluid from the in situ fluid[1]. As is seen, for these test parameters, only in the $\alpha = 0$ are all injection well stream-lines connected to the production well.

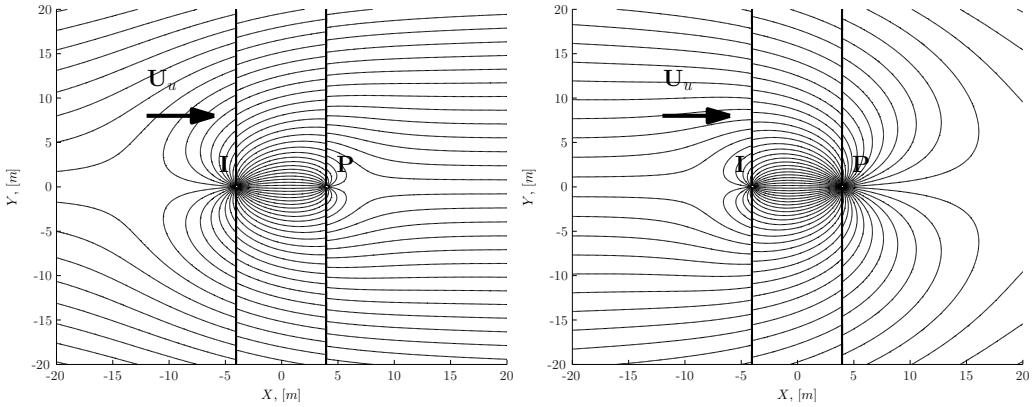

(a) $|Q_p| = Q_i/2$, $\alpha = 0$ (b) $|Q_p| = 2Q_i$, $\alpha = 0$

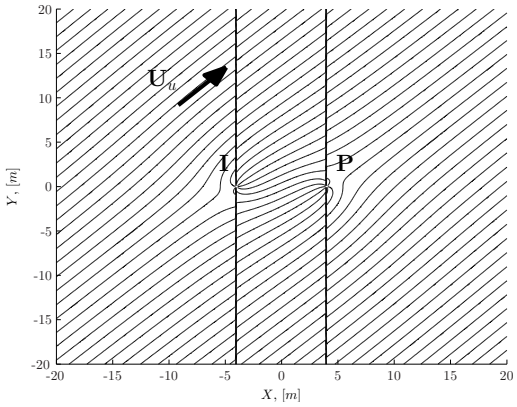

(c) $|Q_p| = Q_i$ but reduced by 90%, $\alpha = \pi/4$

Figure 6.2: Two-well transmission test stream-line patterns. The impact of the injection/production rate ratio as well as the injection/production "strength" compared to the natural drift. The vertical lines are due to the asymptotic behaviour of the arctan parts of Equation 6.1 and represent non-physical stream-line effects. This is also the cause of the "broken" stream-lines.

[1] Some in situ fluid initially located inside the Rankine oval, will be produced before injectant break-through occurs.

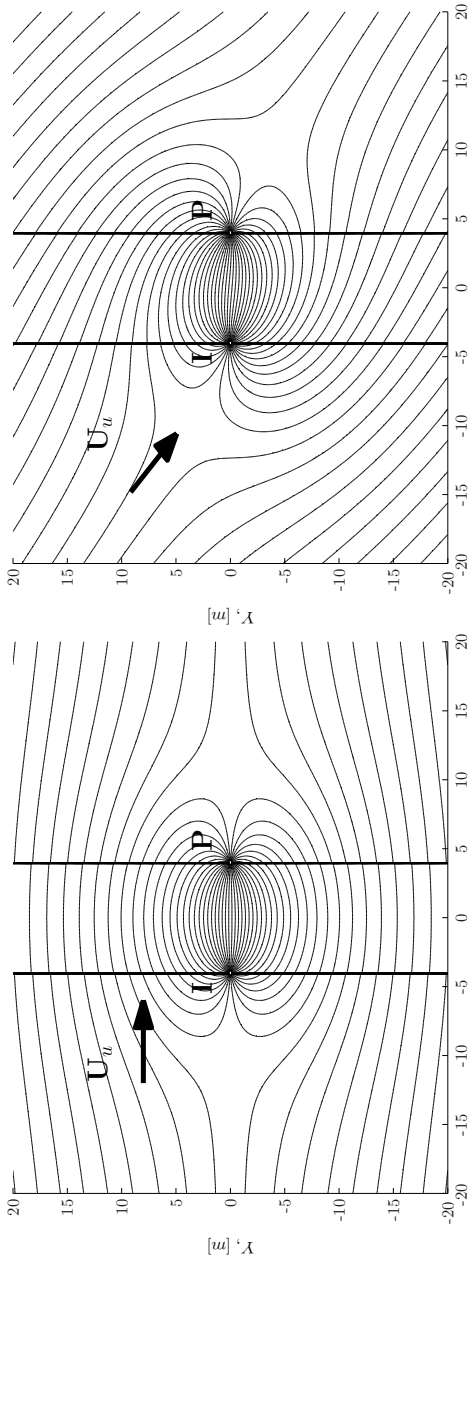

(a) $\alpha = 0$

(b) $\alpha = 7\pi/4$

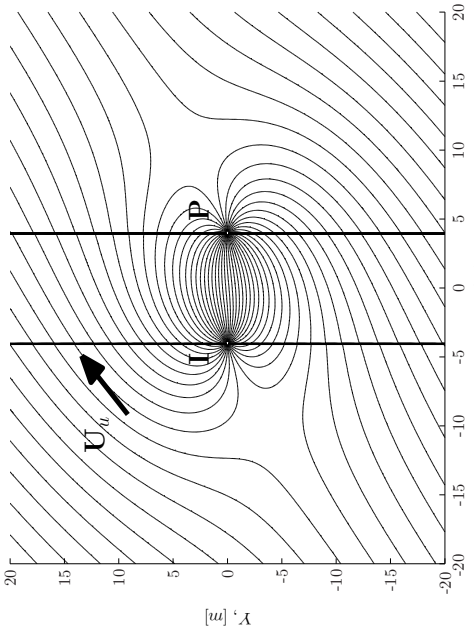

(c) $\alpha = \pi/4$

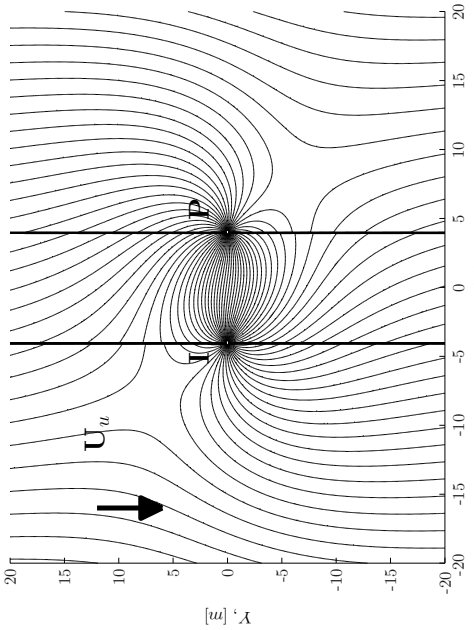

(d) $\alpha = 3\pi/2$

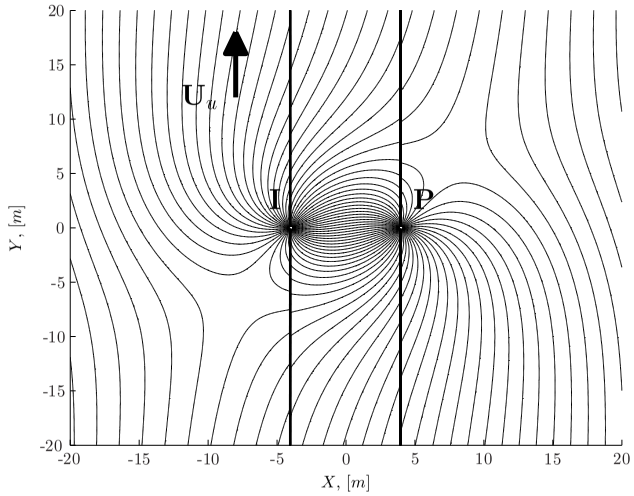

(e) $\alpha = \pi/2$

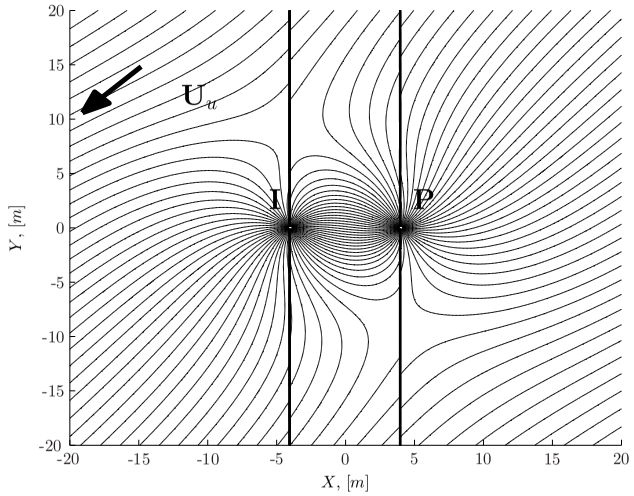

(f) $\alpha = 5\pi/4$

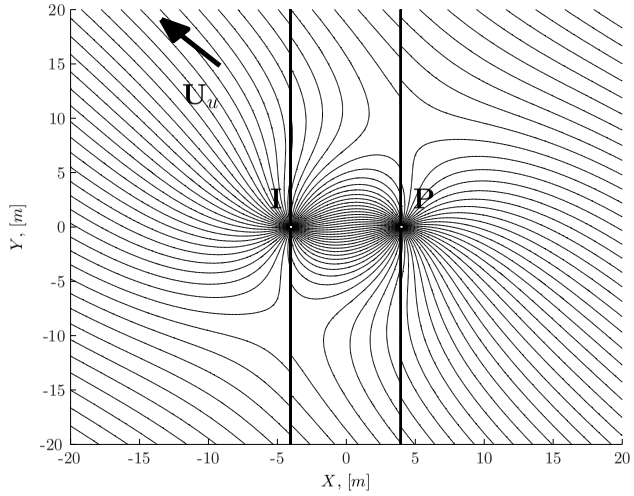

(g) $\alpha = 3\pi/4$

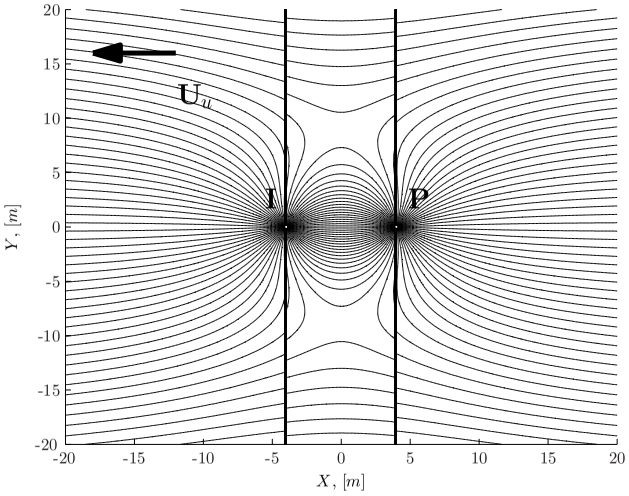

(h) $\alpha = \pi$

Figure 6.3: Two-well transmission test stream-line patterns. The impact of the natural drift direction α, where $\vec{U}_u = U_u(\hat{x}\cos\alpha + \hat{y}\sin\alpha)$. The vertical lines are due to the asymptotic behaviour of the arctan parts of Equation 6.1 and represent non-physical stream-line effects. This is also the cause of the "broken" stream-lines.

6.3 Conclusions

It has been seen, studying stream-line patterns, that two-well transmission tests might be sensitive to natural drift. In addition to the injector/producer strength ratio, the direction of the drift, in relation to the axis on which the test wells lie, is of great importance for the interpretation of the test results. Only for a natural drift going in the injector-producer direction, and only for $Q_i \leq |Q_p|$, are all injector stream-lines connected to the producer, and all the injectant may be recovered.

Before a two-well transmission test is designed one should fully understand the flow regime, else a test where the injector and the producer are not connected by any stream-lines at all can accidentally be designed, and no injectant will be recovered, whatsoever.

The mathematics of the two-well transmission test stream-line based problem is more complex than that of the single-well push-pull test, and it might not be possible finding an analytical solution to the problem. The problem may, however, be solved numerically by applying the same ideas as for the single-well push-pull test, tracing the injectant fronts along each stream-line. For the two-well test, in addition to a time of clean water break-through, a time of injectant break-through must be calculated for each stream-line, relating the problem to the single-well test problem where a drift/residence phase is included in-between the injection and production phases.

References

[1] K. H. Coats, C.H. Whitson, and L.K. Thomas. Modelling conformance as dispersion. SPE Annual Technical Conference and Exhibition, 26-29 September, Houston, Texas, September 2004. SPE 90390.

[2] J.F. Pickens and G.E. Grisak. Scale-dependent dispersion in a stratified granular aquifer. *Water Resources Research*, 17(4):1191–1211, 1981.

[3] The Coats Engineering web page. http://www.coatsengineering.com, 2006.

[4] F.M. White. *Fluid Mechanics*. McGraw - Hill, New York, USA, 5th edition, 2003.

Further Work

- In some cases of push-pull tests, it might be desireable to include a *drift phase* between the injection and production phases, where the injectant plume is allowed to drift naturally with the in situ water without being affected by any induced pressure gradient, [1]. This to increase the residence time of the test solution in the aquifer and allow more time for reactions to proceed. The program code developed along with this thesis does presently not allow for this option. It should, however, not be too difficult implementing this possibility, by letting the stream-line end-points move linearly with the natural drift for some time, before tracing them back to the test well.
  Similarly, it should be possible to introduce the possibility of varying injection/production rates.
  Both ideas would require a kind of "rubber band" geometry of the injectant front. The "rubber band" should not be broken, or the methodology will not work, since this implies more advanced flow regimes. It should also be taken care to keep the test well inside the "rubber band". If the test-well is allowed outside of the injectant covered area,as is actually the case for the two-well test, more advanced approaches must be applied, as there will also be a time of injectant break-through.

- Presently the possibility of modelling deterioration of the injectant tracer content, by radioactive decay, adsorption, chemical or physical reaction, or by any other mechanism, is not included. The tracer is assumed to be ideal, but adding this possibility in the program could prove useful.

- Throughout this work, the physical dispersion and diffusion has been assumed negligible, and there is no possibility of modelling these effects in the present model. By applying the one-dimensional convection-dispersion equation along each stream-line, however, it might be possible to model this as well.

- Two-well transmission tests are also common field tests conducted all over the world. These tests are also readily visualised and modeled using stream-lines, superposing a source and a sink some distance apart, in a uniform flow field, [2]. The mathematics of the front-tracking part, however, becomes significantly more complicated than in the single-well test case, and no great effort has been put into this problem during this study. As for the single-well test, including a drift phase, a time for injectant break-through, in addition to a time of clean water break-through, will be required for each stream-line. The equations developed, but not solved in this thesis, could possibly be solved applying numerical mathematical techniques.

References

[1] Young Kim, Mohammad Azizian, Jonathan Istok, and Lewis Semprini. *Field Push-Pull Test Protocoll for Environmental Security Technology Certification Program*. Oregon State University, Civil, Construction, and Environmental Engineering Department, Corvallis, OR 97331, April 2005.

[2] F.M. White. *Fluid Mechanics*. McGraw - Hill, New York, USA, 5th edition, 2003.

Conclusions

Introducing scale-dependency, velocity dependency, etc., just to cling to the current explanation model, seems like desperation not uncommon in the history of science. Based on the arguments given in this thesis, however, it is believed we need to think again. It is time for a change of paradigm in the well-testing science. The current use of the one-dimensional convection-dispersion equation should be discarded, and well-testing engineers and scientists should consider natural ground-water drift as more important than physical dispersion.

The method of considering ground-water drift will not only explain, in a better way, the current single-well and two-well tests being performed, but it can also be used to assess the ground-water drift in an aquifer. This can prove interesting in many study areas, such as CO_2 sequestration in saline aquifers and transport of contamination, by the ground-water, e.g. salt-water intrusion in fresh-water supplies or transport of environmentally hazardous substances. An important application, for the oil industry, is predicting tilted water-oil-contacts, as a consequence of dynamic aquifers below the oil-zone. Neglecting a tilted WOC may result in an inaccurate estimate of the amount of initial oil in place. Knowing, or assuming, the natural drift velocity, the method proposed may be employed to assess the permeability and/or the porosity of the aquifer, as well.

The main conclusions, related to single-well push-pull tests, from the study reported in this thesis, are:

Paper I

1. In an entirely dispersion free model, it has been shown that real experimental data may be matched well even though apparent dispersivity is large.

2. It has been shown analytically, in an over-simplified reservoir model, that natural drift alone may cause a big part of the apparent dispersivity reported by Pickens and Grisak.

3. The analytically calculated times for clean water break-through and end time of tracer production and the semi-analytical calculations in-between show good agreement with results from numerical simulations run by Coats *et al*, and stream-line based simulation results obtained from Streamsim's 3DSL.

Paper II

1. For injection phase durations, T_i, larger than some critical time, T_c, the tracer production is not conservative, and the Convection-Dispersion equation will no longer fit the tracer producing concentration profile well.

2. For $T_i < T_c$, the Peclet number plots linearly vs. T_i in a log-log diagram, using the SW1 and SW2 test parameters.

3. A strong scale dependency of the apparent dispersivity has been found even though the physical dispersivity of the model per definition is zero.

4. The apparent dispersivity resulting from fitting the one-dimensional convection-dispersion equation cannot be expected to be a measure of the physical dispersivity.

Paper III

1. Time of break-through is not affected by layering in an aquifer with no natural drift.

2. Both time of clean water break-through and end-time of tracer production is affected by layering in the presence of natural groundwater drift.

3. Introducing layering and applying the layering data reported by Pickens and Grisak, it is possible to get an exact match to the experimental data, including the characteristic oscillating behaviour of the production profile. Thus it may be concluded that the oscillations are effects of the stratification of the test-site in combination with the natural drift.

4. In a model free of physical dispersion, it is shown that a model combining groundwater drift and layering heterogeneity may yield a perfect match to production profiles showing large apparent dispersivity.

Chapter 2

1. For injection rates dominating over the natural drift, the no-drift approximation is equivalent to doing a Taylor expansion of the second order, around the well-radius, of the exact up-gradient radial advancement expression, thus being valid for small radial advancements only.

2. For the Pickens-Grisak SW2 test parameters, a thousand stream-lines is sufficient to get an effectively converged production profile.

Chapter 3 - 5

1. Even though numerical dispersion related to the grid refinement, in the Coats *et al.* radial SENSOR model, was minimised and effectively removed,

the model results show some unaccounted-for dispersion compared to the dispersion-free analytical model results.

2. Single-well push-pull "echo" tests are not readily modeled using available commercial simulators, from Coats Engineering, Sensor (FD) and, from Streamsim, 3DSL (SL).

Chapter 6

1. It has been seen, studying stream-line patterns, that two-well transmission tests are sensitive to natural drift, also.

2. In addition to the injector/producer strength ratio, the direction of the drift, in relation to the axis on which the test wells lie, is of great importance for the interpretation of the test results.

3. Only for a natural drift going in the injector-producer direction, and only for $Q_i \leq |Q_p|$, are all injector stream-lines connected to the producer.

4. Unless the natural flow regime is understood, a test where the injector and the producer are not connected by any stream-lines at all can accidentally be designed, and no injectant will be recovered, whatsoever.

Part IV

Appendix

APPENDIX A

SENSOR Input Deck

A.1 Introduction

In [1], Coats *et al.* showed, using the finite difference simulator SENSOR, [2], that the apparent dispersivity in single-well push-pull tests may to a large extent be caused by natural drift of the ground-water. The SW2 SENSOR input deck employed by Coats *et al.* is cited below.

References

[1] K. H. Coats, C.H. Whitson, and L.K. Thomas. Modelling conformance as dispersion. SPE Annual Technical Conference and Exhibition, 26-29 September, Houston, Texas, September 2004. SPE 90390.

[2] The Coats Engineering web page. http://www.coatsengineering.com, 2006.

A.2 Input Deck

```
TITLE
 sw2.dat

    SW2 hydraulic gradient r-theta  dp/dx=.00232 psi/ft
    1000x25x1

ENDTITLE

GRID 1000 25 1

RADIAL
 5
 .17 20. 1405.
 25*7.2

ILU 2 1 1
MAPSPRINT 1 P TRACER  KX  PV TX TY
MAPSFORM 4 P
CPU

C      Bwi    cw   denw   visw  cr   pref
MISC   1.    3.e-6   62.4     1.  4.e-6   5000

SWINIT CON
  1
```

```
TRACEREXPL 1   ! TREAT WELL TERMS EXPLICITLY IN TRACER CONCENTRATIONS
               !(DEFAULT IS IMPLICIT)

TRACER
   2  WATR

C  DEFAULT INITIAL TRACER FRACTIONS ARE 0 1

PVTBO 1
C          #/cuft stoil  #/scf gas
 DENSITY      53.00        .0624
 PRESSURES  1  2    ! nsat  ntot
 300.    6000.      ! psia

 PSAT      P       BO    VISO
   300.   300.    1.0000   .5
         6000.    1.0000    .5

KRANALYTICAL
 .2  .2 .2 0.   ! Swc  Sorw  Sorg  Sgc
  1. 1. 1.      ! krwro krgro krocw
  2 2 2 2       ! nw now ng nog

THICKNESS CON
 1.
DEPTH  CON
 5000
KX CON
  14800.
KY  EQUALS KX
KZ  EQUALS KX
POROS  CON
 .38
INITIAL
  PINIT 5000
  ZINIT 5000.5
ENDINIT         !  end of Initial Data


WELL
   I J K
 WINJ                  !    wellname
 1 1 1
 1 2 1
 1 3 1
 1 4 1
 1 5 1
 1 6 1
 1 7 1
```

```
 1 8 1
 1 9 1
 1 10 1
 1 11 1
 1 12 1
 1 13 1
 1 14 1
 1 15 1
 1 16 1
 1 17 1
 1 18 1
 1 19 1
 1 20 1
 1 21 1
 1 22 1
 1 23 1
 1 24 1
 1 25 1
 PROD
 1 1 1
 1 2 1
 1 3 1
 1 4 1
 1 5 1
 1 6 1
 1 7 1
 1 8 1
 1 9 1
 1 10 1
 1 11 1
 1 12 1
 1 13 1
 1 14 1
 1 15 1
 1 16 1
 1 17 1
 1 18 1
 1 19 1
 1 20 1
 1 21 1
 1 22 1
 1 23 1
 1 24 1
 1 25 1
WINJA
 1000 25 1
PRODA
 1000 1 1
WELLTYPE
```

```
  WINJ   STBWATINJ
  PROD   STBLIQ
  WINJA  STBWATINJ
  PRODA  STBLIQ
BHP
 WINJA 5001.05
 PRODA 4998.95
RATE
 WINJ 7.25
 WINJA 1.E20
 PRODA 1.E20

CFL 1.

 MAPSFREQ 100
 STEPFREQ 10
 WELLFREQ 10

WELLTRACER
  WINJ  WATR
        1 0  ! inject tracer fraction 1
  WINJA WATR
       0 1

TIME 3.93
RATE
 WINJ -1
 PROD  6.1105
TIME 8.5929
TIME 13.256
END


TITLE
  500x25x6
ENDTITLE

GRID 500 25 6

RADIAL
 5
 .17 26. 1405.
 25*7.2

 ILU 2 1 1
MAPSPRINT 1 P TRACER  KX  PV TX TY DEPTH
MAPSFORM 4 P
CPU
```

```
C      Bwi    cw   denw   visw  cr   pref
MISC   1.    3.e-6   62.4     1.  4.e-6   5000

SWINIT CON
  1

TRACEREXPL 1   ! TREAT WELL TERMS EXPLICITLY IN TRACER CONCENTRATIONS
               !(DEFAULT IS IMPLICIT)

TRACER
   2  WATR

C  DEFAULT INITIAL TRACER FRACTIONS ARE 0 1

PVTBO 1
C          #/cuft stoil  #/scf gas
 DENSITY      53.00        .0624
 PRESSURES  1  2    ! nsat  ntot
 300.    6000.      ! psia

 PSAT      P       BO    VISO
   300.   300.    1.0000   .5
         6000.    1.0000    .5

KRANALYTICAL
 .2  .2 .2 0.   ! Swc  Sorw  Sorg  Sgc
  1. 1. 1.      ! krwro krgro krocw
  2 2 2 2       ! nw now ng nog

THICKNESS ZVAR
 .389 .1667 .1111 .1111 .0556 .1667
KX ZVAR
  .453 .865 .7485 1. .943 .612
  MOD
   1 500  1 25  1 6 * 22119.

DEPTH  CON
 5000
KY  EQUALS KX
KZ  CON
   0.
POROS  CON
 .38
INITIAL
  PINIT 5000
  ZINIT 5000.5
ENDINIT         !  end of Initial Data

MODIFY DEPTH
```

```
  1 500 1 25  1 6 = 5000.5
WELL
   I J K1 K2
 WINJ                    !    wellname
 1 1 1 6
 1 2 1 6
 1 3 1 6
 1 4 1 6
 1 5 1 6
 1 6 1 6
 1 7 1 6
 1 8 1 6
 1 9 1 6
 1 10 1 6
 1 11 1 6
 1 12 1 6
 1 13 1 6
 1 14 1 6
 1 15 1 6
 1 16 1 6
 1 17 1 6
 1 18 1 6
 1 19 1 6
 1 20 1 6
 1 21 1 6
 1 22 1 6
 1 23 1 6
 1 24 1 6
 1 25 1 6
 PROD
 1 1 1 6
 1 2 1 6
 1 3 1 6
 1 4 1 6
 1 5 1 6
 1 6 1 6
 1 7 1 6
 1 8 1 6
 1 9 1 6
 1 10 1 6
 1 11 1 6
 1 12 1 6
 1 13 1 6
 1 14 1 6
 1 15 1 6
 1 16 1 6
 1 17 1 6
 1 18 1 6
 1 19 1 6
```

```
 1 20 1 6
 1 21 1 6
 1 22 1 6
 1 23 1 6
 1 24 1 6
 1 25 1 6
WINJA
 500 25 1 6
PRODA
 500 1 1 6
WELLTYPE
  WINJ   STBWATINJ
  PROD   STBLIQ
  WINJA  STBWATINJ
  PRODA  STBLIQ
BHP
 WINJA 5001.28
 PRODA 4998.72
RATE
 WINJ 7.25
 WINJA 1.E20
 PRODA 1.E20

DT -.005512 ! CFL 1

 MAPSFREQ 100
 STEPFREQ 10
 WELLFREQ 10

WELLTRACER
  WINJ  WATR
        1 0  ! inject tracer fraction 1
  WINJA WATR
       0 1

TIME 3.93
RATE
 WINJ -1
 PROD  6.1105
TIME 8.5929
TIME 13.256
END
```

APPENDIX B

3DSL Input Deck

B.1 Introduction

In Chapter 4, the search for a single-well push-pull test model, using Streamsim's, [2], stream-line based commercial simulator, 3DSL, [1], was described. Here is presented the 3DSL input deck representing the best solution that could be found.

References

[1] Streamsim Technologies, Inc. *3DSL User Manual - ver. 2.30*, December 2005. Available at: http://www.streamsim.com.

[2] The Streamsim web page. http://www.streamsim.com, 2006.

B.2 Input Deck

```
- ------------------------------------------------------------
- Single-well push-pull test in a naturally flowing aquifer.
- ------------------------------------------------------------
-
- A (I,J,K) 601x601x1 grid with no-flow boundaries and no inactive cells
- is initiated with a homogeneous fractional porosity of 0.38,
- and a permeability of 14.8 darcy, at 150 kPa uniform pressure,
- and the in situ fluid is "water".
- The grid is based on a 201x201 homogeneous cell size grid of
- 4.6x4.6x8.2 m3.
- Local refinement of the center of the grid has been done,
- such that the grid cells have dimensions 0.1x0.1x8.2 m3.
- Horisontal wells at I=1 and I=601, spanning the width of
- the reservoir, J=1-601, on BHP control ensures a natural
- pressure gradient of ~0.052 kPa/m.  The inecting well is
- injecting the in situ fluid, "water".
- In the middle of the model, I=301, J=301, a test well is located.
- The test well, on rate control, injects "oil" for a certain period,
- then the well starts producing.
- Using the TRACER option, the only difference beween the different
- fluid phases, are their names.  All PVT properties are
- identical.



RUNOPTIONS
   TITLE='Single-well push-pull test in a naturally flowing aquifer.'
```

```
   UNITS=METRIC          !input and output data in metric units
   MODEL=TRACER          !oil, gas and water phases have identical properties
END RUNOPTIONS


GRID
    NX=601               !number of grid cells in the x-direction (I)
    NY=601               !number of grid cells in the y-direction (J)
    NZ=1                 !number of grid cells in the z-direction (K)

    POROSITY
        0.38 /           !fractional porosity

    PERMX
        14800 /          !x-directional permeability, [mD]
    PERMY=PERMX
    PERMZ=PERMX

    DXV
        96*4.6 409*0.1 96*4.6/  !grid cell x-directional size, [m]
    DYV
        96*4.6 409*0.1 96*4.6/  !grid cell y-directional size, [m]
    DZV
        8.2 /                   !grid cell z-directional size, [m]
END GRID


PVT
    SCDENSITIES
        1.0   1.0   1.0 /       !oil, gas and water densities @ SC, [kg/m3]
    CVISCOSITIES
        1.0   1.0   1.0 /       !oil, gas and water viscosity @ SC, [cp]
END PVT


INITIALCOND
    ZINIT
        0 0 1 /          !initial oil, gas and water saturation
    PINIT
        150 /            !initial reservoir pressure
END INITIALCOND


OUTPUT
    3DSLFMT= on          !3DSL ASCII output on
    sat=1                !output grid saturation data at every time-step
    slines=-1            !output stream-line grid coordinates at every
                         !explicit TIME key-word.
    slfreq=1             !output data for every stream-line
```

```
END OUTPUT


RECURRENT
    WELLS               !define well name, type, direction, location, diameter
       NAME=TOP     TYPE=I  DIR=Y   I=1     J=1-601 K=1
       NAME=BOTTOM  TYPE=P  DIR=Y   I=601   J=1-601 K=1
       NAME=INJ     TYPE=I  DIR=Z   I=301   J=301   K=1  DIA=0.001
       NAME=PROD    TYPE=P  DIR=Z   I=301   J=301   K=1  DIA=0.001
    /

    TUNING3D            !3D level simulation run tuning
        DVOLMAX=1 DPVMAX=0.5 DTMAX=500
    END

    TUNING1D            !1D level simulation run tuning
        CFL=0.99 NODESMAX=100000
    END

    -Start the injection phase
    TIME=0

        -horizontal well performance, inject "water"
        NAME=TOP        BHP=173.907 ZWAT=1.0
        NAME=BOTTOM     BHP=126.093

        -Test well performance, inject "oil"
        NAME=INJ        RTRAT=62.12 ZOIL=1.0  ![sm3/day]

    -Start the production phase
    TIME=3.93  NT=30   !do NT time-steps before next TIME key-word

        -Test well performance
        NAME=INJ        SHUT
        NAME=PROD       RTRAT=52.36 ![sm3/day]

    -End of test
    TIME=13
END
```

APPENDIX C

MatLab Source-codes

C.1 Introduction

The following sections include the basis of the MatLab source-codes used to generate the plots presented in this thesis.
"MATLAB is a high-level language and interactive environment that enables you to perform computationally intensive tasks faster than with traditional programming languages such as C, C++, and Fortran." (The MathWorks homepage,[1]).
The program was developed on a Microsoft Windows XP sp2 operating system, using MatLab version 7.1.0.246 (R14) sp3. For details, see the compact disc documentation in Appendix C, and the MathWorks homepage, [1].

The source-codes consist of the PushPullTestModel.m file, being the main body of the program, and several function files that should be located in the relative path */Functions/*. In addition, the main.m file can be used to generate output tables for the MatLab user interface.

References

[1] The MathWorks web page.
http://www.mathworks.com, 2006.

C.2 main.m

This file should be run to generate output tables for the MatLab user interface, from the PushPullTestModel.m file.

```
1 %calls the Push-Pull Test production profile solver.
2 %ATTENTION:
3 %appropriate changes must be applied to the beginning of the
4 %PushPullTestModel.m file.
5
6 %over all production profile is stored in the vectors
7 %ResTBTvecSorted and ResHistvec.
8 %Individual layer production profiles are stored in the matrices
9 %TBTmatrix and Histmatrix.
10
11 [TBTmatrix,Histmatrix,ResTBTvecSorted,ResHistvec] = PushPullTestModel;
```

C.3 PushPullTestModel.m

Main body of the model calculations.

```
%#function ReadInput, calcProdProfile, MakeFile, MakePlots, rm1, rmN,
thetaI, thetam, SW1TestParam, SW2TestParam, TstTestParam
%function [TBTmatrix,Histmatrix,ResTBTvecSorted,ResHistvec] = PushPullTestM
                                                                odel
%function PushPullTestModel
clear all;                      %clean slate
close all hidden;                %close all figure windows
warning off                      %ignore warnings
if not(isdeployed)
    clc;                         %clear matlab command window
    addpath('Functions');        %add the subdirectory functions do the
            matlab work path
end
global rw Ti
%%MATLAB model predicting producing tracer concentration profiles
%%in push-pull "Echo" tests.
%%produced for and published in the PHD dissertation
%%of Sverre Gullikstad Johnsen
%%2003-2006
%%---------------------------------
%%
%%M-file produces plots of the producing tracer concentration cs.
%%dimensionless volume produced, Vp/Vinj,tot.
%%---------------------------------

%%---------------------------------
%%Input file information
%%---------------------------------
%%Input files are located in the sub directory InputData.
%%Input data should include test paramters and layering data.

%%Test paramter data must be on the form (fill inn the missing numbers).
%% qi=    ;% [l/s]     Injection rate
%% qp=    ;% [l/s]     Production rate (absolute value)
```

```
35 %% Ti=    ;% [days]    Total time of injection
36 %% rw=    ;% [m]       Well radius
37 %% dP=    ;% [kPa/m]   natural pressure gradient
38 %% visc=  ;% [cp]=[1E-3 Pa s] Water viscosity
39
40 %%Layering data must be on the form (Two first lines are required):
41 %%  k1  por1    h1
42 %%  k2  por2    h2
43 %%  ...
44 %%  kM  porM    hM
45 %%---------------------------------
46
47
48 %%---------------------------------
49 %%Output file information
50 %%---------------------------------
51 %Output is stored in the directory OutputData, and files are named
52 %according to the date and time they are run.
53 %Data stored includes:
54 %   1.  Date and time of the run
55 %   2.  Test parameters used
56 %   3.  Layering data used
57 %   4.  Reservoir production profile data
58
59
60
61 %%---------------
62 %%Choose experiment
63 %%---------------
64     proceed=0;
65     while proceed==0
66         Experiment = input('Which experiment? (SW1, SW2, Tst=default):',
67                            's');
68         if (isempty(Experiment))
69             Experiment='Tst';
70         end
71         if strcmp(Experiment,'sw1')
72             Experiment='SW1';
73         elseif strcmp(Experiment,'sw2')
74             Experiment='SW2';
75         elseif strcmp(Experiment,'tst')
```

```
76              Experiment='Tst';
77          end
78          if  strcmp(Experiment,'SW1')  || strcmp(Experiment,'SW2') ||
79                      strcmp(Experiment,'Tst')
80              proceed=1;
81          else
82              error('The requested experiment doesnt exist.');
83          end
84      end
85
86
87
88
89
90  %%---------------
91  %%Input datafiles
92  %%---------------
93      [N,qi,qp,Ti,rw,dP,visc, Layering, ExpProfile,NumProfile] = ReadInput(
94                                                                  Experiment);
95
96
97
98  %%---------------
99  %%Geological data preparation
100 %%---------------
101
102     kj=Layering(:,1)                    ;%Layer permeability
103     porj=Layering(:,2)                  ;%Layer porosity
104     hj=Layering(:,3)                     ;%Layer height
105     h=sum(hj)                            ;%Total reservoir height
106     M=length(hj)                         ;%Total number of layers
107
108     kA=sum(kj.*hj)/h                     ;%Arithmetic average permeability
109     porA=sum(porj.*hj)/h                 ;%Arithmetic average porosity
110
111     Cj=porA./porj.*kj/kA                 ;%Layerwise heterogeneity scaling
112        factor
113
114
115
116 %%---------------
```

```
117 %%Summarize data on the screen
118 %%---------------
119     disp(' ------------------------------');
120     disp('|   Push-Pull "Echo" Test Tracer Production Profile Solver   |');
121     disp('|                Sverre Gullikstad Johnsen                   |');
122     disp('|                       2003-2006                            |');
123     disp(' ------------------------------');
124     disp('                                                             ');
125     disp(' ------------------------------');
126
127     disp(['| Number of stream-lines: ' num2str(N) '
128          |']);
129     if strcmp(Experiment,'SW1')
130         disp('| Experiment:             Pickens-Grisak SW1
131              |');
132     elseif strcmp(Experiment,'SW2')
133         disp('| Experiment:             Pickens-Grisak SW2
134              |');
135     elseif strcmp(Experiment,'Tst')
136         disp('| Experiment:             Custom test
137              |');
138     end
139     disp(' ------------------------------');
140     disp(['| Number of Layers:       ' num2str(M,2) '
141          |']);
142     disp(['| Average permeability:   ' num2str(kA,4) ' darcy
143          |']);
144     disp(['| Average porosity:       ' num2str(porA*100) ' %
145          |']);
146     disp(' ------------------------------');
147     disp(['| Injection phase duration:    ' num2str(Ti) '    days
148          |']);
149     disp(['| Injection rate:              ' num2str(qi) '   l/s
150          |']);
151     disp(['| Production rate:             ' num2str(qp) '   l/s
152          |']);
153     disp(['| Natural pressure  gradient:  ' num2str(dP) '   kPa/m
154          |']);
155     disp(' ------------------------------');
156     disp('                                                             ');
157
```

```
158     proceed=0;
159     while proceed==0
160         reply = input('Is it ok to proceed? (Y=default, N):','s');
161         if (isempty(reply))
162             reply='Y';
163         end
164         if (reply~='Y' && reply~='N')
165             proceed=0;
166         end
167         if (reply=='N' || reply=='n')
168             return;
169         end
170         if (reply=='Y' || reply=='y')
171             proceed=1;
172         end
173     end
174
175
176
177 %%---------------
178 %%Calculations
179 %%---------------
180     options = optimset('Display','off','FunValCheck','off');        %give
181               no warnings when fzero terminates unexpectedly
182     t=cputime;
183
184
185     %We want an odd number of stream-lines
186     if mod(N,2)==0
187         N=N+1;
188     end
189
190     %prepare matrices to store layerwise data
191     TBTmatrix=zeros(M,N);
192     Histmatrix=zeros(M,N);
193     ResTBTvec=[];
194     Volrate=[];
195     LostInLayer=[];
196
197     %reformulate the 3-dimensional injection/production rates
198     qi3D=qi*3600*24/1000;          %[l/s]->[m3/day]
```

```
199     qi2D=qi3D/h;                    %[m2/day]        2D injection rate
200     qp3D=qp*3600*24/1000;           %[l/s]->[m3/day]
201     qp2D=qp3D/h;                    %[m2/day]        2D production rate
202
203     %Layerwise natural drift velocity
204     Uuj=(3600*24)*dP*1e3*9.869e-13*kj./(visc*1e-3*porj);%[m/day]
205
206
207
208     %%---------------
209     %for every layer, find the production profile
210     %individual layer profiles are stored in the matrices TBTmatrix and
211     %Histmatrix, so that individual layer profiles may be plotted.
212     %Each layer profile is appended to the vectors ResTBTvec and Volrate.
213     for j=1:M
214         [lost,Volrate,ResTBTvec,TBTmatrix,Histmatrix] = calcProdProfile(qi,
215                                                         qi2D,qp,qp2D,porA,
216                                                         hj,j,Cj,Uuj,M,N,
217                                                         options,ResTBTvec,
218                                                         Volrate,TBTmatrix,
219                                                         Histmatrix);
220         if strcmp(lost,'yes!')
221             LostInLayer=[LostInLayer j];
222         end
223     end
224     %%---------------
225
226
227     %Order the elements of ResTBTvec and Volrate.
228     [ResTBTvecSorted, order]=sort(ResTBTvec);
229     VolrateSorted=Volrate(order);
230
231
232     %generate normalised histogram of  tracer inflow
233     ResHistvec(1)=1-VolrateSorted(1)/qp3D;
234     for i=2:length(ResTBTvecSorted)
235        ResHistvec(i)=ResHistvec(i-1)-VolrateSorted(i)/qp3D;
236                    %rateAddedSorted(i)/J;
237     end
238
239
```

```
240
241
242
243
244 %%---------------
245 %%Making plots
246 %%---------------
247     %Generate figure
248     MakePlots(Experiment,ResTBTvecSorted,ResHistvec,ExpProfile,NumProfile);
249
250     %Generate output file
251     [success,message,filename] = MakeFile(N,qi,qp,visc,dP,kA,porA,Layering,
252                                  Ti,rw,Experiment,ResTBTvecSorted,
253                                  ResHistvec,LostInLayer);
254
255
256
257
258 %%---------------
259 %%Write report to screen
260 %%---------------
261     disp('                                                              ');
262     disp(' -------------------------------');
263     disp('| FINAL REPORT                                                |')
264          ;
265     disp(' -------------------------------');
266     disp(['| cpu-time spent:    ' num2str(cputime-t,4) ' s
267          |']);
268     disp('|                                                             |')
269          ;
270     disp(['| Time of Break-Through (Vp,tbt/Vinj.tot):           ' num2str(
271          ResTBTvecSorted(1),3)   '     |']);
272     if strcmp(lost,'yes!')
273         disp('| Tracer was lost in and the production profile approaches
274              |');
275         disp('| 0 assymptotically.
276              |');
277     else
278         disp(['| End-time of Tracer Production (Vp,eop/Vinj.tot):   '
279              num2str(ResTBTvecSorted(length(ResTBTvecSorted)),3) '     |'])
280              ;
```

```
281     end
282     disp('|                                                          |')
283          ;
284     if success && isempty(message)  %If output directory and file was
285                             created
286         disp('| Production profile data are stored in the file
287              |');
288         disp(['| ' filename '    |']);
289     else
290         disp('| Output data could not be stored.
291              |');
292         disp('| If the program is run from a read-only medium, f.ex. a CD,
293              |');
294         disp('| it should be copied to the harddrive to enable data
295              storage.|');
296     end
297
298     disp(' ------------------------------');
299
300
301
302
303
304
305
306
```

C.4 Functions

The following functions should be put in the sub directory *Functions*.

ReadInput.m

Function used to read the input data.

```
1 function [N,qi,qp,Ti,rw,dP,visc, Layering, ExpProfile,NumProfile] = ReadInp
2                                                                     ut(
3                                                                     Experim
```

```
4                                                                    ent)
5 %Reads input parameters, experimental data and numerical simulation data.
6
7     if strcmp(Experiment,'SW1')
8         TestParam=load('InputData/SW1TestParam.dat');%load file containing
9                   test paramters
10        Layering=load('InputData/SW1LayeringData.dat');%load file
11                containing geological information about layering
12        ExpProfile=load('InputData/SW1PickensProfile.dat');%load the
13                   Pickens-Grisak prod.profile data
14        NumProfile=load('InputData/SW1CoatsProfile.dat')  ;%load the Coats
15                   et al. prod.profile data
16    elseif strcmp(Experiment,'SW2')
17        TestParam=load('InputData/SW2TestParam.dat');%load file containing
18                  test paramters
19        Layering=load('InputData/SW2LayeringData.dat');%load file
20                containing geological information about layering
21        ExpProfile=load('InputData/SW2PickensProfile.dat');%load the
22                   Pickens-Grisak prod.profile data
23        NumProfile=load('InputData/SW2CoatsProfile.dat')  ;%load the Coats
24                   et al. prod.profile data
25    elseif strcmp(Experiment,'Tst')
26        if exist('InputData\TstTestParam.dat','file')
27             TestParam=load('InputData/TstTestParam.dat');%load file
28                       containing test paramters
29        else
30            error('PushPull:noTestParam','\nNo test parameters were
31                  specified. \nSpecifiy test parameters in the file
32                  "InputData\\TstTestParam.m"');
33        end
34
35        if exist('InputData\TstLayeringData.dat','file')
36            Layering=load('InputData/TstLayeringData.dat');%load file
37                     containing geological information about layering
38        else
39            error('PushPull:noLayering','\nNo layering data provided.
40                  \nEven for the single layer solution, average perm. and
41                  por.\nas well as C1 and h1 must be provided.')
42        end
43
44        if exist('InputData\TstExpData.dat','file')
```

```
45              ExpProfile=load('InputData/TstExpdata.dat');%load experimental
46                          data
47          else
48              ExpProfile=[];
49              disp('No experimental data found.');
50              disp('Experimental data may be included in the file
51                   "InputData\TstExpData.dat"');
52          end
53
54          if exist('InputData\TstNumData.dat','file')
55              NumProfile=load('InputData/TstNumdata.dat');%load experimental
56                          data
57          else
58              NumProfile=[];
59              disp('No numerical simulation data found.');
60              disp('Numerical simulation data may be included in the file
61                   "InputData\TstNumData.dat"');
62
63          end
64      end
65
66
67       N= TestParam(1)    ;%                  Number of stream-lines traced in
each
68          layer
69       qi=TestParam(2)    ;% [l/s]         Injection rate
70       qp=TestParam(3)    ;% [l/s]         Production rate (absolute value)
71       Ti=TestParam(4)    ;% [days]        Total time of injection
72       rw=TestParam(5)    ;% [m]           Well radius
73       dP=TestParam(6)    ;% [kPa/m]       Natural pressure gradient
74       visc=TestParam(7)  ;% [cp]=[1E-3 Pa s] Water viscosity
```

calcProdProfile.m

Function used to track the injectant front and generate the production profile data.

```
1 function [lost,Volrate,ResTBTvec,TBTmatrix,Histmatrix] = calcProdProfile(
2                                                          qi,qi2D,qp,qp2D,
3                                                          porA,hj,j,Cj,Uuj,
```

```
4                                                          M,N,options,
5                                                          ResTBTvec,Volrate,
6                                                          TBTmatrix,
7                                                          Histmatrix)
8  global rstart rw Uu Ti Qi Qp psiinj psiprod Cinj i
9  %sub routine to calculate the production profile from a push-pull test
10 %in a single layer reservoir.
11 %for multi layer reservoirs, this routine is called for every layer.
12
13 disp(['Working on layer ' num2str(j) ' of ' num2str(M) '...']);
14
15 %Layer specific rates
16 Qi=qi2D/(2*pi*porA)*Cj(j);       %[m2/day]    Reformulated Injection Rate
17 Qp=qp2D/(2*pi*porA)*Cj(j);       %[m2/day]    Reformulated Production Rate
18    (absolute value)
19 Uu=Uuj(j);                      %[m/day]     Layer natural drift velocity
20
21
22 %reinitialize vectors
23 histweight=[];
24 rate=[];
25 TBTdimless=[];
26
27
28 %-----------
29 %Injection Phase
30 %-----------
31     %Angles at which stream-lines leave the well bore
32     thetaout=(0:pi/(N-1):pi);        %[rad]
33
34
35     %Stream-lines to trace during injection phase
36     psiinj=Uu*rw*sin(thetaout)+Qi*thetaout;
37
38     %Integration constant during injection
39     Cinj=-Uu*rw*cos(thetaout)-Qi*log(sin(thetaout));
40
41     %Find maximum radial advancement for theta=0 and theta=pi
42     thetamax(1)=0;
43     thetamax(N)=pi;
44     rmax=zeros(1,N);
```

```
45      rstart=sqrt(rw^2+2*Qi*Ti);
46      rmax(1)=fzero('rm1',rstart);
47      rmax(N)=fzero('rmN',rstart);
48
49      %Check if up-gradient rmax is valid
50      %rmax(N) cannot be larger than the dist to the stagnation point
51      rmaxboundupgrad=Qi/Uu;
52      while (rmax(N)>rmaxboundupgrad || rmax(N)<0)
53          rstart=rstart*0.99;
54          rmax(N)=fzero('rmN',rstart);
55      end
56
57      %Check if some injectant will be lost
58      rbound=Qp/Uu;
59      lost='nope';
60      if (rmax(1)>rbound) %if max down-stream radial pos. is greater than
61          rbound
62          disp(['Injectant will be lost in layer ' num2str(j) ' of ' num2str(
63              M) '.']);
64          lost='yes!';
65      end
66
67      %Find the angle and maximum radial advancement for each streamline at
68      the
69      %end of the injection phase
70      thetastart=thetaout;
71      for i=2:N-1
72         %Must demand that theta and rmax are monotone functions of psi
73         %Must demand that the fluid left the well-bore
74         while (rmax(i)<=rw)
75              thetamax(i)=fzero('thetam',thetastart(i),options);
76              %Check if all thetamax are numbers.  if NaN calculate again
77              with a
78              %new initial value
79              while (isnan(thetamax(i))==1)
80                  thetastart(i)=thetastart(i)*0.99;
81                  thetamax(i)=fzero('thetam',thetastart(i),options);
82              end
83              rmax(i)=(psiinj(i)-Qi*thetamax(i))/(Uu*sin(thetamax(i)));
84              %Check if the fluid left the well-bore, if not recalculate
85              with new
```

```
86              %initial angle value
87              if (rmax(i)<=rw)
88                  thetastart(i)=thetastart(i)*0.99;
89              end
90          end
91      end
92
93
94
95
96
97
98  %----------
99  %Production Phase
100 %----------
101
102     %calculate stream-line numbers to trace during production phase
103     psiprod=psiinj-(Qp+Qi)*thetamax;
104
105
106     %If injectant is lost, monitor the non-lost streamlines only.
107     %Assume sweep efficiency of remaining stream-lines is good enough
108     if strcmp(lost,'yes!')
109
110         %end-points with a psiprod<0 are recovered, while those with
111         psiprod>=0
112         %are lost
113         recovered=[];
114         for i=1:N
115             if psiprod(i)<0
116                 recovered=[recovered i];
117             end
118         end
119
120
121         %cut off all matrices so that only the i last entries are used in
122         %calculations plus one streamline for theta=0
123         N=length(recovered)+1;              %new number of streamlines to
124           trace
125         psiprod=[0 psiprod(recovered)];
126         thetamax=[0 thetamax(recovered)];
```

```
127
128         %we put the rmax(1) at angle theta=0 close to the stagnation point.
129         rmax=[Qp/Uu*(1-eps) rmax(recovered)];
130
131
132     end
133
134
135     %Calculate angle of arrival at rw
136     thetaintersec=zeros(1,N);
137     for i=2:N-1
138         thetastart=thetamax(i);
139         thetaintersec(i)=fzero('thetaI',thetastart);
140     end
141     thetaintersec(1)=0;
142     thetaintersec(N)=pi;
143
144     %Calculating time of break-through for each stream-line
145
146     %Integration constant
147     Cp=-Uu*rmax.*cos(thetamax)+Qp*log(sin(thetamax));
148
149     %time of break-through
150     TBT=1/Uu^2*(Cp+(Qp*thetaintersec+psiprod).*cot(thetaintersec)-Qp*log(
151         sin(thetaintersec)));
152     TBT(1)=1/Uu^2*(Uu*(rw-rmax(1))+Qp*log((Uu*rw-Qp)/(Uu*rmax(1)-Qp)));
153     TBT(N)=1/Uu^2*(Uu*(rmax(N)-rw)+Qp*log((Qp+Uu*rw)/(Qp+Uu*rmax(N))));
154
155
156     %Dimensionless time conversion
157     qiTOT=Ti*qi;            %   Total Volume Injected into the reservoir
158     TBTdimless(1:N)=qp*TBT/qiTOT;%   Dimensionless time vector
159
160
161     %Production Rate associated with each stream-line, Qp,n,j
162     %sum(rate)=pi*Qp
163     rate(1)=(psiprod(2)-psiprod(1))/2;
164     rate(N)=(psiprod(N)-psiprod(N-1))/2;
165     for i=2:N-1
166         rate(i)=(psiprod(i+1)-psiprod(i-1))/2;
167     end
```

```
168     rate=abs(rate);
169
170
171     %Layer specific histogram (normalised)
172     %Note that Qp is scaled by 2pi and that we are studying the half-plane
173     %only, hence, divide py pi*Qp not 2pi*Qp.
174     histweight(1)=rate(1)/(pi*Qp);
175     for i=2:N
176         histweight(i)=histweight(i-1)+rate(i)/(pi*Qp);
177     end
178
179
180     %Volumetric rate produced from each stream-line in current layer
181     %(assuming the "height" of each stream-line is hj)
182     %(pi is allready accounted for in the rate)
183     rate3D=2*porA*rate*hj(j);
184
185
186     %store layer specific production profile
187     TBTmatrix(j,1:N)=TBTdimless;
188     Histmatrix(j,1:N)=histweight;
189
190
191     %Append layer spesific data to the overall reservoir data
192     ResTBTvec=[ResTBTvec TBTdimless];
193     Volrate=[Volrate rate3D];
194
195
```

rm1.m

Function used to find the down-gradient maximum radial advancement.

```
1 function f = rm1(r)
2 global rw Qi Uu Ti
3
4 f=Uu*(r-rw)-Qi*log(abs(Uu*r+Qi)/abs(Uu*rw+Qi))-Uu^2*Ti;
```

rmN.m

Function used to find the up-gradient maximum radial advancement.

```
function f = rmN(r)
global Qi Uu Ti rw

if (Qi-Uu*r==0)
    r=r*0.9;
end

f = Uu*(r-rw)+Qi*log(abs(Qi-Uu*r)/abs(Qi-Uu*rw))+Uu^2*Ti;


```

thetaI.m

Function used to find the polar angle coordinate of the intersection point of the well-bore and a stream-line.

```
function f = thetaI(theta)
global psiprod Qp Uu rw i

f=rw*Uu*sin(theta)-psiprod(i)-Qp*theta;
```

thetam.m

Function used to find the polar angle coordinate of the injection-phase stream-line end point.

```
function f = thetam(theta)
global Qi psiinj Uu Ti Cinj i

f = (Qi*theta-psiinj(i))*cot(theta)-Qi*log(sin(theta))+Uu^2*Ti-Cinj(i);
```

MakePlots.m

Function used to generate plots.

```
function MakePlots(Experiment,ResTBTvecSorted,ResHistvec,ExpProfile,
                   NumProfile)
%generate production profile plots from a push-pull "echo" test

if strcmp(Experiment,'SW1')
    hold on
    plot (ExpProfile(:,1),ExpProfile(:,2),'ok')
    plot (NumProfile(:,1),NumProfile(:,2),'k','LineWidth',2)
    plot(ResTBTvecSorted,ResHistvec,'g','LineWidth',2)
    legend('Pickens & Grisak SW1 Field Test Data','Coats et al. Numerical
           Simulation Result','Semi-Analytical SW1 Model Data');
elseif strcmp(Experiment,'SW2')
    hold on
    plot (ExpProfile(:,1),ExpProfile(:,2),'ok')
    plot (NumProfile(:,1),NumProfile(:,2),'k','LineWidth',2)
    plot(ResTBTvecSorted,ResHistvec,'g','LineWidth',2)
    legend('Pickens & Grisak SW2 Field Test Data','Coats et al. Numerical
           Simulation Result','Semi-Analytical SW2 Model Data');
elseif strcmp(Experiment,'Tst')
    hold on
    plot(ResTBTvecSorted,ResHistvec,'g','LineWidth',2)
    legendstring='Semi-Analytical Model Data  ';
    %plot experimental data if they exist
    if exist('ExpProfile','var')==1 && not(isempty(ExpProfile))
        plot(ExpProfile(:,1),ExpProfile(:,2),'ok')
        legendstring=[legendstring;  'Experimental Field Test Data'];
    end
    %plot numerical simulation data if they exist
    if exist('NumProfile','var')==1 && not(isempty(NumProfile))
        plot(NumProfile(:,1),NumProfile(:,2),'k','LineWidth',2)
        legendstring=[legendstring; 'Numerical Simulation Data   '];
    end
    legend(legendstring);
end


xlabel('Dimensionless Time, V_{prod}/V_{inj,TOT}');
ylabel('Concentration, C');
axis([0 2 0 1.2]);
```

MakeFile.m

Function used to generate output data files.

```
function [success,message,filename] = MakeFile(N,qi,qp,visc,dP,kA,porA,
                                       Layering,Ti,rw,Experiment,
                                       ResTBTvecSorted,ResHistvec,
                                       LostInLayer)
%generate the output data file from the stream-line based
%semi-analytical push-pull test calculations


%If the OutputData directory does not exists create it
    if exist('OutputData','dir')~=7
        success=mkdir('OutputData');
        if not(success)
            disp('Output directory could not be created.');
            disp('If the program is run from a read-only medium,such as a
                 CD,');
            disp(' it should be copied to the hard drive to enable data
                 storage.');
        end
    else
        success=true;
    end


    %write the production profile to file
    if success  %if the OutputData directory exists
        filename=['OutputData/' Experiment '-ProdProfileData-' datestr(now,
                 'yyyy-mmmm-dd_HH.MM.SS') '.dat'];
        [fid,message] = fopen(filename, 'wt');

        if isempty(message)     %if the outputfile could not be opened for
                  writing
            fprintf(fid, '%%Stream-line based push-pull test production
                    profile\n');
            fprintf(fid, '%%generated from experiment "%s"\n', num2str(
                    Experiment));
            fprintf(fid, '%%the %s at %s.\n', num2str(date), num2str(
```

```
37                  datestr(rem(now,1))));
38          fprintf(fid, '%%------------------------
39                  ----------\n\n');
40          fprintf(fid, '%%Test parameters used were:\n\n');
41          fprintf(fid, '%%N=   %6.0f \n', N);
42          fprintf(fid, '%%qi=\t%6.3f [l/s]\n', qi);
43          fprintf(fid, '%%qp=\t%6.3f [l/s]\n', qp);
44          fprintf(fid, '%%Ti=\t%6.3f [days]\n', Ti);
45          fprintf(fid, '%%rw=\t%6.3f [m]\n', rw);
46          fprintf(fid, '%%dP=\t%6.3f [kPa/m]\n', dP);
47          fprintf(fid, '%%visc=\t%6.3f [cp]\n\n', visc);
48          fprintf(fid, '%%------------------------
49                  ----------\n\n');
50          fprintf(fid, '%%Tracer recovery:\n\n');
51          if isempty(LostInLayer)
52              fprintf(fid, '%%All the injected tracer was recovered.
53                      \n\n');
54          else
55              fprintf(fid, '%%Tracer was lost in layers \n');
56              fprintf(fid, '%%                          %4.0f.\n',
57                      LostInLayer);
58          end
59          fprintf(fid, '\n%%------------------------
60                  -----------\n\n');
61          fprintf(fid, '%%Average permeability was %6.3f darcy.\n', kA);
62          fprintf(fid, '%%Average porosity was     %4.1f%%.\n\n',
63                  porA*100);
64          fprintf(fid, '%%Layering data used were:\n\n');
65          fprintf(fid, '%%Perm.\t Por.\t height\n\n');
66          fprintf(fid, '%%%6.3f  %4.3f\t%6.3f\n', [Layering(:,1);
67                  Layering(:,2); Layering(:,3)]);
68
69          fprintf(fid, '\n\n%%----------------------
70                  ------------\n');
71          fprintf(fid, '%%------------------------
72                  ----------\n');
73          fprintf(fid, '\n%%Production profile data:\n\n');
74
75          fprintf(fid, '%%Dim.less Volume                         \n');
76          fprintf(fid, '%%Produced,\t\t Producing Fractional\n');
77          fprintf(fid, '%%Vp/Vinj,tot\t\t Tracer Concentration\n\n');
```

```
78              fprintf(fid, '%12.9f\t\t %12.10f\n', [ResTBTvecSorted;
79                      ResHistvec]);
80          end
81      end
82
83      fclose('all');
```

APPENDIX D

The Software Compact Disc

D.1 Introduction

Provided with this copy of the thesis, or obtainable upon request, is a compact disc containing an executable of the MatLab, [3] source code cited in Appendix B. Included on the compact disc, is also the MatLab Runtime Environment needed to run the executable, unless MatLab is already installed on the system.
The soft-ware is installed and run from an intuitive menu based user interface.

The compact disc contains two modelling examples, using the Pickens-Grisak SW1 and SW2 test parameters, [2], as well as their reported layering data. Running the stream-line based model, the stream-line based model production profiles are compared to the Pickens-Grisak experimental data as well as the SENSOR simulation results obtained by Coats *et al.*, [1].
Using the compact disc soft-ware, it is also possible to design a custom built simulation, using custom test parameters and layering data. It is possible to input experimental and/or simulation data to compare with the stream-line based model results, as well.

The compact disc should auto run as it is inserted into the cd-rom, and an installation menu should appear. The soft-ware was developed on and for a Windows XP system, however, and might not run smoothly on other systems.

The compact disc documentation is cited in Section D.2.

References

[1] K. H. Coats, C.H. Whitson, and L.K. Thomas. Modelling conformance as dispersion. SPE Annual Technical Conference and Exhibition, 26-29 September, Houston, Texas, September 2004. SPE 90390.

[2] J.F. Pickens and G.E. Grisak. Scale-dependent dispersion in a stratified granular aquifer. *Water Resources Research*, 17(4):1191–1211, 1981.

[3] The MathWorks web page.
http://www.mathworks.com, 2006.

D.2 Compact Disc Documentation

```
Instructions for installation and running
of the push-pull test production profile solver
PushPullTestModel v. 1.0
------------------------------------------------------------------------
developed by
Sverre Gullikstad Johnsen
sverregu@gmail.com

as part of a PHD study at the
department of petroleum technology and applied geophysics
Norwegian University of Science and technology
Norway

2003-2006
------------------------------------------------------------------------



-----------------------------------------
CONTENT:
-----------------------------------------

I   List of files
II  Installation instructions
III Uninstalling
IV  Using the program
    A)  Running simulations
    B)  Input files
    C)  Output files
V   Development environment (MATLAB version)
VI  References




-----------------------------------------
I   LIST OF FILES
-----------------------------------------

Autorun.inf         CD autostart instructions
CD_Start.exe            CD menu
README.txt          This file
Start.txt           Instructions if the CD does not automatically start


Acrobat707/
    Acrobat707.exe      Adobe Acrobat Reader installation file


InstallFiles/
    copyPushPullTestModel.bat   Installation batch file for the PushPullTestModel files.
                    Copies the files needed to the hard drive,
                    creates a desktop shortcut and start menu items.
    MCRInstaller.bat        Copies the MATLAB Component Runtime installation file to a
                    temporary directory on the hard drive, extracts the installation files,
                    starts the installation program and deletes the temporary directory after
                    the installation program is closed.
```

```
    Start Menu Items/
        CleanUp.bat     Automatic removal tool for the PushPullTest Model Files.
                    Removes the files created by the copyPushPullTestModel.bat
        PushPullTestModel.lnk   Executable shortcut


MATLAB Component Runtime/
    MCRInstaller.exe    Self-extracting MATLAB Component Runtime library utility


PushPullTestModel/
    PushPullTestModel.exe   Main program executable
    PushPullTestModel.ctf   Component Technology File archive


PushPullTestModel/
    InputData/
        SW1CoatsProfile.dat     Coats et al. numerical simulation data
        SW2CoatsProfile.dat
        SW1PickensProfile.dat   Pickens and Grisak experimental field test data
        SW2PickensProfile.dat
        SW1TestParam.dat    Pickens and Grisak field test parameters
        SW2TestParam.dat
        SW1LayeringData.dat Pickens and Grisak test-site layering data
        SW2LayeringData.dat

        TstLayeringData.dat     Custom model layering data
        TstTestParam.dat        Custom model test parameters

    May be added by the user:
        TstExpData.dat      Custom model experimental data to compare with
        TstNumData.dat      Custom model numerical simulation data to compare with


Thesis/
    Thesis.pdf  The PHD thesis on which the PushPullTestModel is based.
    PaperI.pdf  Papers published as part of the PHD work.
    PaperII.pdf
    PaperIII.pdf



----------------------------------------
II      INSTALLATION INSTRUCTIONS
----------------------------------------

The CD is created on and for a Windows XP environment.  Thus, the automatic
installation procedures might not function properly on any other operative system.
The CD has been run and tested on a Windows 2000 computer, where the automatic installation failed.
However, the MCRInstaller and the PushPullTestModel program functioned smoothly when manually copied
to the hard drive.

As the CD is inserted into the CD ROM, a menu should autostart.
If this is not so, manually run the CD_Start.exe from the CD.


1)  This step may be performed automatically by choosing the
    "Install MATLAB Component Runtime" in the CD menu.

    The MATLAB Component Runtime is needed to run the PushPullTestModel
    executable.
    You need administator privileges to install the MCR as it makes
```

```
    changes to both your registry and your system path, however you
    need user-level privileges, only, to run the push-pull test solver.

    IF YOU ALLREADY HAVE MATLAB INSTALLED, YOU DO NOT NEED TO INSTALL MCR!
    (see below for information about matlab and compiler versions used)

    Copy to the hard drive and run the file MCRInstaller.exe to
    install the MATLAB component runtime library utility.
    MCR will be extracted in the directory from where it is run.
    When the setup files have been extracted, an installation wizard
    starts automatically.  After the installation wizard has been run,
    the extracted files may be deleted.
    You need administator privileges to install the MCR as it makes
    changes to both your registry and your system path, however you
    need user-level privileges, only, to run the push-pull test solver.

    For more information on running the MCR Installer utility, see the
    MATLAB compiler User's guide, f.ex. at www.matlab.com .

    IF YOU ALLREADY HAVE MATLAB INSTALLED, YOU DO NOT NEED TO INSTALL MCR!
    (see below for information about matlab and compiler versions used)


2)  Choose the "Copy the PushPullTest Model Files to the Hard Drive"
    in the CD menu to copy the necessary files to the hard drive, create
    a desktop shortcut and start menu/programs items.

    This step might not function properly on non-Windows XP systems.
    In that case, copy the PushPullTestModel/ directory to the hard drive
    manually, and create short-cuts yourself.

    The push-pull test solver is executable from any media, but to
    enable the storage of output data, the program files should all
    be copied to the hard drive or any other writable media.

3)  The program is ready to be run.
    If the automatic procedure in step 2 was succesful, the program
    may be run by double clicking the desktop shortcut or by
    clicking the start menu/programs/PushPullTestModel shortcut.

    First time execution of the
    PushPullTestModel.exe program file will create a directory,
    PushPullTestModel_mcr, containing necessary program files.




-----------------------------------------
III     UNINSTALLING
-----------------------------------------
    These steps might not function properly on a non-Windows XP system.
    In such a case remove all files manually from the hard drive.


1)  Go to "control panel/Add or Remove Programs" and choose to "remove"
    the "MATLAB Component Runtime".

2)  This step may be performed automatically by clicking the
    start menu/programs/PushPullTestModel CleanUp shortcut, or by running
    the CleanUp.bat located in the PushPullTestModel directory on the
    hard drive or on the CD.
```

```
    Delete all files/directories and shortcuts you copied/created to/on
    the hard drive.




-----------------------------------------
IV  USING THE PROGRAM
-----------------------------------------

A)  RUNNING SIMULATIONS
    1)  Execute the file PushPullTestModel.exe.

    2)  The program will ask you which of three different experiments
        you want to simulate, SW1 or SW2 by Pickens and Grisak or the
        custom-built test Tst.  The custom-built test parameters and
        input data could be altered to suit the user's needs.

    3)  The program will list some of the key parameters of the simulation
        and ask if you are ok with running the simulation with these
        parameters.

    4)  The simulation finishes by producing a graphical representation
        of the production profiles, summarizing some of the simulation
        key figures to the screen and creating an output file.
        Note that the medium from which the program is run must be
        writable to do so.


B)  INPUT FILES
    In the directory /InputData/ several .dat files are provided.
    Files whose names begin with SW1 or SW2 should not be altered, as these
    represent simulations of the Pickens-Grisak field tests SW1 and SW2.

    Files with names beginning with Tst may be altered by the user.

    TstTestParam.dat     contains key test parameters such as number
                of streamlines, injection and production rates,
                duration of the injection phase, well radius,
                natural reservoir pressure gradient and viscosity.

                The file should contain seven numbers, representing,
                in the following order,
                N, number of stream-ines to be traced in each layer,
                qi, injection rate, in liters per second,
                qp, production rate in liters per second,
                Ti, duration of the injection phase in days,
                rw, well radius in meters,
                dP, natural pressure gradient in kilopascal per meter,
                visc, viscosity of the injectant/reservoir fluid in
                    centipoise


    TstLayeringData.dat contains stratification data.
                At least one line must be included, consisting of
                permeability, fractional porosity and layer thickness.
                If more than one line is included, each line will
                represent an individual layer in a multi-layered
                reservoir model.
```

```
    The user may add files containing experimental data and/or
    numerical simulation data, TstExpData.dat and TstNumData.dat.
    Data should be listed in two columns, whereas column 1 contain
    dimensionless volumes produced, Vp/Vinj,tot, and column 2 contain
    fractional concentration of injectant in the producing well-stream.
    The experimental/numerical data will be presented graphically along
    with the stream-line based production profile in the resulting plot.



C)  OUTPUT FILES
    If the medium, from which PushPullTestMode.exe is run, is writable,
    output files will be created in the directory /OutputData/.  If the
    directory does not exist, it will be created.

    The output filenames are on the form
    Experiment-ProdProfileData-yyyy-mmm-dd_hh.mm.ss.dat
    where Experiment=SW1, SW2 or Tst.

    The output file contains:
    *  Date and time of the simulation.
    *  Test parameters used.
    *  A list of the layers where tracer was lost, if any.
    *  Layering data used, including permeabilities, porosities, layer
       heights, average permeability and average porosity.
    *  Production profile data generated, in two columns, where column 1
       contain dimenionless volumes produced, Vp/Vinj,tot, and column 2
       contain fractional concentration of injectant in the producing
       well-stream.



-----------------------------------------
V   DEVELOPMENT ENVIRONMENT
    (MATLAB version and WINDOWS version)
-----------------------------------------

The program is developed in MATLAB where the "ver" command resulted in the following


--------------------------------------------------------------------------------
MATLAB Version 7.1.0.246 (R14) Service Pack 3
MATLAB License Number: 159436
Operating System: Microsoft Windows XP Version 5.1 (Build 2600: Service Pack 2)
Java VM Version: Java 1.5.0 with Sun Microsystems Inc. Java HotSpot(TM) Client VM mixed mode
--------------------------------------------------------------------------------
MATLAB                                                Version 7.1        (R14SP3)
Simulink                                              Version 6.3        (R14SP3)
Communications Toolbox                                Version 3.2        (R14SP3)
Control System Toolbox                                Version 6.2.1      (R14SP3)
Data Acquisition Toolbox                              Version 2.7        (R14SP3)
Excel Link                                            Version 2.3        (R14SP3)
Extended Symbolic Math                                Version 3.1.3      (R14SP3)
Financial Toolbox                                     Version 2.5        (R14SP3)
Fixed-Point Toolbox                                   Version 1.3        (R14SP3)
Fuzzy Logic Toolbox                                   Version 2.2.2      (R14SP3)
Image Processing Toolbox                              Version 5.1        (R14SP3)
Instrument Control Toolbox                            Version 2.3        (R14SP3)
MATLAB Compiler                                       Version 4.3        (R14SP3)
Model Predictive Control Toolbox                      Version 2.2.1      (R14SP3)
Neural Network Toolbox                                Version 4.0.6      (R14SP3)
Optimization Toolbox                                  Version 3.0.3      (R14SP3)
```

```
Partial Differential Equation Toolbox                Version 1.0.7      (R14SP3)
Real-Time Workshop                                   Version 6.3        (R14SP3)
Robust Control Toolbox                               Version 3.0.2      (R14SP3)
Signal Processing Toolbox                            Version 6.4        (R14SP3)
SimPowerSystems                                      Version 4.1.1      (R14SP3)
Simulink Accelerator                                 Version 6.3        (R14SP3)
Simulink Control Design                              Version 1.3        (R14SP3)
Simulink Fixed Point                                 Version 5.1.2      (R14SP3)
Simulink Verification and Validation                 Version 1.1.1      (R14SP3)
Spline Toolbox                                       Version 3.2.2      (R14SP3)
Stateflow                                            Version 6.3        (R14SP3)
Statistics Toolbox                                   Version 5.1        (R14SP3)
Symbolic Math Toolbox                                Version 3.1.3      (R14SP3)
System Identification Toolbox                        Version 6.1.2      (R14SP3)
Wavelet Toolbox                                      Version 3.0.3      (R14SP3)
```

```
-----------------------------------------
VI      REFERENCES
-----------------------------------------
```


http://www.mathworks.com/
    The Mathworks, creator of MATLAB.

Coats KH, Whitson CH, Thomas L (2004) Modelling Conformance as Dispersion.
    SPE Annual Technical Conference and Exhibition, Houston, Texas, USA,
    SPE 90390

Pickens J, Grisak G (1981) Scale-dependent Dispersion in a Stratified Granular Aquifer.
    Water Resources Research 17(4):1191-1211

Part V

Papers

Paper I

Analytical Treatment of a Push-Pull "Echo" Test.
Part I - Development of a Single Layer Solution.

Sverre G. Johnsen and Curtis H. Whitson
Submitted to *The Journal of Transport in Porous Media*

Abstract

Analysis of stream-line-based formulations are used to calculate, analytically, the time of break-through for clean water and the end-time of tracer production in addition to overall producing tracer concentration vs. time, in a single-well tracer push-pull test. As a main topic we study injection/production in unconfined homogeneous aquifers of infinite extent, subject to natural groundwater drift. Injectant and in situ groundwater are assumed to be miscible, incompressible fluids with identical fluid properties. Only macroscopic flow is considered, and flow is assumed to experience no in situ fluid mixing (physical dispersion) so fluid interfaces remain sharp. Analytical results are compared to field study data provided by Pickens and Grisak and numerical simulation data obtained by Coats *et al*. The good match with experimental data and numerical simulation data validate the physical dispersion-free method proposed.

Keywords Analytical, Contamination, Echo test , Macroscopic dispersion, Natural drift, Push-pull test, Stream-line, Tracer, Water

1 Introduction

In 1981 Pickens and Grisak, [[8]], reported from two full-scale single-well push-pull tests, SW1 and SW2, performed using two neighbouring wells in the same aquifer. Push-pull tests, also known as echo or injection-withdrawal tests, are single-well tests where an injection phase "pushing" injectant containing a tracer into the well is followed by a production phase where fluids are "pulled" out of the well. Normalised tracer concentrations are measured during the production phase.
Laboratory experiments on core-samples from the test site gave a dispersivity of approximately $0.035cm$, whereas the field tests, neglecting natural groundwater-drift, gave $3cm$ and $9cm$, respectively, fitting the one-dimensional convection-dispersion equation (1D CD-EQ) to the test data. Pickens and Grisak conclude that the great variations are due to a strong scale dependency in apparent dispersivity; others also suggest the same, [[1]], [[7]].

Recently Coats *et al*. have shown that the large dispersivity reported by Pickens and Grisak may be mainly due to natural drift of the in situ ground water, [[3]]. Coats *et al.* remind that all experimental evidence show that dispersivity is a rock property and that any "apparent" scale dependence of dispersivity derived from produced-well concentration profiles[1] must be due to other physical phenomena such as drift.

[1] *Production profiles* and *concentration profiles* refer to the plot of the normalised concentration

In this paper a "source/sink in a uniform stream"-problem is solved for the boundary values provided by the Pickens-Grisak test site by introducing and tracing individual stream-lines. Pickens and Grisak report a fractional porosity of 0.38 and a hydraulic conductivity of approximately $1.4 \cdot 10^{-2} cm/s$. In the numerical simulations run by Coats *et al.*, and also in this paper, a permeability of $14.8 darcy$ has been used. Interpretation of the Pickens-Grisak Figure 2 gives a hydraulic head gradient of about $0.05 kPa/m$. The Coats *et al.* value of $0.0023 psi/ft$ ($\sim 0.052 kPa/m$) has been used. Based on these figures, the natural macroscopic velocity of the groundwater is $0.17 m/day$, [[6]], see Appendix B. It was assumed that the areal extent of the aquifer was infinite, that the reservoir thickness was $8.2m$, as reported by Pickens and Grisak, and that the test well fully penetrated the reservoir. Test parameters for the two single-well tests, SW1 and SW2, are given in **Table I**. Steady state injection/production was assumed.

In **Figure 1** stratigraphic interpretations by Cherry et al, [[2]], are shown. The Pickens-Grisak test site is marked with the circle in Figure 1(a) , and the stratigraphic cross-sections are indicated also. The Y-Y' line is from Cherry's own figure, while the X-X' line has been added based on Figure 1 in [[4]]. The piezometer KO indicated in Figure 1(b) as well as in Figure 1(c) is located approximately where the Y-Y' and the X-X' lines are crossing. The stratification along the X-X' cross-section is close to horisontal, and the thickness of the various strata does not vary much. It will be assumed that this is the situation for all cross-sections perpendicular to the Y-Y' cross-section, hence it is assumed that the natural drift is parallel to the Y-Y' cross-section. Furthermore, it was assumed that both the injectant and the in situ groundwater are incompressible fluids with identical fluid properties. Viscosity was assumed constant and temperature, pressure and density variations were neglected, i.e., no gravitational, viscous or thermodynamic effects were taken into account. It was assumed that the tracer[2]

of tracer in the produced fluid either as a function of time, t_p, or as a function of dimensionless volume produced, $Q_D = \frac{|Q_p| t_p}{Q_i T_i}$.

[2]Usually tracers are added to the injectant in relatively small concentrations to obtain near ideal

Table I: Test Parameters for the two single-well tests performed by Pickens and Grisak.

Parameter	Test SW1		Test SW2	
Well Radius	0.057	m	0.057	m
Injection Phase				
Rate	76.55	m^3/day	62.12	m^3/day
Duration	1.25	*days*	3.93	*days*
Production Phase				
Rate	76.55	m^3/day	52.36	m^3/day
Duration	2.0	*days*	16.9	*days*

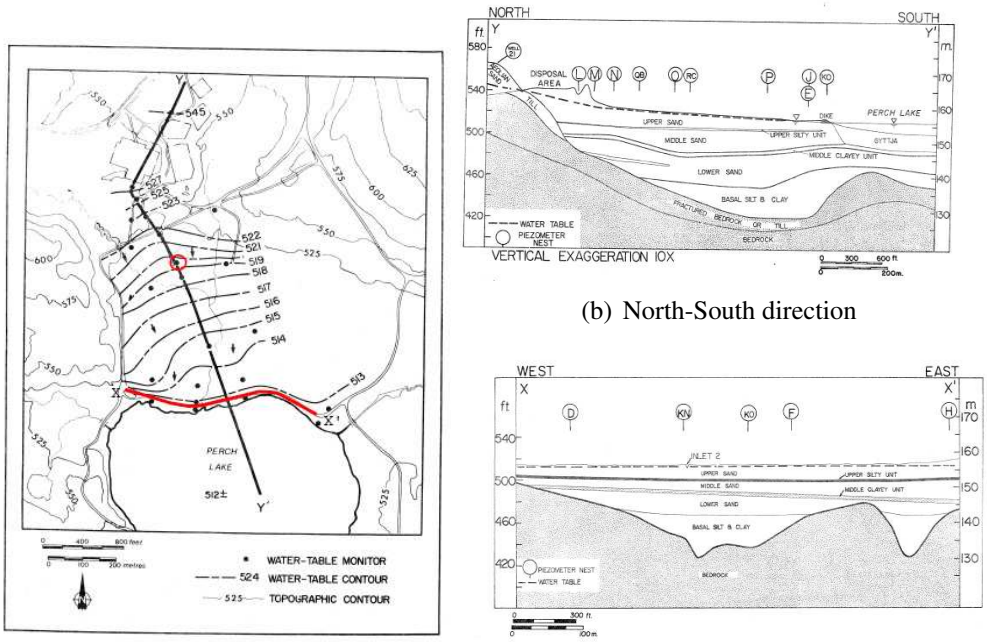

(a) Perch Lake Overview

(b) North-South direction

(c) West-East direction

Figure 1: Figure 10, 6 and 7 in [[2]]; Physical hydrogeology of the Lower Perch Lake Basin. The X-X' line in (a) is based on Figure 1 in [[4]].

was ideal, i.e., chemically and physically stable, not interacting with in situ fluids or solids and not naturally present in the reservoir.

Even though microscopic flow in porous media will be affected by physical dispersion, it has been assumed that the physical dispersion is negligible and that no in situ mixing takes place. The injectant and the groundwater are miscible and displace each other perfectly, maintaining a sharp interface between the two fluids, i.e., all mixing will occur in the well-bore.

For injection phases lasting longer than some critical time, T_c, some fluid will cross the $\psi_p = 0$ production phase stream-line. For given production phase parameters, this fluid will be lost and cannot be recovered unless the production rate is increased. In this paper, the T_c will not be addressed, and it will be assumed that $T_i < T_c$, so that all injected fluid is recoverable. In the follow-up paper, Part II, [[5]], we will, however, give T_c attention.

tracer behaviour. In this paper, though, the notations *injectant* and *tracer* will be used equivalently about the fluid being injected, and in situ water containing no tracer will be referred to as *clean water*. Produced water may consist of a mixture of injected water and clean water, whereas the tracer concentration will be in the range $(0,1)$. The producing tracer concentration at some time, t, is accordingly the ratio of injectant volume to total volume produced in an infinitesimal time interval.

2 No Drift

Considering a homogeneous reservoir of infinite areal extent, with a test-well located at the origin, the Darcy velocity field due to injection/production at a constant two-dimensional rate of q is given by

$$U_r = \frac{q}{2\pi\phi r} = \frac{Q}{r}\,, \tag{1a}$$

$$U_\theta = 0\,, \tag{1b}$$

where q is positive for injection and negative for production.
Equation 1a is a separable differential equation, and the solution is given by

$$\frac{1}{2}\,r^2 = Qt + \mathscr{C}\,. \tag{2}$$

In a push-pull test the injectant front position will be r_w at the start of injection and r_{max} at the end of injection/start of production. The radius of the injectant-covered area is hence given by

$$r(t \le T_i) = \sqrt{r_w^2 + 2Q_i t_i}\,, \tag{3}$$

and

$$r(T_i < t \le T_i + T_p) = \sqrt{r_{max}^2 - 2|Q_p|t_p} \tag{4}$$

during the injection and production phases, respectively. From Equation 3 , we get an expression for r_{max} by inserting $t = T_i$, and from Equation 4 we get

$$T_p = \left|\frac{Q_i}{Q_p}\right| \cdot T_i\,, \tag{5}$$

when $r(t = T_i + T_p) = r_w$, as expected for piston-like displacement. Owing to the symmetry of the problem, the above calculations are valid for any angle, θ, so we get $T_{BT} = T_p$, for all θ, i.e., the producing fractional concentration of tracer drops from 1 to 0 instantaneously. In **Figure 2** a schematic of the different time variables referred to, can be seen.

3 Drift

In nature we often find a steady velocity component due to natural variations in the hydraulic head, and the most obvious example is a river. Natural drift may,

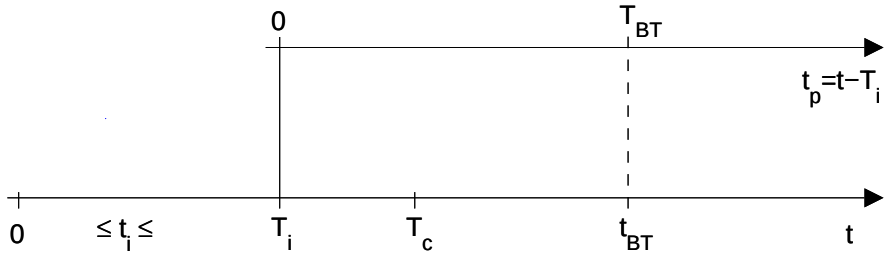

Figure 2: Schematic of different times involved in the analytical derivations. For $T_c > T_i$ we have so-called conservative injection, where all injectant may be recovered.

however, also occur sub-surface, in groundwater reservoirs. In such a situation Equation 1a and Equation 1b has to be added to terms from the natural velocity field, and the total velocity field is now given by, [[10]],

$$U_r = U_u \cos\theta + \frac{Q}{r}\,, \tag{6a}$$

$$U_\theta = -U_u \sin\theta\,, \tag{6b}$$

which in Cartesian coordinates become

$$U_x = U_u + \frac{Qx}{x^2+y^2} \tag{7a}$$

$$U_y = \frac{Qy}{x^2+y^2} \tag{7b}$$

It is assumed that the uniform stream velocity vector points in the positive x-direction, and the test well is still located at the origin. We can see that stagnation-points, i.e., spatial points where all velocity components become zero, exist for $(x,y) = \left(-\left|\frac{Q_i}{U_u}\right|, 0\right)$ and $\left(\left|\frac{Q_p}{U_u}\right|, 0\right)$ in the injection and production phases, respectively. Assuming miscible flow, i.e., the injectant perfectly displaces the in situ fluid, the stream-lines passing through the stagnation-points will represent absolute boundaries between the injectant and the in-situ fluid during the injection phase and between recoverable fluid and escaped fluid in the production phase, as seen in **Figure 3**. The shape of these boundaries is the Rankine half-body, [[10]].

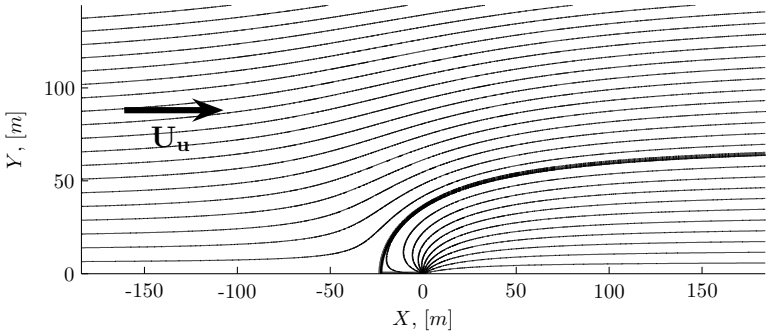

(a) Injection phase

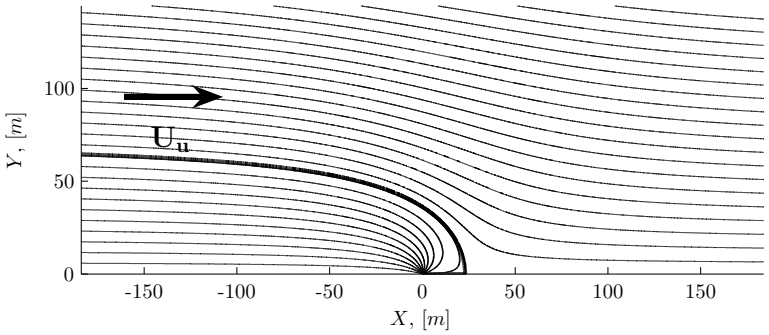

(b) Production phase

Figure 3: General picture of stream-lines, or constant ψ contours, in the upper half-plane, in the sink/source in a uniform stream model. Injection- and production-rates are symmetrical, so the two cases are mirror images of each other. The Rankine Half-body is shown as the emphasised stream-lines. Source, in (a), and Sink, in (b), are located at the origin and the uniform stream velocity vector points in the positive x-direction, as indicated.

3.1 Stream-line Contours

The stream-line contours are identified by real numbers ψ, [[10]], which are given by

$$\frac{\partial \psi}{\partial r} = -U_\theta \bigwedge \frac{\partial \psi}{\partial \theta} = r \cdot U_r \ , \tag{8a}$$

or

$$\frac{\partial \psi}{\partial y} = U_x \quad \bigwedge \frac{\partial \psi}{\partial x} = -U_y \ , \tag{8b}$$

which, from Equation 6 and Equation 7 , respectively, result in

$$\psi = U_u \cdot r \sin\theta + Q \cdot \theta \ . \tag{9a}$$

and

$$\psi = U_u \cdot y + Q \cdot \arccos\left(\frac{x}{\sqrt{x^2+y^2}}\right) \tag{9b}$$

From Equation 9a we get

$$r = \frac{\psi - Q\theta}{U_u \sin\theta} \ , \tag{10}$$

which gives, from Equation 8a ,

$$\frac{d\theta}{dt} = -\frac{1}{r}\frac{\partial\psi}{\partial r} = -\frac{U_u \sin\theta}{r} = -\frac{(U_u \sin\theta)^2}{\psi - Q\theta} \ , \tag{11}$$

where we have used that $U_\theta = r \cdot \frac{d\theta}{dt}$.

The ψ denote stream-lines or flow-paths. By definition, [[10]], the fluids on a stream-line are confined there, i.e., a fluid particle with a given ψ will stick to this number until the streaming conditions are altered. Plotting lines of constant ψ, we can visualize the flow pattern of the fluid system.

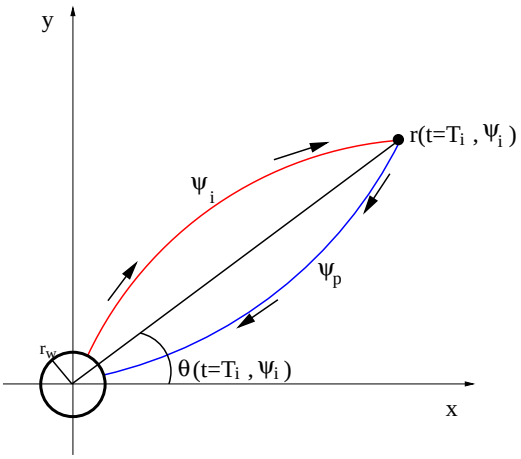

Figure 4: General view of the trace of a fluid particle leaving the wellbore at the radius r_w at the time $t = 0$. The trace is described by the injection phase stream-line ψ_i until the particle reaches it's maximum radial advancement r_{max} at the time $t = T_i$ and thereafter by the production phase stream-line ψ_p until it is back at the well-bore radius r_w.

Since there may be no cross-flow between stream-lines, the stream-lines are uniquely identified by one set of r and θ values. It follows from Equation 9a that a fluid particle situated at the injection phase stream-line ψ_i and at the angle θ at the end of injection, is bound to flow along the production phase stream-line

$$\psi_p = \psi_i - (|Q_p| + Q_i)\,\theta \ , \tag{12}$$

for $t_p > 0$. If the particle did not cross the $\psi_p = 0$ boarder during the injection phase, i.e., ψ_p from Equation 12 is less than 0, the particle will move back towards the production well as shown in **Figure 4**, else, if $\psi_p > 0$, the particle will keep moving away from the production well and is lost. In Figure 3 a selection of stream-lines have been shown for the "source/sink in a uniform stream" problem, for the injection phase (source) and the production phase (sink), respectively.

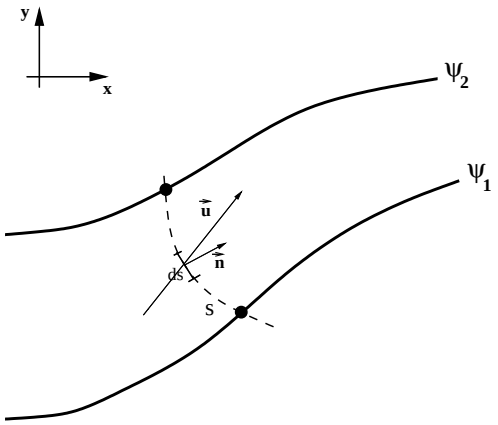

Figure 5: Geometrical interpretation of stream-lines, ψ: volume flow between two stream-lines.

Furthermore, the two-dimensional rate between two stream-lines, ψ_1 and ψ_2, are found by integrating along some path, s, as seen in **Figure 5**,

$$q = \int_s dq \ , \tag{13}$$

where dq is given by

$$dq = (\vec{u} \cdot \vec{n})\, ds \ . \tag{14}$$

The normal vector, $\vec{n}$, to the line segment ds is given by

$$\vec{n} = \hat{\mathbf{x}} \frac{dy}{ds} - \hat{\mathbf{y}} \frac{dx}{ds} \ . \tag{15}$$

Applying Equation 8b , Equation 14 and Equation 15 to Equation 13 we get

$$q \ = \ \int_s (U_x dy - U_y dx) = \int_{\psi_1}^{\psi_2} d\psi = \psi_2 - \psi_1 \ . \tag{16}$$

Hence, the numerical stream-line number difference between two arbitrary stream-lines is a measure of the two-dimensional rate flowing between them.

3.2 Break-through, $\theta = \pi$

Injection Phase

Break-through (BT) is defined as the earliest time at which clean water enters the well-bore during the production phase. BT may, hence, both refer to the earliest time clean water enters the well-bore from *any* stream-line or the earliest time clean water enter the well-bore from a *specific* stream-line.

From Equation 6a we see that the radial particle velocity is monotonically decreasing with $\theta \in [0, \pi]$. For all radii and angles, the injection phase radial fluid velocity is positive and the production phase radial fluid velocity is negative (for recoverable fluids).
This means that the tracer front will be closest to the well at $\theta = \pi$ at all times. Hence, break-through will happen for the $\theta \equiv \pi$ producing stream-line, first. From Equation 6b , we see that at angles $\theta = 0$ and $\theta = \pi$, the velocity is radial only, and for $\theta = \pi$, the particle velocity, during the injection phase, is given by

$$\vec{u}_i = \left(-U_u + \frac{Q_i}{r} \right) \hat{\boldsymbol{r}} \, . \tag{17}$$

Solving for r, the differential equation, Equation 17 , we get

$$U_u \, (r - r_w) + Q_i \ln \left| \frac{Q_i - U_u \cdot r}{Q_i - U_u \cdot r_w} \right| = -U_u^2 \cdot t, \;\; t \in [0, T_i] \, . \tag{18}$$

Production Phase

Breakthrough will occur at the time when the fluid located in the position $(r, \theta) = (r_{max}, \pi)$ at the start of the production phase, $t_p = 0$, is produced back and arrives at the well perimeter, r_w. Hence we must calculate the time it takes for a particle to travel this distance. For $\theta = \pi$, the particle velocity, during the production phase, is given by

$$\vec{u}_p = \left(-U_u - \frac{|Q_p|}{r} \right) \hat{\boldsymbol{r}} \, , \tag{19}$$

which results in the time-radius relation

$$U_u \, (r - r_{max}) - |Q_p| \ln \left| \frac{|Q_p| + U_u \cdot r}{|Q_p| + U_u \cdot r_{max}} \right| = -U_u^2 \cdot t, \;\; r \in [r_w, r_{max}] \, . \tag{20}$$

The time of break-through, T_{BT}, may now easily be found by inserting r_w for r in Equation 20 . r_{max} is found by inserting T_i for t in Equation 18 and solving for r.

3.3 End of Tail, $\theta = 0$

Assuming all injectant can be recovered, we deduce, from the same argument as above, that the last drop of injectant to be produced back comes from the injection/production stream-lines with $\theta \equiv 0$. The calculations are identical to those for $\theta = \pi$ and we get that the down-gradient tracer front position, r, is implicitly given by

$$U_u\,(r - r_w) - Q_i \ln\left(\frac{Q_i + U_u r}{Q_i + U_u r_w}\right) = U_u^2 t, \quad t \in [0, T_i] \tag{21a}$$

during the injection phase, and

$$U_u\,(r - r_{max}) + |Q_p| \ln\left(\frac{|Q_p| - U_u r}{|Q_p| - U_u r_{max}}\right) = U_u^2 t, \quad r \in [r_w, r_{max}] \tag{21b}$$

during the production phase. Finding the maximum down-stream radius from Equation 21a , Equation 21b can be used to calculate at what time the last drop of injectant is produced back, i.e., when the producing injectant concentration reaches zero.

3.4 Angles between 0 and π

Injection

Owing to the symmetry about the x-axis, it suffices to investigate the upper half-plane, $\theta \in [0, \pi]$.
Solving the separable differential equation, Equation 11 , for the injection phase, we get

$$(Q_i\theta - \psi_i)\cot\theta - Q_i \ln|\sin\theta| = -U_u^2 t + \mathscr{C}(\psi_i)\ , \tag{22}$$

where $\theta \equiv \theta(t, \psi_i)$ and $\mathscr{C}(\psi_i)$ is an integration constant depending on the stream-line in question. For $t = 0$ we have the boundary condition $r = r_w$, so we get from Equation 9 that

$$\Big[\, Q_i\theta(t = 0, \psi_i) - \psi_i \,\Big] = -U_u r_w \sin\big[\theta(t = 0, \psi_i)\big]\ , \tag{23}$$

and we get an expression for the integration constant,

$$\mathscr{C}(\psi_i) = -U_u r_w \cos\theta - Q_i \ln|\sin\theta|\Big|_{\theta=\theta(t=0,\psi_i)}\ . \tag{24}$$

As $\theta(t = T_i, \psi_i)$ can be found from Equation 22 , we can use Equation 10 to calculate the maximum radial advancement for each injection phase stream-line, ψ_i,

$$r_{max} = r(t = T_i, \psi_i) = \left.\frac{\psi_i - Q_i\theta}{U_u \sin\theta}\right|_{\theta=\theta(t=T_i,\psi_i)}\ . \tag{25}$$

Solving Equation 22 for θ may result in multiple solutions. The relevant solution will be in the interval $(0,\pi)$, if we study the upper half-plane, and result in an r_{max} in the range $\big(r_{max}(\theta=\pi), r_{max}(\theta=0)\big)$. Both $\theta(T_i)$ and r_{max} must be monotone functions of ψ_i.

Production

During the production phase the rate is by definition negative, but except for the sign of Q, Equation 6 and Equation 7 remain the same, so it suffices to let $Q_i \rightarrow -|Q_p|$ in Equations 22-25 to get the production phase equations;

$$\psi_p = U_u r \sin\theta - |Q_p|\theta \tag{26}$$

$$r = \frac{\psi_p + |Q_p|\theta}{U_u \sin\theta} \tag{27}$$

$$-U_u^2 t + \mathscr{C}(\psi_p) = -\left(|Q_p|\theta + \psi_p\right)\cot\theta + |Q_p|\ln|\sin\theta| \tag{28}$$

$$\mathscr{C}(\psi_p) = -U_u r_{max}\cos\theta + |Q_p|\ln|\sin\theta|\Big|_{\theta=\theta(t=T_i,\psi_i)} \tag{29}$$

From Equation 27 it is possible to calculate at what angle a given production phase stream-line enters the well bore, $\theta(r_w, \psi_p)$ by setting $r = r_w$. The production phase stream-line will be known from Equation 26 , putting in the r_{max} and $\theta(t = T_i, \psi_i)$ values obtained from Equation 25 and Equation 22 , respectively.
When the polar coordinates at which the production phase stream-line intersects the well-bore are found, these can be used to calculate the "time of break-through" for clean water, T_{BT,ψ_p}, for each production phase stream-line, using Equation 28 with the integration constant in Equation 29 .

4 Comparing the Analytical Solution with Experimental Data

To generate a production profile based on the theory presented, we have to abandon the analytical approach. There is no way to find an analytical expression for the producing tracer concentration as a function of time. We can, however, generate a semi-analytical production profile by keeping track of a finite, but large, number of stream-lines and employing the analytical approach to calculate the T_{BT} for each of them.

Using a finite number of stream-lines, the production profile is in reality not a

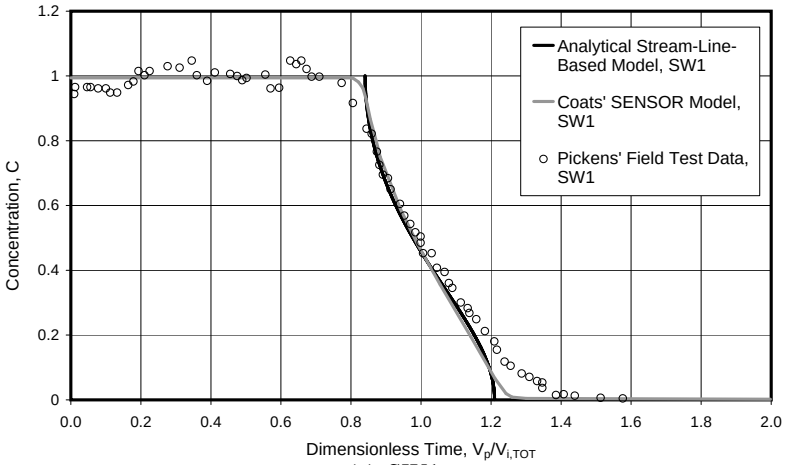

(a) SW1

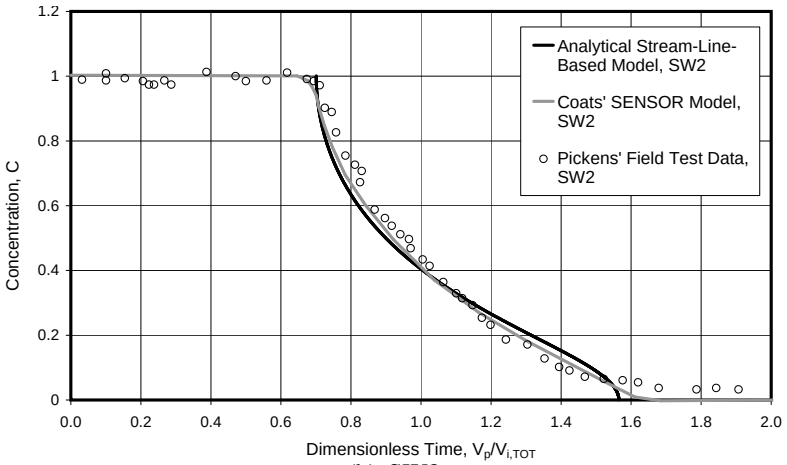

(b) SW2

Figure 6: Producing tracer concentration vs. dimensionless time, Volume produced/Total volume injected , comparing the Pickens-Grisak field test data, numerical simulation results from the Coats *et al.* SENSOR model and this paper's semi-analytical stream-line-based model.

continuous line, but rather a series of points. As the inflow rate associated with each stream-line is an approximation[3], the points are error prone. Tracing a large number of stream-lines, however, the error becomes negligible, and the production profile points become so dense that the space between them vanish, hence there is no need for interpolation.

Only the upper half-plane was studied and the N traced injection phase stream-lines intersect the well-perimeter, at $r = r_w$, at uniform angle intervals such that $\Delta\theta_i = \frac{\pi}{N-1}$ and $n = 1$ and $n = N$ corresponds to the angles $\theta = 0$ and $\theta = \pi$,

[3]Modelling a finite number of stream-lines, a finite inflow rate has to be associated with each stream-line such that the sum equals the actual injection/production rate.

respectively. As described in the previous sections, the $r_{max,\psi_{i,n}}$ were calculated for each stream-line, $\psi_{i,n}$, and the corresponding $T_{BT,\psi_{p,n}}$ were calculated for each stream-line, $\psi_{p,n}$.

As shown in Equation 16 , the two-dimensional rate between two stream-lines, ψ_m and ψ_n is simply $\psi_m - \psi_n$. Half of this rate may be associated with each of the two stream-lines, so the total in-flow rate associated with a given stream-line, ψ_n where $n \in [2, N-1]$, is

$$\begin{aligned} q_{p,n} &= \frac{1}{2}\left(\psi_{p,n+1} - \psi_{p,n}\right) + \frac{1}{2}\left(\psi_{p,n} - \psi_{p,n-1}\right) \\ &= \frac{1}{2}\left(\psi_{p,n+1} - \psi_{p,n-1}\right) , \end{aligned} \tag{30a}$$

and as we study the upper half-plane only, we have

$$q_{p,1} = \frac{1}{2}\left(\psi_{p,2} - \psi_{p,1}\right) , \tag{30b}$$

and

$$q_{p,N} = \frac{1}{2}\left(\psi_{p,N} - \psi_{p,N-1}\right) . \tag{30c}$$

We now get that

$$\begin{aligned} \sum_{n=1}^{N} q_{p,n} &= \frac{1}{2}\left(\psi_{p,2} - \psi_{p,1}\right) + \frac{1}{2}\left(\psi_{p,N} - \psi_{p,N-1}\right) + \frac{1}{2}\sum_{n=2}^{N-1}\left(\psi_{p,n+1} - \psi_{p,n-1}\right) \\ &= \psi_{p,N} - \psi_{p,1} \qquad (31) \\ &= Q_p \cdot \pi = \frac{q_p}{2\phi} , \qquad (32) \end{aligned}$$

where $\frac{q_p}{\phi}$ is the rate through the effective area $A \cdot \phi$.

Assuming dispersion-free piston displacement, each stream-line produce injectant at the partial rate given by Equation 30 until the time of break-through for that particular stream-line. After the time of break-through, the stream-line produces clean water at the same rate. Hence the total inflow concentration of injectant will be equal to

$$C_{N^*} = \frac{\sum_{n=1}^{N^*} Q_{p,n}}{Q_p} , \tag{33}$$

where N^* is the number of stream-lines still producing tracer.
Since this way of plotting, in reality, generates step-functions of N steps, we

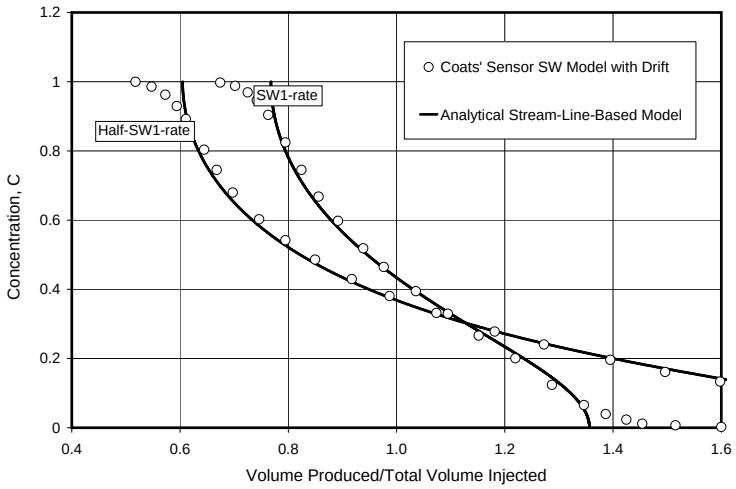

Figure 7: Comparing semi-analytical model results with the Coats *et al.* Sensor model results shown in their Figure 18. Pickens-Grisak SW test area with drift for two injection=production rates; 3 days at SW1-rate and 6 days at half SW1-rate.

would, for a small number of stream-lines, get into the dilemma of plotting upper or lower value of each step, i.e., choosing N^* as the number of stream-lines with $T_{BT,n} > t_p$ or $\geq t_p$. However, as this will only be a problem for small N's, which will also result in several other inaccuracies and problems, this will not be addressed any further. Here, $\geq t_p$ was chosen.

The semi-analytical solution plots in **Figure 6(a)** and **Figure 6(b)** are generated from a thousand data-points $\left(T_{BT,n}, C_{N-n+1}\right)$, based on tracing a thousand stream-lines, and are compared to the Pickens-Grisak field test data and the numerical simulation data provided by Coats *et al.*

In **Figure 7** results from the semi-analytical model is compared to the Coats *et al.* SENSOR results using SW1 and half SW1 rates, from their Figure 18, [[3]]. As is seen, there is good agreement between the semi-analytical model and results from the simulator, SENSOR, but the SENSOR model shows a somewhat more dispersed result. In **Figure 8** a selection of stream-lines as well as the injectant-covered area, at $t_i = T_i$, is shown for SW1 and SW2 injection and production phases, respectively. It can be seen how the injectant-covered area deviates somewhat from a perfect circle.

To verify the semi-analytical solution described in this paper, and to compare with the results obtained by Coats *et al.*, a commercially available stream-line based simulator, 3DSL, [[9]], was employed. An equivalent model to that of the stream-line based semi-analytical model and the Coats *et al.* model was built and run, both for SW1 and SW2 test parameters. The resulting production profiles were more or less identical to the Coats *et al.* results, but somewhat more dis-

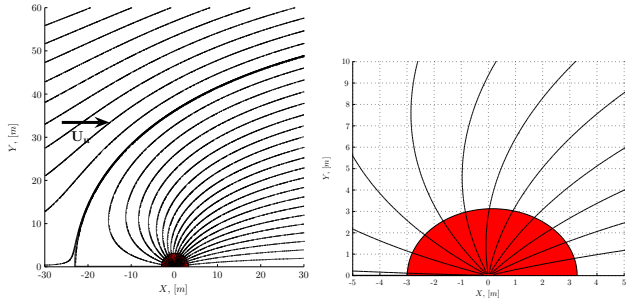

(a) SW1 - Injection phase

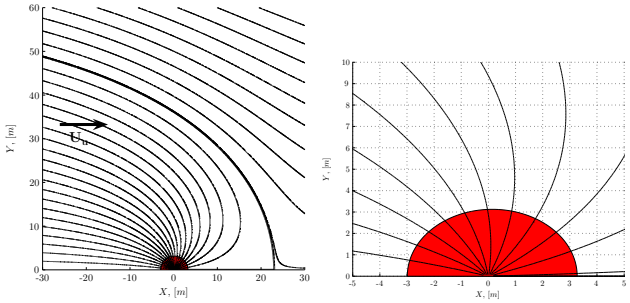

(b) SW1 - Production phase

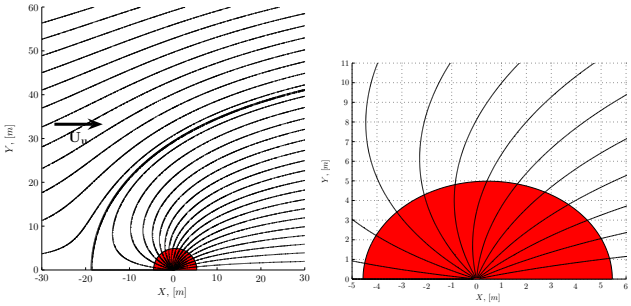

(c) SW2 - Injection phase

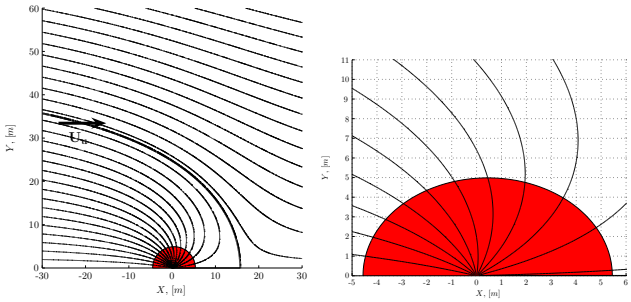

(d) SW2 - Production phase

Figure 8: Injection and Production phase stream-lines for SW1 and SW2 test-parameters, respectively. Injectant covered areas at the end of the injection phase are shown as the hatched area. The test-well is located at the origin, and, as indicated, the uniform stream velocity vector points in the positive x-direction.

persed than the semi-analytical profile, depending on the number of data-points generated, i.e. the number of time-steps taken. Based on our study of the semi-analytical model, the SENSOR model and the 3DSL model, and correspondence with Marco Thiele at Streamsim Technologies Inc., [[9]], we are under the impression that our semi-analytical solution represent the most accurate solution and that the single-well push-pull test is not readily modelled using available simulators, finite difference based or stream-line based.

5 Conclusions

1. In an entirely dispersion free model, it has been shown that real experimental data may be matched well even though apparent dispersivity is large.

2. It has been shown analytically, in an over-simplified reservoir model, that natural drift alone may cause a big part of the apparent dispersivity reported by Pickens and Grisak.

3. The analytically calculated times for clean water break-through and end time of tracer production and the semi-analytical calculations in-between show good agreement with results from numerical simulations run by Coats *et al* and stream-line based simulation results obtained from Streamsim's 3DSL.

A Hydraulic Head - Hydrostatic Pressure Conversion

Hydraulic head, h, is commonly used to denote the pressure of a water column of a certain height. The pressure at a given depth is found by solving the differential equation

$$\frac{dP}{dh} = \rho_w g \ , \tag{A1}$$

where ρ_w, the water density, is assumed to be constant and g is the gravity. The hydraulic head is hence related to the pressure by the formula

$$h = \frac{P}{\rho_w g} \ . \tag{A2}$$

B Darcy's Law and the Natural Drift Velocity

The Darcy velocity is given by

$$v = K \cdot \frac{dh}{dx} = \frac{K}{\rho_w g} \frac{dP}{dx} \ , \tag{B3}$$

where the hydraulic conductivity, K, is related to the permeability, k, by

$$K = k \cdot \frac{\rho g}{\mu} \ , \tag{B4}$$

where ρ and μ is the density and viscosity of the fluid in question. The unit of permeability is frequently given as $darcy = 9.869 \cdot 10^{-13}\ m^2$. For flow in a porous media of porosity ϕ, the macroscopic fluid velocity will be given by

$$u = \frac{v}{\phi} = \frac{K}{\phi} \cdot \frac{dh}{dx} = \frac{k}{\mu\phi} \ \frac{dP}{dx} \ . \tag{B5}$$

References

[1] A. Arya, T.A. Hewett, R.G. Larson, and L.W. Lake. Dispersion and reservoir heterogeneity. *SPERE*, 3:139–148, 1988. SPE 14364.

[2] J.A. Cherry, R.E. Jackson, D.C. McNaughton, J.F. Pickens, and H. Woldetensae. *Physical Hydrogeology of the Lower Perch Lake Basin, in PJ Barry* Hydrological Studies on a Small Basin on the Canadian Shield, pages 625–680. Number AECL 5041/II. Atomic Energy of Canada, Ltd., Chalk River Nuclear Laboratories., Ontario, Canada, September 1975.

[3] K. H. Coats, C.H. Whitson, and L.K. Thomas. Modelling conformance as dispersion. SPE Annual Technical Conference and Exhibition, 26-29 September, Houston, Texas, September 2004. SPE 90390.

[4] R.M. Gagne. *Seismic Investigation of the Perch Lake Study Area, Chalk River Nuclear Laboratories, in PJ Barry* Hydrological Studies on a Small Basin on the Canadian Shield, pages 139–143. Number AECL 5041/I. Atomic Energy of Canada, Ltd., Chalk River Nuclear Laboratories., Ontario, Canada, September 1975.

[5] Sverre G. Johnsen and Curtis H. Whitson. Analytical Treatment of a Push-Pull "Echo" Test, Part II - Application of the Convection-Dispersion Equation. Submitted to Transport in Porous Media, 2007.

[6] G.P. Kruseman and N.A. de Ridder. *Analysis and Evaluation of Pumping Test Data, Bulletin 11*. International Institute for Land Reclamation and Improvement, Wageningen, The Netherlands, 1970.

[7] J. Mahadevan, L.W. Lake, and R.T. Johns. Estimation of true dispersivity in field scale permeable media. SPE/DOE Improved Oil recovery Symposium, Tulsa, Oklahoma, USA, April 2002. SPE 75247.

[8] J.F. Pickens and G.E. Grisak. Scale-dependent dispersion in a stratified granular aquifer. *Water Resources Research*, 17(4):1191–1211, 1981.

[9] The Streamsim web page. http://www.streamsim.com, 2006.

[10] F.M. White. *Fluid Mechanics*. McGraw - Hill, New York, USA, 5th edition, 2003.

Paper II

Analytical Treatment of a Push-Pull "Echo" Test.
Part II - Application of the Convection-Dispersion Equation.

Sverre G. Johnsen and Curtis H. Whitson
Submitted to *The Journal of Transport in Porous Media*

Abstract

The semi-analytical stream-line based model developed and validated in a previous paper is used to study the effects of varying the injection phase duration. It is shown that for a given set of boundary values and test-parameters there exists a theoretical maximum injection phase duration giving conservative tracer production. The model is used to study the tracer production profiles as the injection phase duration is extended to values larger than this limit. The applicability of the one-dimensional convection-dispersion equation on calculating apparent dispersivity Peclet numbers is studied, as the injection phase duration is increased. It is shown how it fails to predict the volume of recoverable tracer and how it fails to fit the measured data. It is also shown how a strongly scale depending apparent dispersivity may occur in a model, with no physical dispersion, due to natural drift only.

Keywords Analytical, One-dimensional Convection-Dispersion Equation, Contamination, Echo test, Macroscopic dispersion, Natural drift, Push-pull test, Stream-line, Tracer

1 Introduction

In 1981 Pickens and Grisak, [[8]], reported from two full-scale single-well push-pull tests, SW1 and SW2, performed using two neighbouring wells in the same aquifer. Push-pull tests, also known as echo or injection-withdrawal tests, are single-well tests where an injection phase "pushing" injectant containing a tracer into the well is followed by a production phase where fluids are "pulled" out of the well. Tracer concentrations in the producing fluids are measured during the production phase.
Laboratory experiments on core-samples from the test site gave a dispersivity of approximately $0.035cm$, whereas the field tests, neglecting natural groundwater-drift, gave $3cm$ and $9cm$, respectively, fitting the one-dimensional convection-dispersion equation (1D CD-EQ) to the test data. Pickens and Grisak conclude that the great variations are due to a strong scale dependency in apparent dispersivity; others also suggest the same, [[3]], [[7]].

Recently Coats *et al.*, [[4]], have shown that the large dispersivity reported by Pickens and Grisak may be mainly due to natural drift of the in situ ground water. Coats *et al.* remind that all experimental evidence show that dispersivity is a rock property and that any "apparent" scale dependence of dispersivity derived from

produced-well concentration profiles[4] must be due to other physical phenomena such as drift.

In part I of this work, [[6]], we introduced a stream-line based model with no physical dispersion, and we showed how natural drift alone might cause the apparent dispersivity reported by Pickens and Grisak. In the stream-line based model it was assumed that the injectant and the in situ fluids were incompressible fluids with identical fluid properties. Viscosity was assumed constant and temperature, pressure and density variations were neglected, i.e., no gravitational, viscous or thermodynamic effects were taken into account. It was furthermore assumed that the tracer was ideal, i.e., chemically and physically stable, not interacting with in situ fluids or solids and not naturally present in the reservoir. It was also assumed that the injectant and the in situ fluids were miscible and displace each other perfectly, maintaining a sharp interface between the two fluids, hence all mixing will occur in the well-bore, during the production phase. Unless otherwise stated all results shown in this paper are obtained using the stream-line based model developed in [[6]], with constant injection/production rates. For a complete understanding of the mathematics of the stream-line based model, we refer to part I. Only a few of the key-equations are given in this text.

As will be shown, there exists, in the stream-line based model, a theoretical maximum injection phase duration, T_c, for which tracer-production is conservative[5]. The T_c depends on injection-rate, production-rate, natural groundwater drift velocity and well radius. For injection phase durations, T_i, larger than this limit, some of the injected tracer will be lost and cannot be produced back unless the production-rate is increased. As T_i increases, the tracer production profile will obtain an increasingly long tail, and when $T_i \geq T_c$ the production profile approaches 0 asymptotically. The effect of injection phase durations larger than T_c has been studied for $T_i \in [T_c, \infty)$, and it is shown that the dimensionless time of breakthrough as well as the integral of the tracer production-profile goes to zero as $T_i \to \infty$. Production profiles were created for a selection of T_is and the 1D CD-EQ were fitted to the profiles. The apparent dispersivities from the best fit procedure were plotted versus length travelled, and even though the model is free of physical dispersion, the system shows a strong scale dependency of the apparent dispersivity. It is also argued that the 1D CD-EQ lack some of the key properties of a real concentration profile and that fitting the 1D CD-EQ to experimental data has no value for large T_is. First, a real concentration profile must take the value 1 at $t_p = 0$, whereas the 1D CD-EQ concentration profile will be smaller than 1

[4] *Production profiles* and *concentration profiles* refer to the normalised concentration of tracer in the produced fluid either as a function of time, t_p, or as a function of dimensionless volume produced, $Q_D = \frac{|Q_p| t_p}{Q_i T_i}$.

[5] By conservative tracer-production we mean that all the injectant is recoverable.

for all $t_p \geq 0$, for any N_{Pe}. Second, the integral of the concentration profile, from 0 to ∞ should be 1 or smaller, whereas the integral of the CD-EQ concentration profile seems to be larger than 1, although this is not strictly proven. The apparent dispersivity resulting from fitting the 1D CD-EQ to experimental data cannot be expected to be a measure of the physical dispersivity.

1.1 The Stream-Line Based Model

The Velocity Field

The model presented in [[6]] is based on solving the source/sink in a uniform stream problem, [[10]]. The problem is charaterised by the velocity field

$$U_r = U_u \cos\theta + \frac{Q}{r} , \tag{1a}$$

$$U_\theta = -U_u \sin\theta , \tag{1b}$$

where U_u is the natural drift velocity of the ground-water and $Q = \frac{q}{2\pi\phi}$ is the re-formulated 2-dimensional rate of injection/production. By definition Q is positive when injecting and negative when producing.

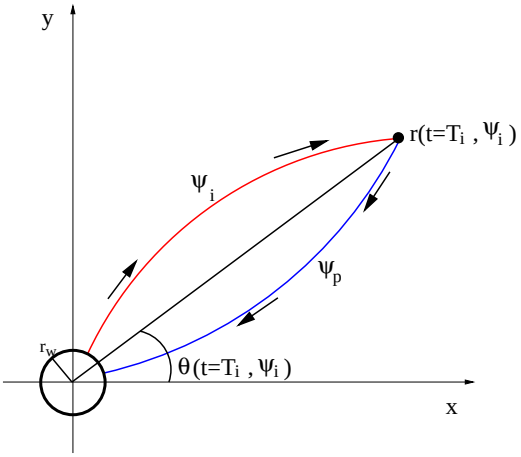

Figure 1: General view of the trace of a fluid particle leaving the wellbore at the radius r_w at the time $t = 0$. The trace is described by the injection phase stream-line ψ_i until the particle reaches it's maximum radial advancement r_{max} at the time $t = T_i$ and thereafter by the production phase stream-line ψ_p until it is back at the well-bore radius r_w.

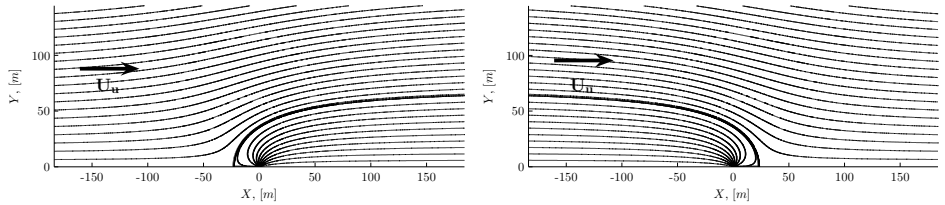

(a) Injection phase (b) Production phase

Figure 2: General picture of stream-lines, or constant ψ contours, in the upper half-plane, in the sink/source in a uniform stream model. Injection- and production-rates are symmetrical, so the two cases are mirror images of each other. The Rankine Half-body is shown as the emphasised stream-lines. Source, in (a), and Sink, in (b), are located at the origin and the uniform stream velocity vector points in the positive x-direction, as indicated.

Stream-Lines

In [[6]] it was shown how a push-pull test could be solved semi-analytically by tracing a finite number of individual flow-paths and keeping track of the tracer front position along each path. The tracer front position will move along the stream paths in the same way as the fluid particles will, as shown in **Figure 1**. The flow-paths or stream-line contours are given by the real numbers

$$\psi_i = U_u \cdot r \sin\theta + Q_i \theta \ , \tag{2a}$$

and

$$\psi_p = U_u \cdot r \sin\theta - |Q_p| \theta \ , \tag{2b}$$

during the injection and production phases, respectively. By definition, [[10]], the fluids on a stream-line are confined there, i.e., a fluid particle with a given ψ will stick to this number until the streaming conditions are altered, hence, knowing the stream-line number, ψ, we have a relation between angle and radius, and knowing the velocity field, we may calculate the tracer front position at any given time. In **Figure 2(a)** and **Figure 2(b)**, it can be seen how the constant ψ contours form flow-paths during the injection and production phases, respectively.

Break-Through

In [[6]] it was shown how the time of break-through for clean water[6], for each stream-line, may be calculated. Tracing a thousand stream-lines, using the test parameters, given by Pickens and Grisak, [[8]], [[6]], **Figure 3(a)** and **Figure 3(b)** were obtained, comparing the two Pickens-Grisak field tests with numerical simulation results by Coats *et al.* and results from the semi-analytical stream-line based model.

[6]Clean water is defined as water containing no tracer.

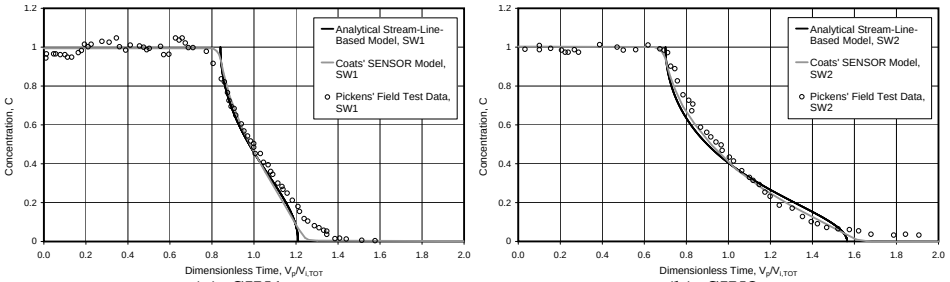

(a) SW1 (b) SW2

Figure 3: Producing tracer concentration vs. dimensionless time, Volume produced/Total volume injected , comparing the Pickens-Grisak field test data, numerical simulation results from the Coats *et al.* SENSOR model and results from the Johnsen-Whitson semi-analytical stream-line-based model, for SW1 and SW2 test parameters, respectively.

2 The Effect of Long-Lasting Injection Phases

2.1 Asymptotic Value for the Time of Break-Through

As the duration of the injection phase increases, the maximum up-stream radial position approaches the injection phase stagnation point in $(x,y) = \left(-\frac{Q_i}{U_u}, 0\right)$ asymptotically. As the time of break-through is a direct consequence of the up-stream radial position at time T_i, the time of break-through must also approach some value asymptotically, as the injection phase duration is increased. The time of break-through, as a function of injection phase duration, keeping all other parameters constant, is shown in **Figure 4**, for both SW1 and SW2 test-parameters. The times needed, for a particle located in the injection phase stagnation-point at $t_p = 0$, with SW1 and SW2 test-parameters, to travel back to the test-well, $T_{BT,max}$, are shown as horizontal asymptotes. The critical times, T_c, are shown as vertical lines. In **Figure 5** the dimensionless volume produced at the time of break-through, $\frac{|Q_p|T_{BT}}{Q_i T_i}$, is shown as a function of injection phase duration, T_i. It can be seen how the dimensionless volume produced at $t_p = T_{BT}$ goes to zero as T_i is increased.

2.2 Lost Injectant

As can be seen from Equation 1 , there exists a production-phase stagnation point, where all velocity components become zero, in $(x,y) = \left(\left|\frac{Q_p}{U_u}\right|, 0\right)$. From Equation 2 we see that the stagnation point is passed through by the stream-line defined by $\psi_p = 0$. In Figure 2(b) the $\psi_p = 0$ stream-line is emphasised. Injectant that crosses the boarder defined by this production phase stream-line is lost and cannot

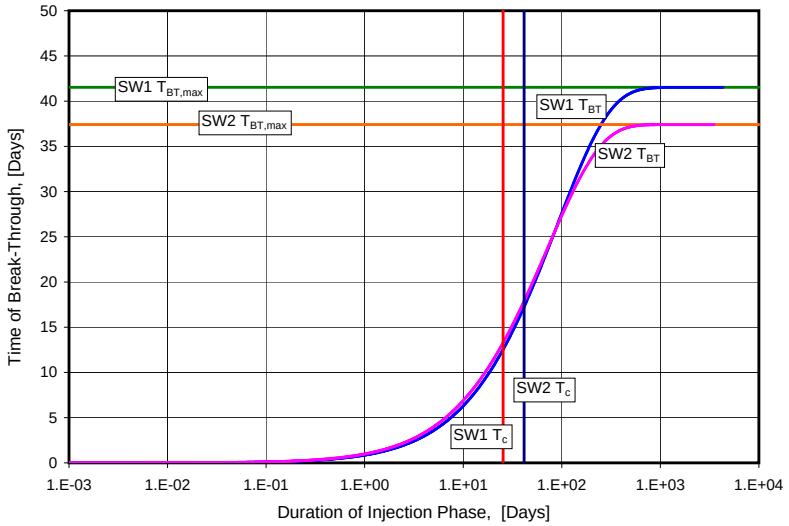

Figure 4: Time of clean water break-through, T_{BT}, versus duration of the injection phase, for the Pickens-Grisak SW1 and SW2 conditions, calculated with the semi-analytical model developed in [[6]]. The $T_{BT,max}$ horizontal lines show the time needed to produce back a fluid particle situated at the injection phase stagnation point at $t_p = 0$. As T_i increases, the tracer front gets closer to the stagnation point, and the time of break-through gets closer to the asymptote defined by $T_{BT,max}$. The critical times, T_c, are represented by the vertical lines.

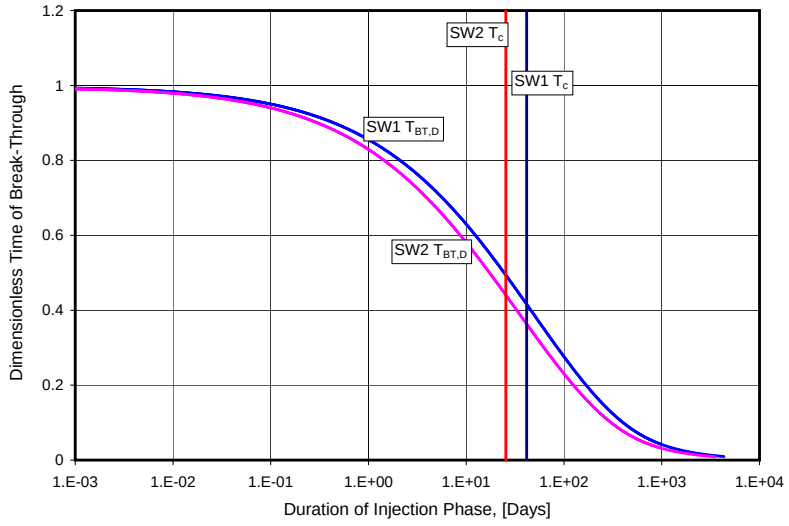

Figure 5: Dimensionless time of break-through, $\frac{Q_p T_{BT}}{Q_i T_i}$, versus duration of the injection phase, T_i, calculated using the semi-analytical model developed in [[6]]. Vertical lines represent the critical times, T_c, for SW1 and SW2, respectively.

be recovered unless the production rate is increased.
$\psi_p = 0$ gives

$$r = \frac{|Q_p|}{U_u} \cdot \frac{\theta}{\sin\theta} , \tag{3a}$$

$$\Downarrow$$

$$\frac{dr}{d\theta} = \frac{|Q_p|}{U_u} \cdot \frac{\sin\theta - \theta\cos\theta}{\sin^2\theta} \geq 0 \; \forall \; \theta \in [0,\pi] , \tag{3b}$$

which means that the distance from the well to the $\psi_p = 0$-stream-line is monotonically increasing and is at it's minimum for $\theta = 0$.
The velocity vector field gives

$$\vec{u}_i = \frac{1}{r}\left(U_u \cdot r\cos\theta + Q_i\right)\hat{\boldsymbol{r}} - U_u \sin\theta \cdot \hat{\boldsymbol{\theta}} , \tag{4a}$$

$$\Downarrow$$

$$|\vec{u}_i|^2 = \frac{2U_u Q_i}{r}\cos\theta + U_u^2 + \frac{Q_i^2}{r^2} , \tag{4b}$$

$$\Downarrow$$

$$\frac{d|\vec{u}_i|^2}{d\theta} = -\frac{2U_u Q_i}{r}\sin\theta \leq 0 \; \forall \; \theta \in [0,\pi] , \tag{4c}$$

meaning that the velocity at a given radius is decreasing monotonically with θ. Since the angle $\theta = 0$ both give the shortest path to the $\psi_p = 0$ boundary and at all radii give the highest fluid velocity, the $\psi_p = 0$ boundary will be crossed by the $\theta = 0$ injectant first.

During the injection phase, we have, for $\theta = 0$, from Equation 1 ,

$$\vec{u}_i = \frac{dr}{dt} \cdot \hat{\boldsymbol{r}} = \left(U_u + \frac{Q_i}{r}\right)\hat{\boldsymbol{r}} , \tag{5}$$

and by integrating

$$dt = \frac{dr}{|\vec{u}_i|} \tag{6}$$

from $r = r_w$ to $\left|\frac{Q_p}{U_u}\right|$, we find that the $\psi_p = 0$ stream-line will be crossed at the time

$$T_c = \frac{1}{U_u^2}\left(|Q_p| - U_u r_w + Q_i \ln\left|\frac{U_u r_w + Q_i}{|Q_p| + Q_i}\right|\right) , \tag{7}$$

which will be referred to as *the critical time*. If $T_i \geq T_c$ some of the injectant will be lost.

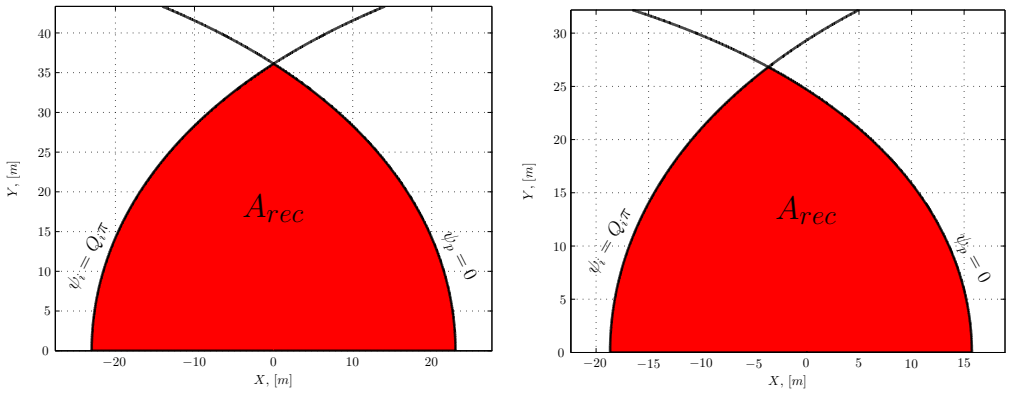

(a) SW1 (b) SW2

Figure 6: Theoretically recoverable tracer covered area, A_{rec}, bound by the injection and production phase boundary stream-lines, for SW1 and SW2 test-parameters.

2.3 Infinite Injection Phase

During the injection phase, the up-stream tracer transport is limited by the injection phase stream-line $\psi_i = Q_i\pi$, but the down-stream tracer transport is unbound. During the production phase the stream-line $\psi_p = 0$ defines a boundary between recoverable and non-recoverable fluids, as seen in Figure 2(b) . Hence, the maximal volume of tracer produced back will be proportional to the area bound by these two boundary stream-lines, as shown in **Figure 6**. The hatched area is, however, an asymptotic value, and it will neither be entirely covered with tracer nor entirely recovered within a finite time-scale. The shape of the area is determined by the test-parameters as well as the porosity, permeability and natural groundwater velocity.

As is shown in Figure 4 , the time of break-through approaches an asymptotic value as the duration of the injection phase goes to infinity. The asymptotic value is the time needed, for a particle located in the injection phase stagnation-point at $t_p = 0$, to travel to the production well. The total volume of tracer injected, Q_iT_i, however, is not limited, so

$$\lim_{T_i \to \infty} \frac{|Q_p| T_{BT}}{Q_i T_i} = 0 \, . \tag{8}$$

That is, the dimensionless volume produced at the time of break-through will go to zero as the duration of the injection phase goes to infinity, as indicated in Figure 5 . The total recoverable volume of tracer is given by

$$V_{t,tot} = \int_0^\infty V_t(t_p) dt_p \, , \tag{9}$$

where $V_t(t_p)$ is the volume of injectant recoverable in the time interval $(t_p, t_p + dt_p)$. For $T_i < T_c$, all the injected tracer is recoverable, and $V_{t,tot} = |Q_p|T_p = Q_i T_i$. $V_t(t_p)$ may be expressed by a concentration-function, $0 \leq C(t_p) \leq 1$, multiplied by the production rate, so that

$$V_{t,tot} = \int_0^\infty |Q_p| C(t_p) dt_p \ . \tag{10}$$

Making the change of variable, $Q_D = \frac{|Q_p| t_p}{Q_i T_i}$, we get

$$\int_0^\infty C(Q_D) dQ_D = \frac{V_{t,tot}}{Q_i T_i} \ , \tag{11}$$

so the integral of the concentration, $C(Q_D)$ equals one, for $T_i < T_c$. We have no analytical expression for the concentration profile, and neither do we have an analytical expression for the shape of the tracer front, so we cannot, in general, calculate the integral of C. All we can say is that for $T_i > T_c$, the integral of $C(Q_D)$ is, due to the loss of tracer, smaller than one. We can summarise our knowledge of $C(t)$ in the following way;

$$C(t_p) = \begin{cases} 1 & \text{for } t_p < T_{BT} \\ 0 & \text{for } t_p \to \infty \end{cases} \ , \tag{12a}$$

$$\int_0^\infty C(Q_D) dQ_D = \begin{cases} 1 & \text{for } T_i < T_c \\ 0 & \text{for } T_i \to \infty \end{cases} \ . \tag{12b}$$

In **Figure 7** concentration profiles are shown, for various injection phase durations, for SW1 and SW2 parameters, respectively.

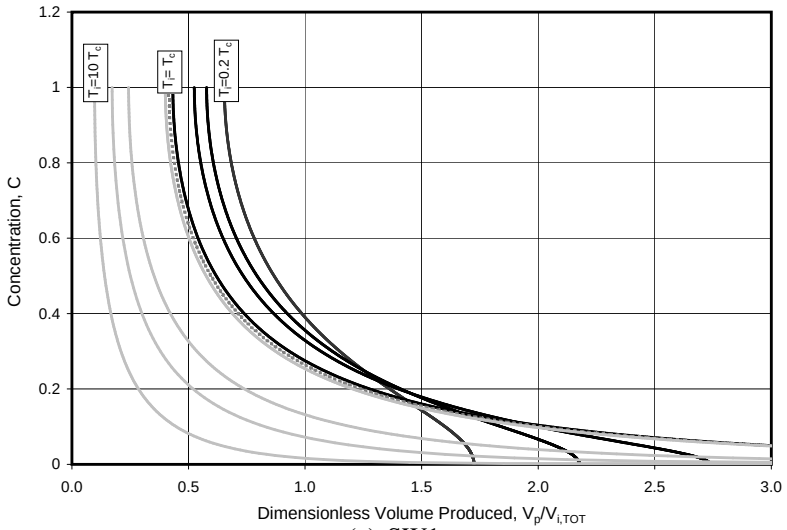

(a) SW1

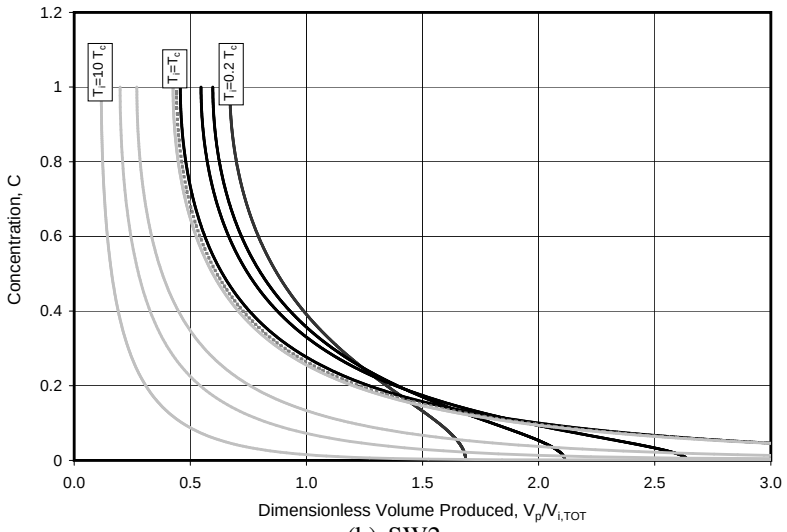

(b) SW2

Figure 7: Concentration profiles for various injection phase durations, $T_i = a \cdot T_c$, for SW1 and SW2 test parameters, respectively, where $a \in \left[0.2,\ 0.35,\ 0.5,\ 0.9,\ 1.0,\ 1.1,\ 3.0,\ 5.0,\ 10.0\right]$, calculated using the semi-analytical model developed in [[6]].

3 The 1-Dimensional Convection-Dispersion Equation

The Aronofsky-Heller, [[2]], convection-dispersion equation (CD-EQ), at a fixed spatial point, is widely used to fit the producing concentration profiles in single-well tests, C_{CD} for concentration of clean water and $(1-C_{CD})$ for injectant concentration[7]. The CD-eq is given by, [[4]],

$$C_{CD}(PV_{inj}) = \frac{1}{2}\text{erfc}\left(\frac{1-PV_{inj}}{2\sqrt{PV_{inj}/N_{Pe}}}\right) + \frac{e^{N_{Pe}}}{2}\text{erfc}\left(\frac{1+PV_{inj}}{2\sqrt{PV_{inj}/N_{Pe}}}\right) , \quad (13)$$

where, [[1]],

$$\text{erfc}(z) = 1-\text{erf}(z) , \quad (14)$$

$$\text{erf}(z) = \frac{2}{\sqrt{\pi}}\int_0^z e^{-t^2}dt , \quad (15)$$

and the Peclet number, N_{Pe}, is a shaping parameter. The Peclet number is defined as the scale, L, divided by the dispersivity, α, [[4]]. $C_{CD}(PV_{inj})$ has the the following properties, [[2]];

$$C_{CD}(PV_{inj}) = \begin{cases} 0 & \text{for } PV_{inj}=0 \\ 1 & \text{for } PV_{inj}\to\infty \end{cases} . \quad (16)$$

The Aronofsky-Heller dimensionless pore-volumes injected, PV_{inj}, is related to the dimensionless volume produced, Q_D, by the relation,

$$PV_{inj} = \frac{1}{2}(Q_D+1) , \quad (17)$$

as seen in Equation A3 . Using the CD-EQ to fit the Pickens-Grisak field data, we obtain Peclet numbers of 56.4 and 27.4, for the SW1 and SW2 tests, respectively. For the semi-analytical model developed in [[6]], using the SW1 and SW2 test parameters, we obtain Peclet numbers of 161.5 and 70.0, respectively, as seen in **Figure 8**. In **Figure 9** it can be seen how the CD-equation best-fit Peclet number varies with the ratio T_i/T_c for SW1 and SW2 parameters, respectively. The sum-of-squares error is plotted along with the Peclet numbers. For $T_i > T_c$, some of the tracer front points being traced are in the non-recoverable area. The stream-lines belonging to these points were simply discarded, hence the number of stream-lines traced will decrease as T_i is increased. It can, in Figure 9 , be seen that the

[7]For two-well transmission-tests, C_{CD} is the concentration of injectant, and $(1-C_{CD})$ is the concentration of clean water.

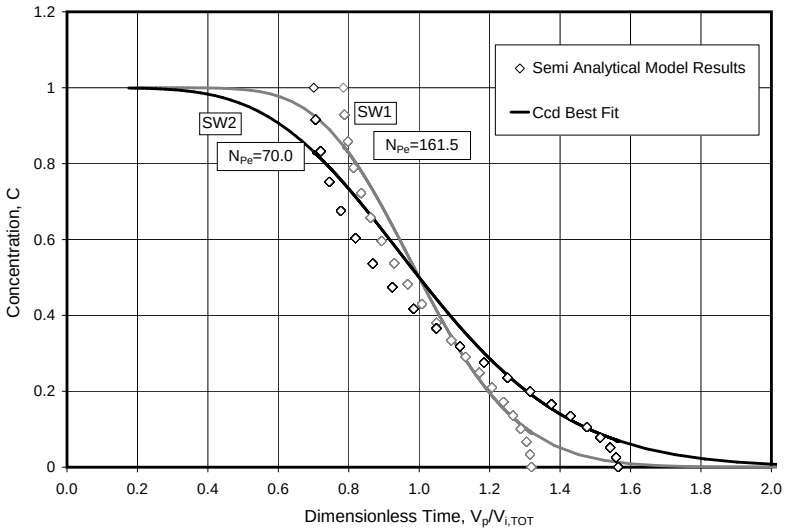

Figure 8: CD-EQ best fit to the analytical model results for SW1 and SW2 test parameters, respectively. The best fit Peclet numbers were 161.5 for SW1 parameters and 70.0 for SW2 parameters, respectively. The fits are based on a thousand data-points, and were not significantly affected by increasing the number of points.

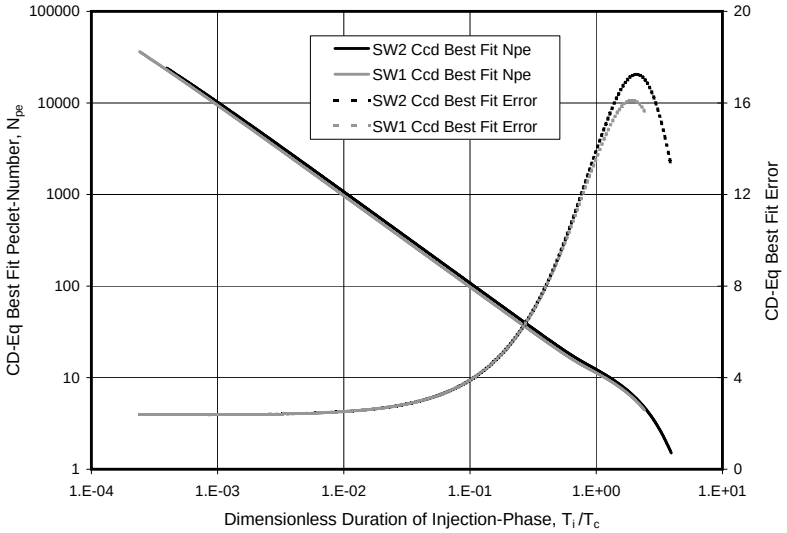

Figure 9: CD-eq. best-fit Peclet numbers and respective sum-of-square-errors for SW1 and SW2 test parameters, as functions of $\frac{T_i}{T_c}$.

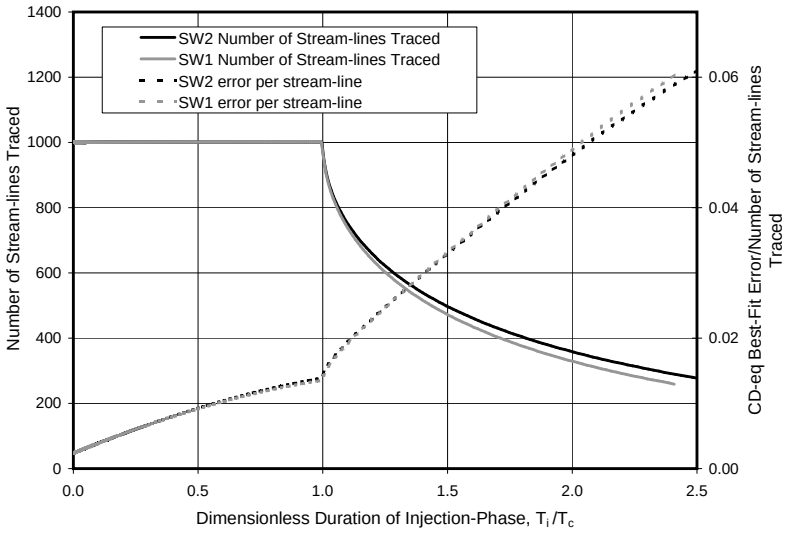

Figure 10: The number of stream-lines traced and average square error per stream-line versus $\frac{T_i}{T_c}$ for the Pickens-Grisak SW1 and SW2 parameters.

total N_{pe} sum-of-squares error decreases as T_i increases. However, as can be seen in **Figure 10**, the number of stream-lines traced decreases also, so that the average error per stream-line keeps increasing as T_i is increased beyond T_c.

3.1 Scale-Dependency of the Dispersivity

Figure 11 is the same as the Coats *et al.* Fig.17, [[4]], where apparent dispersivity versus length traveled is added for the semi-analytical model results. The apparent dispersivity is given by

$$\alpha_a = \frac{L}{N_{Pe}}\ , \tag{18}$$

where L is the length traveled. $L = 2 \cdot L_m$, where
$L_m = \left(\sqrt{2Q_i \cdot T_i + r_w^2} - r_w\right)$ is the mean maximal tracer front travel distance, has been used. Even though the semi-analytical model is free of physical dispersion, there is a strong scale-dependency in the CD-EQ-calculated apparent dispersivity of the model results.

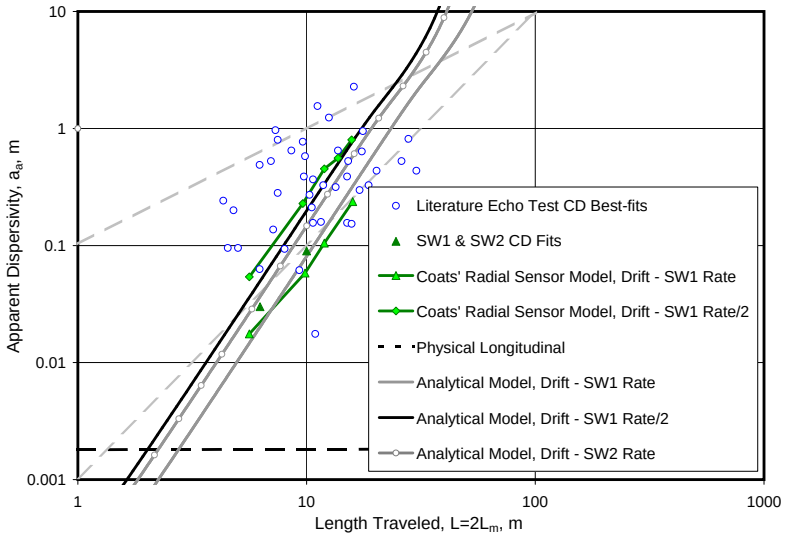

Figure 11: The Coats *et al.* Fig. 17, [[4]], with apparent dispersivity scale dependency for the stream-line based SW1 and SW2 models.

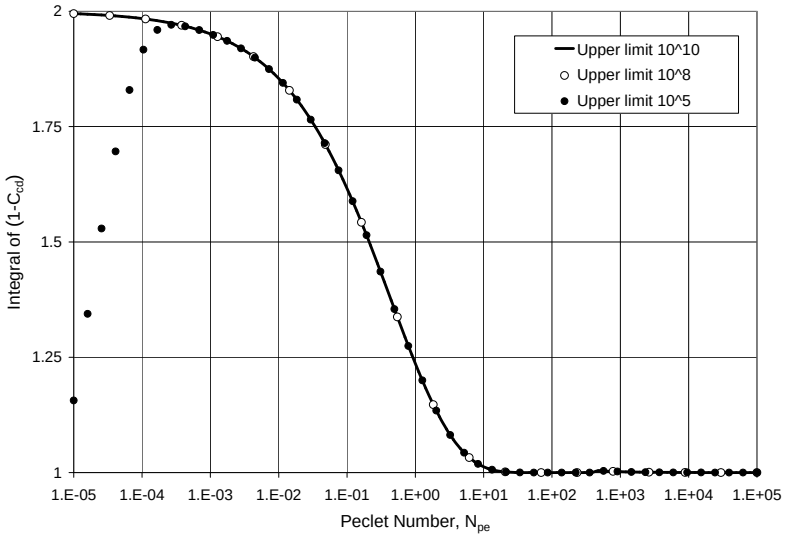

Figure 12: Numerical calculation of $\int_0^{limit} (1 - C_{CD}(Q_D))\, dQ_D$, as a function of the Peclet number, N_{Pe}. The integral is calculated for three different upper limits, 10^5, 10^8 and 10^{10}.

3.2 The Integral of the Production Profile

Using the *quadl*[8] routine in The Mathworks's MATLAB, [[9]], we have calculated the integral $\int_0^\infty (1 - C_{CD}(Q_D))\ dQ_D$ for different Peclet numbers, as seen in **Figure 12**. As the *quadl* routine may not use an infinite upper limit, we have calculated the integral using the upper limits $Q_D = 10^5$, 10^8 and 10^{10}. As can be seen in Figure 12 , there is no noticeable difference in the results, for $N_{Pe} > 10^{-3}$, so we conclude that the left-out tail of the integral is negligible. It can be seen from Figure 9 that the Peclet number is about 10 for $T_i = T_c$ and is decreasing for increasing T_is. In Figure 12 we see that the integral starts deviating noticeably from 1 at approximately $N_{Pe} = 10$. As T_i becomes larger than T_c we no longer have conservative tracer production, and we would expect the integral of the production profile to decrease, becoming smaller than 1 and approaching zero for $T_i \to \infty$. The integral of the $\left(1 - C_{CD}\right)$ concentration profile, however, increases and we therefore have to realise that the 1D CD-EQ will provide an increasingly poor fit when extending the injection phase duration, T_i.

3.3 Boundary Values of the CD-EQ

Another problem with the CD-equation becomes clear when we look at the concentration profile at $t_p = 0$, or rather $Q_D = 0$, where $PV_{inj} = 1/2$. Here, a real concentration profile must take the value 1. The 1D CD-EQ, however, takes the value 0 for $PV_{inj} = 0$ and increases monotonically, so in general $\left(1 - C_{CD}(PV_{inj} > 0)\right) < 1$, which contradicts Equation 12a . For relatively large N_{Pe} the deviation from 1 is negligible, but for large T_i, the N_{Pe} decreases and $\left(1 - C_{CD}(PV_{inj} > 0)\right)$ becomes noticeably smaller than 1.

In **Figure 13** 1D CD-EQ best fits are shown for injection phase durations of 0.2 and 10 times the critical time, T_c, for SW1 and SW2 test parameters. Peclet numbers are 49.0, 0.91, 54.1 and 0.11 for the short and long injection phases, for SW1 and SW2, respectively. It is evident that the fit to the $10 \cdot T_c$ production profile is of little value.

[8]The MATLAB *quadl* routine approximates the integral of a function between two finite limits to within a default error of 10^{-6} using recursive adaptive Lobatto quadrature, [[9]], [[5]].

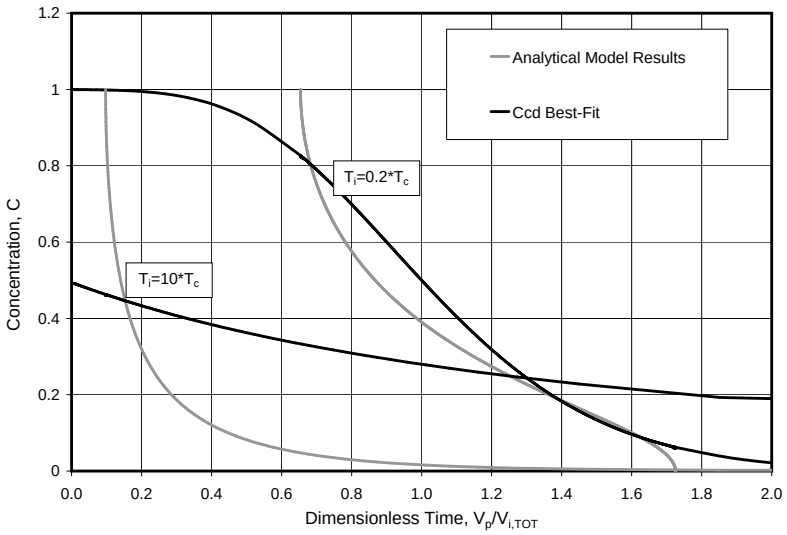

(a) SW1

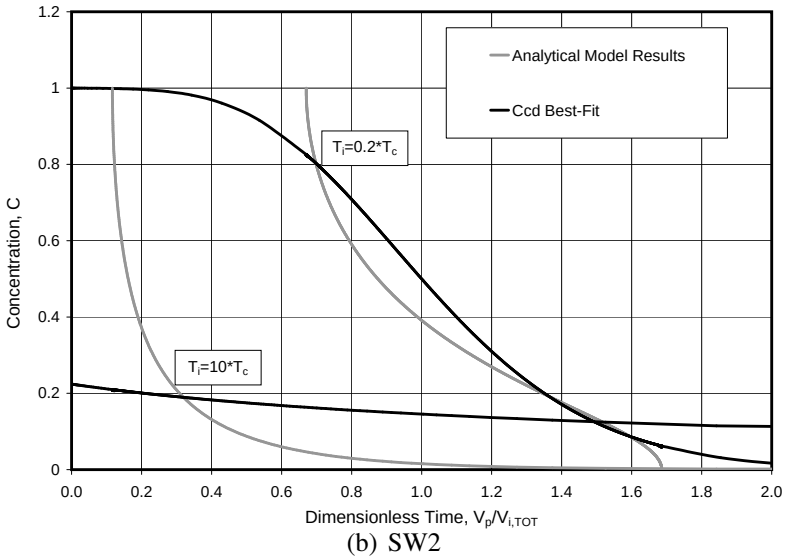

(b) SW2

Figure 13: CD-equation best fits to analytical model results for $T_i = 0.2 \cdot T_c$ and $T_i = 10 \cdot T_c$, for SW1 and SW2 test parameters, respectively.

4 Conclusion

1. For injection phase durations, T_i, larger than some critical time, T_c, the tracer production is not conservative, and the 1-dimensional Convection-Dispersion equation will no longer fit the producing tracer concentration profile well.

2. For $T_i < T_c$, the Peclet number plots linearly vs. T_i in a log-log diagram, using the SW1 and SW2 test parameters.

3. A strong scale dependency of the apparent dispersivity has been found even though the physical dispersivity of the model per definition is zero.

4. The apparent dispersivity resulting from fitting the one-dimensional convection-dispersion equation cannot be expected to be a measure of the physical dispersivity.

A Converting from PV_{inj} to Q_D

In the Aronofsky-Heller CD equation, [[2]], the variable used is Pore-Volumes injected, PV_{inj}, when comparing single-well field test data with the CD-EQ solution it is, however, convenient to introduce the variable dimensionless volume produced, $Q_D \equiv \frac{V_p}{V_{i,TOT}}$. The Aronofsky-Heller 1D CD-EQ applies to an infinitely

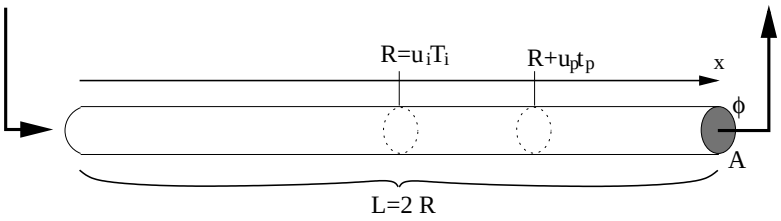

Figure 14: The Aronofsky-Heller two-well transmission test stream-tube of length $L = 2R$, cross-section A and fractional porosity ϕ.

long stream-tube where tracer is injected at one end and the tracer concentration is measured at the other end, as in a two-well transmission test. Frequently however, the 1D CD-EQ is used to assess the dispersivity in single-well push-pull tests as well. To convert the Aronofsky-Heller PV_{inj} to Q_D in a single-well test, we need to view the single-well test as an equivalent two-well test. Studying one stream-tube only, assume that the tracer front[9] has moved the distance R at the end of the injection phase, such that $R = u_i \cdot T_i$, where u_i is the constant fluid velocity

[9]The tracer front is defined as where the tracer concentration is 0.5.

during the injection phase and T_i is the duration of the injection phase. During the production phase, the tracer front must move the same distance back to the producer. Hence, the 1-dimensional stream-tube single-well test, where the tracer front moves the distance $2R$, is equivalent to the 1-dimensional stream-tube two-well test, where the tracer front moves the distance $L = 2R$, as shown in **Figure 14**. In the two-well test, the tracer front will reach the producer the moment one Pore-Volume has been injected, i.e., $PV = A\phi L$, and

$$PV_{inj} = \frac{V_{inj}}{PV} \ . \tag{A1}$$

During the production phase of the single-well test we get

$$PV_{inj} = \frac{A\phi R + q_p t_p}{2A\phi R} \ , \tag{A2}$$

where $V_{i,TOT} = A\phi R$ is the total volume injected during the injection phase, and $V_p = q_p t_p$ is the volume produced, so

$$PV_{inj} = \frac{1}{2}\left(\frac{V_p}{V_{i,TOT}} + 1\right) = \frac{1}{2}\left(Q_D + 1\right) \ . \tag{A3}$$

References

[1] M. Abramowitz and I.A. Stegun, editors. *Handbook of Mathematical Functions*. Dover Publications, inc., 1964.

[2] J.S. Aronofsky and J.P. Heller. A diffusion model to explain mixing of flowing miscible fluids in porous media. *Trans AIME*, 210:345–349, 1957.

[3] A. Arya, T.A. Hewett, R.G. Larson, and L.W. Lake. Dispersion and reservoir heterogeneity. *SPERE*, 3:139–148, 1988. SPE 14364.

[4] K. H. Coats, C.H. Whitson, and L.K. Thomas. Modelling conformance as dispersion. SPE Annual Technical Conference and Exhibition, 26-29 September, Houston, Texas, September 2004. SPE 90390.

[5] W. Gander and W. Gautschi. Adaptive quadrature - revisited. *BIT*, 40(1):84–101, March 2000.

[6] Sverre G. Johnsen and Curtis H. Whitson. Analytical Treatment of a Push-Pull "Echo" Test, Part I - Development of a Single Layer Solution. Submitted to Transport in Porous Media, 2007.

[7] J. Mahadevan, L.W. Lake, and R.T. Johns. Estimation of true dispersivity in field scale permeable media. SPE/DOE Improved Oil recovery Symposium, Tulsa, Oklahoma, USA, April 2002. SPE 75247.

[8] J.F. Pickens and G.E. Grisak. Scale-dependent dispersion in a stratified granular aquifer. *Water Resources Research*, 17(4):1191–1211, 1981.

[9] The Mathworks web page. http://www.mathworks.com/, 2006.

[10] F.M. White. *Fluid Mechanics*. McGraw - Hill, New York, USA, 5th edition, 2003.

Paper III

Analytical Treatment of a Push-Pull "Echo" Test.
Part III - Layering Treatment.

Sverre G. Johnsen and Curtis H. Whitson
Submitted to *The Journal of Transport in Porous Media*

Abstract

Based on a semi-analytical stream-line based model developed in a previous paper, we study injection/production in stratified aquifers of infinite areal extent, subject to natural groundwater drift. Injectant and in situ groundwater are assumed to be miscible, incompressible fluids with identical fluid properties. Only macroscopic flow is considered, and flow is assumed to experience no in situ fluid mixing (physical dispersion) so fluid interfaces remain sharp, and all mixing occurs in the well-bore. Analytical results give an excellent match to field study data provided by Pickens and Grisak.

Keywords Analytical, Contamination, Dynamic Aquifer, Echo test, Layering, Natural drift, Push-pull test, Stratification, Stream-line, Tracer, Water

1 Introduction

In a previous paper, Part I, [[3]], we developed a semi-analytical single-layer, stream-line based model to predict production profiles in single-well push-pull “Echo” tests. The model was verified by comparing with experimental data, from two field-scale single-well tests, SW1 and SW2, provided by Pickens and Grisak, [[7]], and with numerical simulation data provided by Coats *et al.*, [[2]], as seen in **Figure 1**.

In Part II, [[4]], we pointed out several weaknesses in the traditional way of applying the 1-dimensional Convection-Dispersion Equation to assess dispersivity in single-well push-pull tests.

This paper, Part III, is basically an extension of part I, [[3]], and the two papers should really be read as one. Topics covered in Part I is generally not covered here.

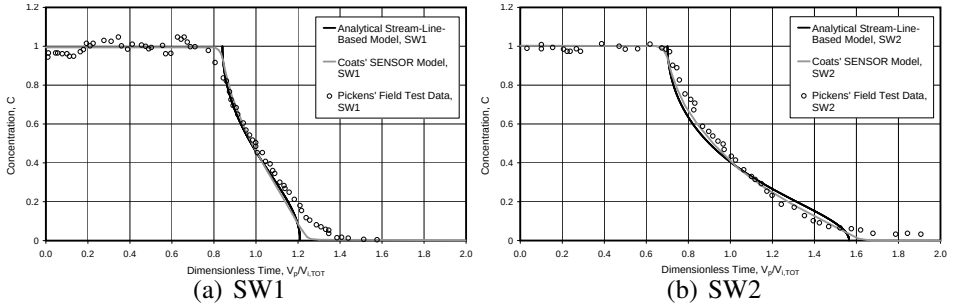

(a) SW1 (b) SW2

Figure 1: Producing tracer concentration vs. dimensionless time, Volume produced/Total volume injected , comparing the Pickens-Grisak field test data, numerical simulation results from the Coats *et al.* SENSOR model and results from the Johnsen-Whitson semi-analytical stream-line-based model, for SW1 and SW2 test parameters, respectively.

In Section 2, however, we give a short summary of the mathematical formulae derived in Part I. Part II does not supply much mathematical foundation for this paper, but will provide motivation for understanding and applying the techniques we propose.

For years the natural groundwater drift has been neglected when assessing push-pull test production profiles, and field scale dispersivities have been over predicted by several orders of magnitude compared to laboratory dispersivities. Coats *et al.*, [[2]], suggest that the natural drift affects the apparent dispersivity more than the physical dispersivity does. Their numerical simulation results support their suggestion, and so does our semi-analytical model where physical dispersion is zero per definition, and the apparent dispersion is all due to the natural groundwater drift.

In this paper the single-layer homogeneous model developed in [[3]], is extended to a stratified heterogeneous model, where porosity and/or permeability may vary from layer to layer. Pickens and Grisak, [[7]], provided stratification data from their test site, which is used in the model. We judge the excellent match to the experimental data, by the layered model presented in this paper, to be a conclusive verification of the Coats *et al.* suggestion.

Comparing the Part I-model to the Pickens-Grisak field data, it was assumed that the areal extent of the aquifer was infinite, that the reservoir thickness was 8.2 m, as reported by Pickens and Grisak, and that the test well fully penetrated the reservoir. Furthermore it was assumed that the aquifer had a homogeneous fractional porosity of 0.38 and permeability of 14.8 *darcy*. Following Coats *et al.*, a natural gradient of 0.052 kPa/m was assumed.

In this paper, the homogeneous single-layer methodology is applied to each layer in a multi-layered aquifer model consisting of a finite number of horizontal layers of equal or varying thickness and rock properties, and we study the effect of layering on the producing tracer concentration. It is assumed that the natural pressure gradients in each layer are identical and that pressure changes spread momentarily throughout the reservoir. It is also assumed that there is no cross-flow between different layers, that all flow is strictly 2-dimensional. Partial producing tracer rates from each layer are summed and normalised to present the fractional tracer concentration of the producing well-stream. For a reservoir with no natural drift it is shown that there is no effect of varying permeability and/or porosity. It is shown, however, that the effect of varying permeability and/or porosity in a reservoir subject to natural drift is the same as that of multiplying the injection phase duration, T_i, with the scaling factor $\mathscr{C}_j = \frac{\phi_A}{\phi_j}\frac{k_A}{k_j}$ in each layer, j.

In **Figure 2** the well configuration at the Pickens-Grisak test site is shown. The Pickens-Grisak SW1 and SW2 tests were performed in the wells P1 and P3, respectively. Stratigraphic interpretations by Cherry et al, [[1]], are shown in

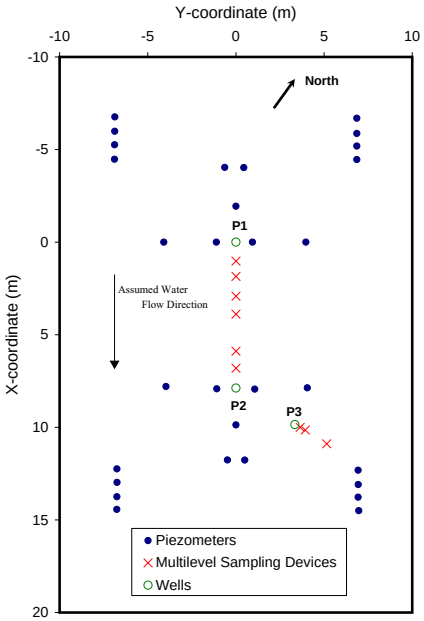

Figure 2: Test site well configuration. Well coordinates are taken from Fig. 4 in [[7]] and the direction of the north arrow is taken from Fig. 5 in [[6]]. Assumed water flow direction is interpreted from Figure 1 in [[3]].

Figure 1 in Part I, [[3]]. The north-arrow in Figure 2 makes an angle of 29.5° to the line passing through the wells P1 and P2, and the Y-Y' line, in Figure 1 of Part I, makes an angle of between 24° and 31.5° with the north-arrow. It will be assumed that the natural drift is parallel to the line passing through the wells P1 and P2.

Based on 23 piezometer hydraulic head measurements, Pickens and Grisak arrived on a hydraulic head vs. radial distance correlation, neglecting the natural drift. They did not state, however, which of the thirty piezometers indicated in Figure 2 they used. We have developed an alternative hydraulic head equation, depending on both radius and angle, taking into account the natural gradient. We show how the Pickens-Grisak regression equation is in good agreement with our alternative equation at a number of piezometer coordinates.

Pickens and Grisak used their hydraulic head regression equation to calculate hydraulic conductivities, and we show how the resulting hydraulic conductivities may be affected by (1) including natural drift and (2) the angle at which the measurements are performed, compared with the drift direction. The SW1 and SW2 multi-level sampling devices were not lined up using the same angle to the natural direction of flow, as seen in Figure 2 . We also show how the hydraulic conductivity calculations are greatly simplified when the multi-level sampling devices are placed directly down-stream from the test-well, as for SW1, compared to putting

them at an angle to the natural direction of flow, as for SW2.

2 Single-Layer Model

In [[3]] it was shown how the single-well push-pull test could be modeled as a "source/sink in a uniform stream" stream-line based problem. A method for tracing the injectant front along a finite number of stream-lines was proposed, and it was shown how the time of break-through for clean water, for each stream-line, may be calculated. Here we give a short review of the formulae derived in Part I.

For each stream-line traced, it is necessary to calculate the tracer front position at the end of injection, $t = T_i$, first. The equations needed to be solved for $r_{max} = r(t = T_i)$ are

$$U_u\,(r - r_w) + Q_i \ln\left|\frac{Q_i - U_u \cdot r}{Q_i - U_u \cdot r_w}\right| = -U_u^2 \cdot t \ , \tag{1a}$$

for the stream-line with constant $\theta = \pi$,

$$U_u\,(r - r_w) - Q_i \ln\left(\frac{Q_i + U_u r}{Q_i + U_u r_w}\right) = U_u^2 t \ , \tag{1b}$$

for the stream-line with constant $\theta = 0$, and

$$r(t = T_i, \psi_i) = \left.\frac{\psi_i - Q_i\theta}{U_u \sin\theta}\right|_{\theta=\theta(t=T_i,\psi_i)} , \tag{1c}$$

where θ is given by

$$(Q_i\theta - \psi_i)\cot\theta - Q_i \ln|\sin\theta| = -U_u^2 t + \mathscr{C}(\psi_i) \ , \tag{2a}$$

and

$$\mathscr{C}(\psi_i) = -U_u r_w \cos\theta - Q_i \ln|\sin\theta|\Big|_{\theta=\theta(t=0,\psi_i)} , \tag{2b}$$

for the stream-lines with $\theta \in (0, \pi)$. As the problem is symmetrical, it suffices to study the upper half-plane.

When r_{max} is found for a given stream-line, the time of break-through, i.e., the time a fluid particle with $r = r_{max}$ at the start of the production phase arrives back at the well perimeter, r_w, can be found. The times of break-through can be found by solving, for t_p and $r = r_w$, the equations

$$U_u\,(r - r_{max}) - |Q_p| \ln\left|\frac{|Q_p| + U_u \cdot r}{|Q_p| + U_u \cdot r_{max}}\right| = -U_u^2 \cdot t_p \ , \tag{3a}$$

for the stream-line with constant $\theta = \pi$,

$$U_u\,(r - r_{max}) + |Q_p| \ln\left(\frac{|Q_p| - U_u r}{|Q_p| - U_u r_{max}}\right) = U_u^2 t_p \ , \tag{3b}$$

for the stream-line with constant $\theta = 0$, and

$$-U_u^2 t + \mathscr{C}(\psi_p) = -\left(|Q_p|\theta + \psi_p\right)\cot\theta + |Q_p| \ln|\sin\theta| \ , \tag{3c}$$

where

$$\mathscr{C}(\psi_p) = -U_u r_{max}\cos\theta + |Q_p| \ln|\sin\theta|\Big|_{\theta=\theta(t=T_i,\psi_i)} \ , \tag{4a}$$

$\theta(r_w, \psi_p)$ is found from

$$r = \frac{\psi_p + |Q_p|\theta}{U_u \sin\theta} \ , \tag{4b}$$

and the stream-line numbers are given by

$$\psi_p = \psi_i - (|Q_p| + Q_i)\theta \ , \tag{4c}$$

for the stream-lines with $\theta \in (0, \pi)$. The $\theta(t = T_i, \psi_i)$, needed to find ψ_p , is known from solving Equation 2a .

3 The Effect of Layering

Assume we have a fully penetrated aquifer of height b, consisting of M homogeneous layers of different or equal permeability and porosity, k_j, ϕ_j, and equal height[10], $b_j = \frac{b}{M}$, as shown in **Figure 3**. Also assume that there is no cross-flow between the layers, i.e., we have strict 2-dimensional flow, and that the reservoir pressure and pressure gradients are the same in all layers. All fluid properties are subject to the assumptions given in Part I. We define the arithmetic average of permeability and porosity as

$$k_A \equiv \frac{\sum k_j b_j}{\sum b_j} = \frac{\sum k_j}{M} \ , \tag{5a}$$

and

$$\phi_A \equiv \frac{\sum \phi_j b_j}{\sum b_j} = \frac{\sum \phi_j}{M} \ . \tag{5b}$$

[10]Assuming that all layers have equal height is sufficiently accurate since we do not require different permeability/porosity for all layers, i.e., one thick physical layer may be considered as many thin layers to meet the assumption.

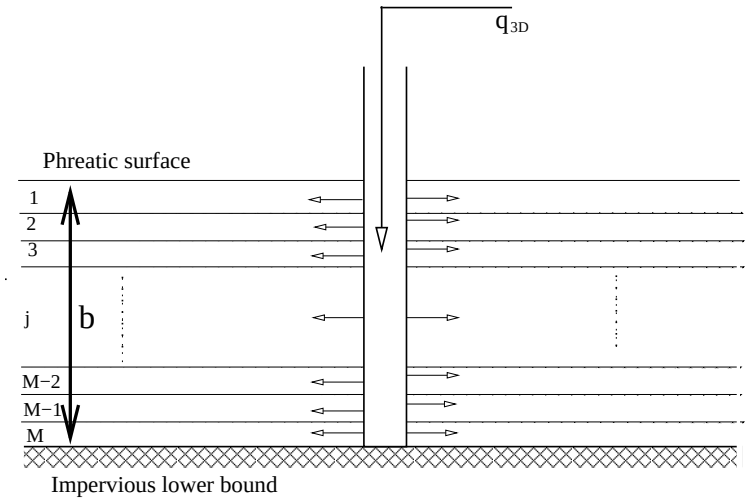

Figure 3: Schematic diagram of a fully penetrated layered unconfined/phreatic aquifer.

Using Darcy's law (see the appendix of Part I), the volumetric rate of flow between the well and layer number j is

$$q_{3D,j} = -\frac{A_j \nabla P \, k_j}{\mu} = -\frac{2\pi r_w \frac{b}{M} \nabla P \, k_j}{\mu} \,, \tag{6}$$

and because the volumetric well rate must be the sum of all layer rates, we get

$$q_{3D} = \sum_j q_{3D,j} = -\frac{2\pi r_w \frac{b}{M} \nabla P \, \sum_j k_j}{\mu} = -\frac{2\pi r_w b \nabla P \, k_A}{\mu} \,, \tag{7}$$

and when rearranging, we get

$$-\frac{2\pi r_w b \nabla P}{\mu} = \frac{q_{3D}}{k_A} \,, \tag{8}$$

so the layer-specific rate into/out of layer number j may be written

$$q_{3D,j} = \frac{q_{3D}}{M} \cdot \frac{k_j}{k_A} \,, \tag{9}$$

which we formulate as 2-dimensional areal rates by dividing by the layer height, b/M,

$$q_j = \frac{q_{3D,j}}{b/M} = q \cdot \frac{k_j}{k_A} \,, \tag{10}$$

and

$$Q_j = \frac{q_j}{2\pi\phi_j} = \frac{q}{2\pi\phi_A} \cdot \frac{\phi_A}{\phi_j}\frac{k_j}{k_A} = Q \cdot \mathscr{C}_j \ , \tag{11}$$

where $\mathscr{C}_j \equiv \frac{\phi_A}{\phi_j}\frac{k_j}{k_A}$.

3.1 No drift

The layer specific fluid particle velocity due to the injection/production becomes

$$u_j(r) = \frac{Q_j}{r} = \frac{Q}{r} \cdot \mathscr{C}_j \ , \tag{12}$$

which gives the expression for the tracer front radial position in layer j as a function of time,

$$r_j(t) \quad = \quad \begin{cases} \sqrt{r_w^2 + 2 \cdot \mathscr{C}_j Q_i t_i} & t \le T_i \\ \sqrt{r_{max,j}^2 - 2 \cdot \mathscr{C}_j |Q_p| t_p} & T_i < t \le T_{p,j} \end{cases} \ , \tag{13}$$

assuming $r_j(0) = r_w$ and $r_j(T_i) = r_{max,j}$. For $r_j(T_{p,j}) = r_w$, we get

$$r_w = r_j(T_p) = \sqrt{r_w^2 + 2\mathscr{C}_j \cdot \left(Q_i T_i - |Q_p| T_{p,j}\right)} \ . \tag{14}$$

Squaring both sides and reorganising, we get

$$T_{p,j} = \frac{Q_i}{|Q_p|} \cdot T_i \ , \tag{15}$$

which means that the time of break-through in a permeability and/or porosity layered reservoir with no natural drift, is neither affected by the permeability- nor the porosity-distribution, since the time of breakthrough in an arbitrary layer is independent of the layer-specific properties.

3.2 Drift

The natural drift velocity, in layer j, due to some natural pressure gradient is

$$U_{u,j} = \frac{\nabla P \, k_j}{\mu \phi_j} = U_u \cdot \frac{\phi_A}{\phi_j}\frac{k_j}{k_A} \ . \tag{16}$$

We can now write the layer specific velocity field as

$$\left(\frac{dr}{dt}\right)_j = \mathscr{C}_j\left(U_u\cos\theta+\frac{Q}{r}\right), \tag{17a}$$

$$\left(\frac{d\theta}{dt}\right)_j = -\mathscr{C}_j\frac{U_u\sin\theta}{r}. \tag{17b}$$

If we make the change of variable, $\tau = \mathscr{C}_j \cdot t$, we get exactly the single-layer velocity field, [[3]]. The solution to the set of differential equations, 17a and b, are thus found by letting $t \rightarrow \mathscr{C}_j \cdot t$ in Equations 1a, 1c, 2a, 3a and 3c. Hence, the effect of layer-wise permeability/porosity variations, on injection phase tracer advancement in each layer, will be the same as the effect of changing the injection phase duration in the single-layer model. Changing the T_i will affect the $r_{max,j}$, for each stream-line, so the time of clean water break-through, along each stream-line, will not only be adjusted by the scaling factor $\mathscr{C}_j$, but will also be affected by the altered $r_{max,j}$.

In **Figure 4** the time of clean water break-through, i.e., the T_{BT} for the $\theta = \pi$ stream-line, and the end-time of tracer production, i.e., the T_{BT} for the $\theta = 0$ stream-line, are shown, using the analytical method described in [[3]], for a range of different T_is smaller than the critical time, T_c, [[4]]. Neither the time of clean water breakthrough nor the end-time of tracer production is linearly related to the duration of the injection phase, as is the case in the no-drift model (see Equation 15), which means that layering will have an effect on both the time of break-

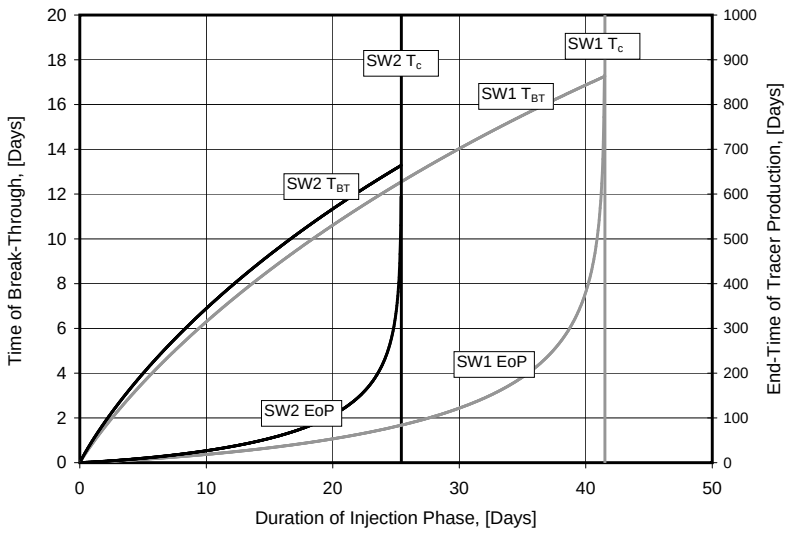

Figure 4: Time of clean water break-through (T_{BT}) and End-time of tracer production (EoP) versus duration of the injection phase, up to T_c, for the Pickens-Grisak SW1 and SW2 conditions.

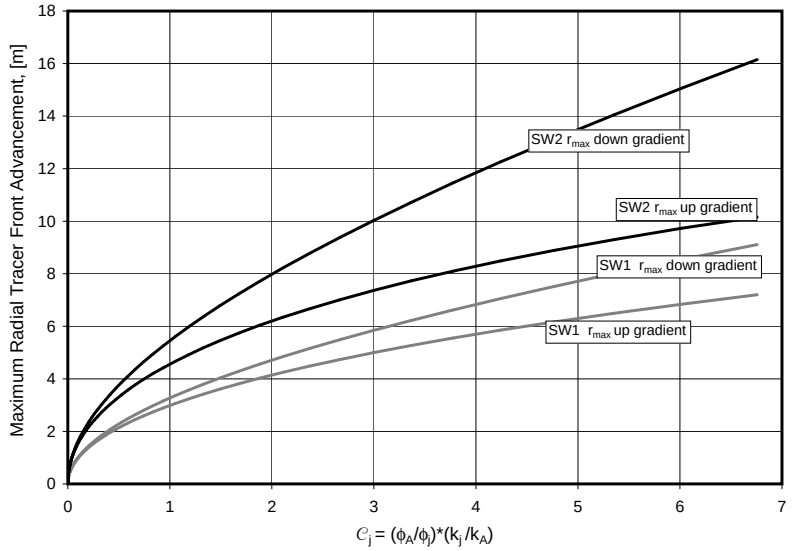

Figure 5: Single-layer maximum up- and down-gradient tracer front advancement, for the Pickens-Grisak SWT conditions, as functions of $\mathscr{C}_j$.

through and the end-time of production in the presence of natural groundwater drift.

By letting $U_u \rightarrow U_u \cdot \left(\frac{k_j}{k_A}\frac{\phi_A}{\phi_j}\right)$ and $Q \rightarrow Q \cdot \left(\frac{k_j}{k_A}\frac{\phi_A}{\phi_j}\right)$ in Equation 1a , 1b, 3a and 3b, we can calculate the time of break-through and the end time of tracer production in the j'th layer, using the same method as described in [[3]]. In **Figure 5** the maximum radial tracer front advancement is shown for both $\theta = 0$ and π for SW1 and SW2 test parameters, as functions of $\mathscr{C}_j$. In **Figure 6** the time of clean water break-through and the end time of tracer production is shown for SW1 and SW2 test parameters as functions of $\mathscr{C}_j$.

The injection-phase duration limit for conservative tracer production, the critical time, T_c, [[4]], will also be affected by permeability/porosity variations. In **Figure 7**, the relation between T_c and $\mathscr{C}_j$ is compared to the actual Pickens-Grisak injection phase durations, T_i, for SW1 and SW2 test conditions. Supposing some layers have a high $\mathscr{C}_j$, tracer might be lost in these layers ($T_i > T_{c,j}$) even though all the tracer may be recoverable from the other layers.

In **Figure 8** the effect, of layering, on the overall production profile is shown for a synthetic system of 29 layers of equal thickness and $\mathscr{C}_j$s uniformly distributed in the range $[0.054, 1.946]$, with an average of 1, for SW1 test parameters. The lowest $\mathscr{C}_j$ layer give the steepest tracer concentration profile, while the $\mathscr{C}_j = 1$ layer, which behave identically to the single layer model, is marked with the thick grey curve, and the highest $\mathscr{C}_j$ layer obtain both the earliest time of clean water break-through and the latest end-time of tracer production.

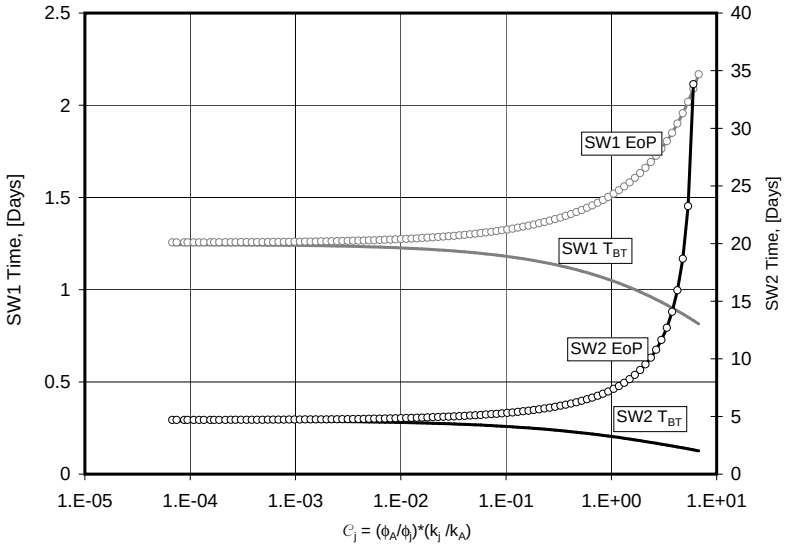

Figure 6: Time of clean water break-through (TBT) and End-time for tracer production (EoP) as functions of $\mathscr{C}_j$, for SW1 and SW2 test parameters.

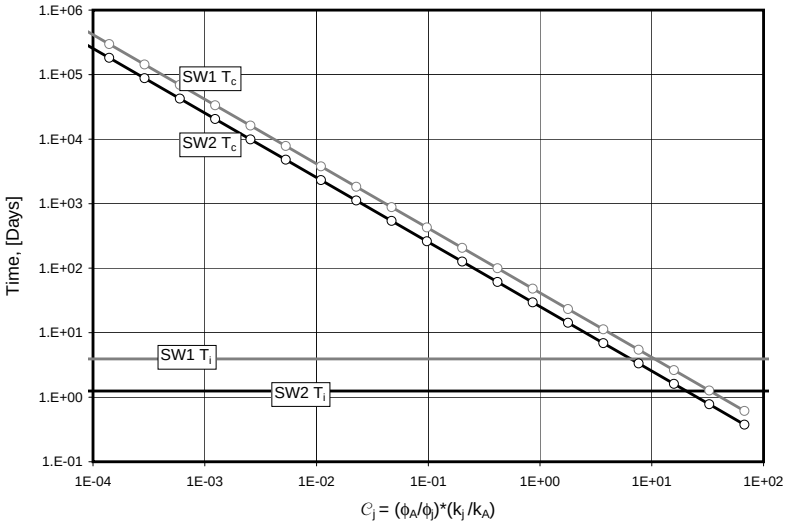

Figure 7: Critical time, T_c, compared to actual duration of the injection phase, T_i, in the Pickens-Grisak SWTs, as a function of $\mathscr{C}_j$.

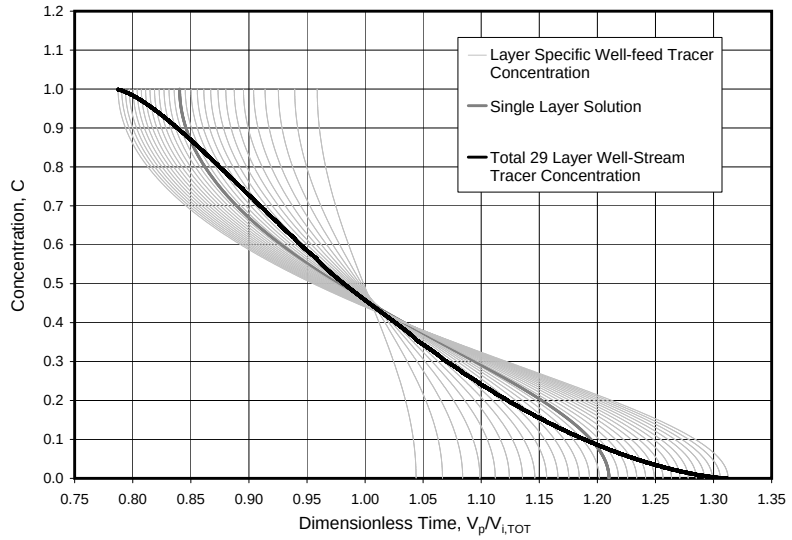

Figure 8: The Pickens-Grisak SW1 parameter production profile in a layered reservoir of 29 equally thick layers. Total well-stream tracer concentration, due to the production from all the layers, is shown as the black curve, and individual layer production profiles are shown in gray.

4 Layering in Practice

Assuming layers of equal thickness is no problem mathematically. In practise, however, when modelling realistic layering data, an infinite number of layers of infinitesimal thickness would be needed. Thus, modifying the method previously outlined is necessary.

When considering each single layer, the layer thickness is of no concern, as two-dimensional flow is assumed. Only when calculating the fraction of the well-stream entering/leaving each layer is the height of any importance, since the volumetric flow depends on the layer thickness. Let $b_j = \frac{b}{M} \to 0$, i.e. $M \to \infty$, and assume that all the layers between b_{m_1} and b_{m_2} have the same properties. Now, consider these $m_2 - m_1$ layers as one single layer of thickness $b_{j^*} = \int_{z_{m_1}}^{z_{m_2}} db$, where z_j is the depth of layer j. We now get that

$$q_{3D,j^*} = \int_{z_{m_1}}^{z_{m_2}} q_j db = q_j b_{j^*} \ , \tag{18}$$

since all $\{q_{m_1}, \ldots, q_{m_2}\}$ must be equal. The fractional volumetric rate contributed to the well-stream from the production phase stream-line $\psi_{p,n}$ in layer j^* is now

simply

$$\frac{q_{3D,j^*,n}}{q_{3D}} = \frac{Q_{p,n,j^*}\phi_{j^*}b_{j^*}}{Q_p\phi_A b} \ , \tag{19}$$

and the producing tracer concentration becomes (see Equation 33 in [[3]])

$$C_{N^*} = \frac{\sum_{j^*}\sum_{n=1}^{N^*} Q_{p,n,j^*}\phi_{j^*}b_{j^*}}{Q_p\phi_A b} \ . \tag{20}$$

5 Layering Data Provided by Pickens and Grisak

Pickens and Grisak present, in their Table 6, layer-wise data for the SW1 test. Layer height, depth and radial distance of the measurements and the time at which the tracer concentration reached 0.5 is presented. Neglecting natural drift, they assumed that

$$q_{3D,j} \cdot t_{0.5} = \pi r^2 b_j \phi \ , \tag{21}$$

where r is the radial position of the piezometer. Furthermore, they use the Thiem equation,[[5]],

$$q_{3D,j} = \frac{2\pi K_j b_j (h_1 - h_2)}{\ln(r_2/r_1)} \ , \tag{22}$$

and their own regression equation obtained from a fit of 23 hydraulic head measurements,

$$h_i = 0.512 - 0.275 \cdot \log_{10} r_i \ , \tag{23}$$

where h_i is the hydraulic head at radial distance r_i, to calculate the hydraulic conductivity, K_j, using $r_1 = r_w$. For some of the layers, Pickens and Grisak report measured data at more than one radial distance without calculating the corresponding hydraulic conductivity. In **Table I** the missing conductivities are calculated using the Thiem equation and the Pickens-Grisak hydraulic head regression equation. As can be seen there is significant uncertainty within each layer regarding the conductivity, and the average hydraulic conductivity, from the Pickens-Grisak Table 6, is not equal to the full-aquifer hydraulic conductivity they reported from SW1. Additionally, hydraulic conductivities obtained from Equation 28 , K_{anal}, where $K_A = 1.4 \cdot 10^{-2} {}^{cm}/_{s}$ are presented. It was assumed that the measurements were performed directly down-gradient from the test well.

The Pickens-Grisak hydraulic head regression equation, Equation 23 , is based on 23 piezometer measurements, but it is not stated which of the 30 piezometers indicated in their Figure 4, they used. Pickens and Grisak disregard the fact that the natural drift perturbs the angular symmetry around the P1 well, but

Table I: Table 6 in [[7]], where missing values and analytically calculated conductivities, K_{anal}, have been added.

Depth	**Layer thickness**	**Radial distance**	$\mathbf{t_{0.5}}$	$(\frac{\mathbf{q_{3D,j}}}{\mathbf{b_j}})$	$\mathbf{K_{Thiem}}$	$\mathbf{K_{anal}}$
m	**m**	**m**	**days**	$m^2/\mathbf{day}$	$\mathbf{10^{-2}}cm/\mathbf{s}$	$\mathbf{10^{-2}}cm/\mathbf{s}$
1.37		1.00				
2.13	0.44	1.00	0.3670	3.26	0.503	0.472
		2.00	1.1500	4.15	0.640	0.588
2.74	0.53	1.00	0.4040	2.95	0.457	0.429
3.19	0.45	1.00	0.3210	3.72	0.575	0.540
3.64	0.45	1.00	0.2540	4.70	0.726	0.683
4.08	0.45	1.00	0.2680	4.45	0.688	0.647
		2.00	1.0920	4.37	0.674	0.620
4.53	0.45	1.00	0.2980	4.01	0.620	0.582
4.98	0.45	1.00	0.2170	5.51	0.852	0.799
5.43	0.45	1.00	0.1830	6.51	1.010	0.947
		2.00	0.6390	7.47	1.153	1.059
5.87	0.45	1.00	0.1440	8.30	1.280	1.204
6.32	0.45	1.00	0.1130	10.61	1.640	1.534
6.77	0.45	1.00	0.1160	10.27	1.590	1.495
		2.00	0.3940	12.13	1.872	1.717
		3.00	1.0380	10.36	1.599	1.429
7.21	0.45	1.00	0.0929	12.85	1.990	1.866
7.66	0.45	1.00	0.0875	13.64	2.110	1.981
8.11	0.45	1.00	0.0917	13.02	2.010	1.891
		2.00	0.3170	15.08	2.327	2.134
		3.00	0.8420	12.77	1.971	1.761
		4.00	1.0830	17.63	2.721	2.374
8.56	0.45	1.00	0.0792	15.08	2.330	2.189
9.00	0.45	1.00	0.0896	13.33	2.060	1.935
9.45	0.53	1.00	0.1210	9.88	1.530	1.433
		2.00	0.3850	12.39	1.912	1.757
		3.00	1.1290	9.32	1.469	1.314
10.05	0.40	1.00	0.3000	3.98	0.615	0.578
		2.00	0.7250	6.39	1.017	0.933
10.82		1.00				

the hydraulic head will in reality be a superposition of two parts, one originating from the natural hydraulic head gradient and one originating from the injection/production,[[5]] ,

$$h(r,\theta) = h_u(x) + h_w(r) \ , \tag{24}$$

where we have

$$\frac{dh_u}{dx} = -5.3 \cdot 10^{-3} \ m/m \tag{25a}$$

and

$$\frac{dh_w}{dr} = \frac{-q}{2\pi K r} \ . \tag{25b}$$

Solving the two differential equations, we get

$$h(r,\theta) = -5.3 \cdot 10^{-3} \cdot r \cdot \cos\theta - \frac{q}{2\pi K} \ln|r| + \mathscr{C}_w(\theta) \ , \tag{26}$$

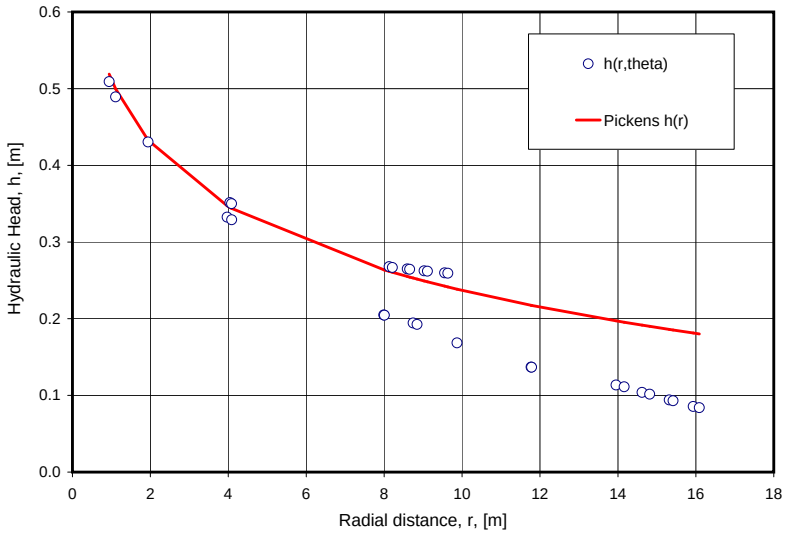

Figure 9: The Pickens-Grisak hydraulic head regression equation compared to a theoretical θ-dependent hydraulic head based on natural groundwater drift.

and assuming the Pickens-Grisak formula is correct for $r = r_w$ we may calculate the θ-dependent integration constant, and we get

$$h(r,\theta) = -5.3 \cdot 10^{-3} \cdot (r - r_w)\cos\theta - \frac{q}{2\pi K}\ln\frac{r}{r_w} + 0.854\ m\ . \qquad (27)$$

The main difference between Equation 27 and the Pickens-Grisak regression equation is the angle dependency of Equation 27 , taking care of the broken symmetry due to the natural drift. In **Figure 9** the θ-dependent hydraulic head equation, Equation 27 , is plotted for all thirty piezometer coordinates along with the Pickens-Grisak regression equation. The theoretical hydraulic head is calculated at the coordinates of the thirty piezometers in the Pickens-Grisak instrumentation layout, Figure 2 . The Pickens-Grisak regression equation is in good agreement with a selection of the theoretically calculated points.

Employing the Darcy equation (see the Appendix of Part I) and reorganising Equation 1b , for layer j, requiring that all sampling points lie on the streamline $\psi_i = 0$, we can calculate the hydraulic conductivity in each layer from

$$K_j = \frac{1}{\left(\frac{1}{\rho_w g\phi}\frac{dP}{dx}\right)^2 t_{0.5}}\left[\frac{1}{\rho_w g\phi}\frac{dP}{dx}(r_2 - r_w) - \frac{Q_i}{K_A}\ln\left(\frac{\frac{Q_i}{K_A} + \frac{r_2}{\rho_w g\phi}\frac{dP}{dx}}{\frac{Q_i}{K_A} + \frac{r_w}{\rho_w g\phi}\frac{dP}{dx}}\right)\right]\ , \qquad (28)$$

where r_2 is the radial distance between the well and the sampling point and $t_{0.5}$ is the time at which the injectant concentration reaches 0.5 at the sampling point. Comparing hydraulic conductivities, reported by Pickens and Grisak and calcu-

lated from Equation 28 , the Pickens-Grisak values are about 6% higher calculated at the $r_2 = 1\ m$ sampling points and increasing until about 13% higher at the $r_2 = 4\ m$ sampling point. Hydraulic conductivities from Equation 28 are shown in Table I .

Pickens and Grisak also reported sampling point break-through data for the SW2 test, in their Table 9, however they have not provided hydraulic conductivities. Using the equations developed, we can calculate the hydraulic conductivities in a similar fashion as for the SW1 test. The SW2 test, however, is a little more complicated, since the sampling points, as can be seen in Figure 2 , are not directly down-stream, i.e., on the $\psi_i = 0$ stream-line. The sampling points are located on a line at an angle of $\theta_{msp} \simeq 63^\circ$ to the line between the wells P1 and P2, which is assumed to be parallel to the direction of the groundwater drift. Hence, we cannot use Equation 28 . We know, however, both the radius and the angle for each of the three sampling points, (r_{msp}, θ_{msp}), as well as the time, $t_{0.5}$, at which the injectant reached the sampling points, so it is possible to numerically calculate the $\mathscr{C}_j$, and thus the K_j. The equation needed to be solved is Equation 2a , where $U_u \rightarrow \mathscr{C}_j U_u$, $Q_i \rightarrow \mathscr{C}_j Q_i$, $\psi_i \rightarrow \mathscr{C}_j \psi_i$ and $\mathscr{C}(\psi_i) \rightarrow \mathscr{C}_j \mathscr{C}(\psi_i)$. Employing the $r - \theta$ formulation of the stream-line number ψ_i, [[3]], we get

$$U_u r_{msp} \sin\theta_{msp} + Q_i \theta_{msp} = U_u r_w \sin\theta_0 + Q_i \theta_0 \ , \tag{29}$$

from which we can find the $\theta_0 = \theta(t_i = 0, \psi_i)$, numerically. Knowing θ_0, we may find the $\mathscr{C}(\psi_i)$, and we may find the K_j from

$$K_j = \frac{-K_A}{U_u^2 t_{0.5}} \left[(Q_i \theta_{msp} - \psi_i) \cot\theta_{msp} - Q_i \ln|\sin\theta_{msp}| - \mathscr{C}(\psi_i) \right] \ , \tag{30}$$

assuming that the porosity is the same in all layers. Assuming that the average hydraulic conductivity is the same as the Pickens-Grisak reported hydraulic conductivity for the SW1 test, $K_A = 1.4 \cdot 10^{-2} {}^{cm}/_{s}$, we get the hydraulic conductivities reported in **Table II**. Neither for the Pickens-Grisak K_j values nor for the K_j values calculated here, we get an average of $K_A = 1.4 \cdot 10^{-2} {}^{cm}/_{s}$, so there must be some error in the data provided. For the $K_{j,anal}$ we get an average of $1.21 \cdot 10^{-2} {}^{cm}/_{s}$ and $1.43 \cdot 10^{-2} {}^{cm}/_{s}$ for SW1 and SW2, respectively[11]. Using a hydraulic head gradient of $0.052\ {}^{kPa}/_{m}$, a constant fractional porosity of 0.38 and using $K_A = 1.4 \cdot 10^{-2} {}^{cm}/_{s}$ despite the fact that this is wrong, we get the layering data, h_j and $\mathscr{C}_j$, reported in **Table III**. For the SW1 data it has been assumed that measurements have been performed down-gradient from the test well, for the SW2 data, however, the measurements have been performed at an angle of 63° to the natural drift direction.

[11] For layers where multiple K_j are calculated, an average, $\Sigma {}^{K_j}/_{n}$, has been used in calculating the arithmetic average defined in Equation 5a .

Table II: Table 9 in [[7]] where analytically calculated conductivities have been added.

Depth	Layer thickness	Radial distance	$t_{0.5}$	$(\frac{q_{3D,j}}{h_j})_b$	K_{Thiem}	K_{anal}
m	m	m	days	m^2/day	$10^{-2} cm/s$	$10^{-2} cm/s$
2.29	0.48	0.36	0.028	5.53	0.853	0.989
		0.66	0.094	5.53	0.853	1.004
		2.06	0.88	5.74	0.886	1.030
2.67	0.38	0.36	0.028	5.53	0.853	0.989
		0.66	0.085	6.12	0.944	1.110
		2.06	1.06	4.78	0.738	0.855
3.05	0.95	0.36	0.087	1.78	0.275	0.318
		0.66	0.213	2.44	0.377	0.443
		2.06	1.43	3.54	0.546	0.634
4.57	2.515	0.36	0.038	4.07	0.628	0.729
		0.66	0.132	3.94	0.608	0.715
		2.06	1.22	4.15	0.640	0.743
8.08	3.875	0.66	0.053	9.81	1.514	1.780
		2.06	0.34	14.9	2.299	2.666

Table III: Layer thickness and $\mathscr{C}_j$ used in generation of the plots in Figure 10 for hydraulic conductivities from both the Thiem equation and based on the analytical model.

SW1			SW2		
Layer Thickness m	$C_{j,Thiem}$	$C_{j,anal}$	Layer Thickness m	$C_{j,Thiem}$	$C_{j,anal}$
0.44	0.359	0.379	0.48	0.617	0.720
0.53	0.326	0.307	0.38	0.604	0.703
0.45	0.411	0.386	0.95	0.285	0.332
0.45	0.519	0.488	2.52	0.447	0.521
0.45	0.491	0.452	3.88	1.362	1.588
0.45	0.443	0.416			
0.45	0.609	0.571			
0.45	0.721	0.716			
0.45	0.914	0.860			
0.45	1.171	1.096			
0.45	1.136	1.105			
0.45	1.421	1.333			
0.45	1.507	1.415			
0.45	1.436	1.457			
0.45	1.664	1.564			
0.45	1.471	1.382			
0.53	1.093	1.072			
0.40	0.439	0.540			

Since

$$\mathscr{C}_j = \frac{k_j}{k_A} = \frac{bk_j}{\sum(b_j k_j)} \,, \tag{31}$$

we have to demand, in general, that

$$\sum \mathscr{C}_j b_j \equiv b \,. \tag{32}$$

If this condition is not met the material balance fails. Hence, we must find a way to mend the reported data, so that the resulting average is equal to the assumed

average. We have assumed constant porosity, but more realistic $\mathscr{C}_j$'s might be obtained if more detailed porosity data are introduced. Here the $\mathscr{C}_j$ values have been exchanged for a new set of $\mathscr{C}_j^*$ values, which have been used in generating production profiles, defined as

$$\mathscr{C}_j^* = \mathscr{C}_j \cdot f \ , \tag{33}$$

where $f = \frac{\Sigma(\mathscr{C}_j b_j)}{b}$.

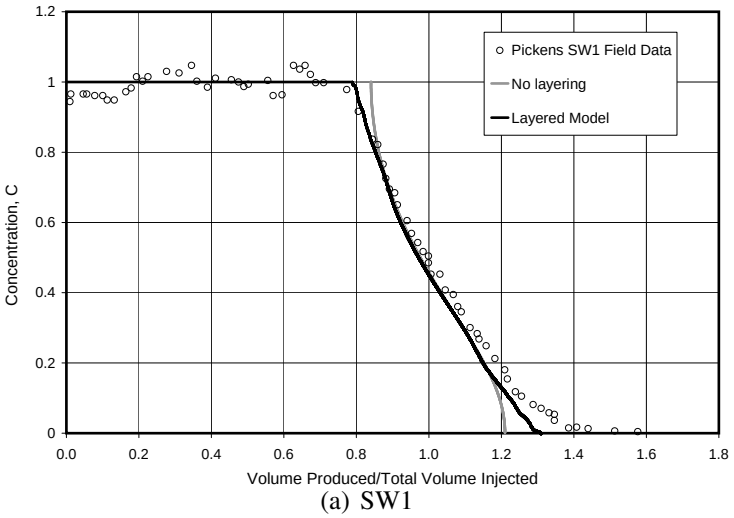

(a) SW1

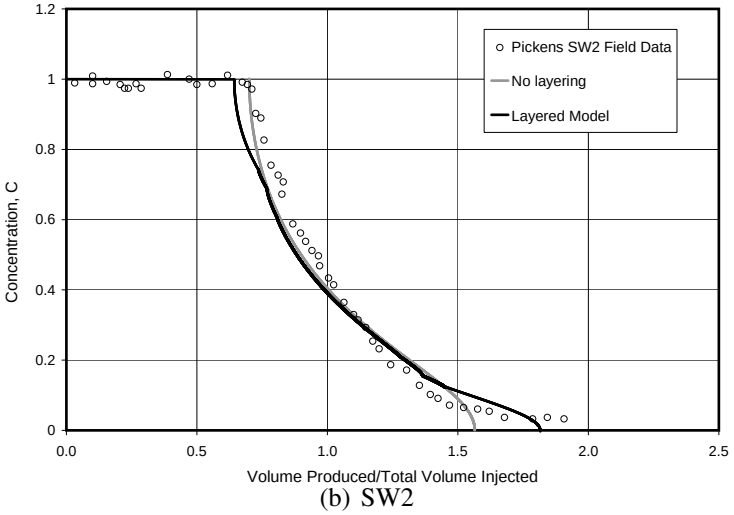

(b) SW2

Figure 10: The Pickens-Grisak field SWT tracer concentration profiles compared to results obtained from the 0.052 $^{kPa}/_{m}$ semi-analytical model with and without layering.

In **Figure 10** results from the layered model is compared to the single-layer model as well as the field data reported by Pickens and Grisak. Layering data

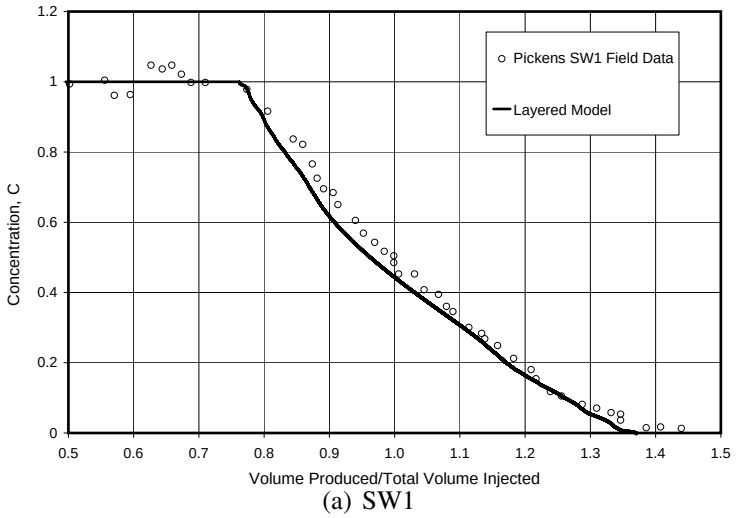

(a) SW1

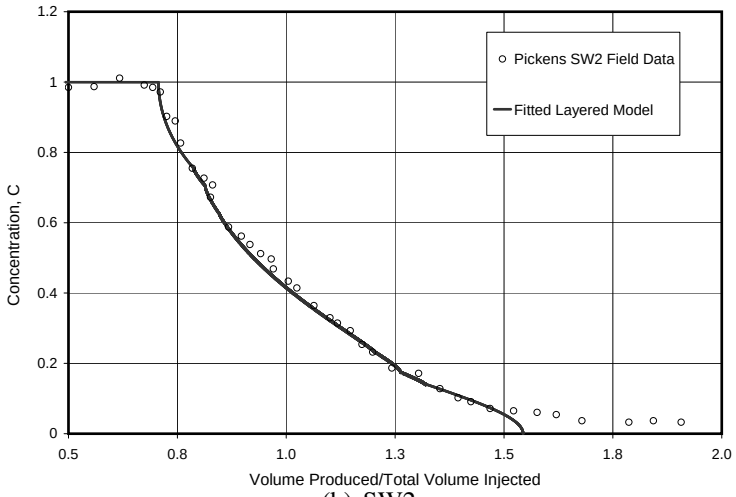

(b) SW2

Figure 11: The Pickens-Grisak field SWT tracer concentration profiles compared to results obtained from the semi-analytical model with layering, doing regression on the hydraulic head gradient.

used are reported in the tables I to III. Both SWT assumed a natural gradient of 0.052 $^{kPa}/_{m}$. Comparing results from the layered model run with the Thiem hydraulic conductivities and the stream-line based ones, there was no difference, for SW1 or SW2. Comparing the single-layer and the layered models it can be seen how the layered model gives a better match to the experimental TBT and EoP. Even though the layered model does not give an exact match, it seems to be able to predict some of the characteristics of the experimental data.

The experimental production profiles do not decrease evenly from 1 to 0, but decreases in an oscillating manner. These oscillations are also present by the

layered model. The oscillations in the experimental data may easily be taken for errors or uncertainty in the measured data, but we conclude that they are effects of the stratification of the aquifer in combination with the natural drift; that they can be predicted by the stream-line based layered model. Due to the superposing of single-layer production profiles, to get the multi-layered profile, dominating layers will be more visible in the final profile than other less dominant layers.

There is great uncertainty in both the drift parameters as well as the layering parameters for the two single-well tests, and by playing with these parameters it should be possible to gain an exact match to experimental data. In **Figure 11** a good fit has been obtained by playing with the hydraulic head gradient only. Since the stream-line based calculations of hydraulic conductivities depend on the groundwater drift velocity, they will also change when adjusting the hydraulic head gradient. The plots are obtained by employing gradients of 0.06 $^{kPa}/_{m}$ and 0.04 $^{kPa}/_{m}$, for the SW1 and SW2 tests, respectively.

6 Conclusion

1. Time of break-through is not affected by layering in an aquifer with no natural drift.

2. Both time of clean water break-through and end-time of tracer production is affected by layering in the presence of natural groundwater drift.

3. Introducing layering and applying the layering data reported by Pickens and Grisak, it is possible to get an exact match to the experimental data, including the characteristic oscillating behaviour of the production profile. Thus it may be concluded that the oscillations are effects of the stratification of the test-site in combination with the natural drift.

4. In a model free of physical dispersion, it is shown that a model combining groundwater drift and layering heterogeneity may yield a perfect match to production profiles showing large apparent dispersivity.

References

[1] J.A. Cherry, R.E. Jackson, D.C. McNaughton, J.F. Pickens, and H. Woldetensae. *Physical Hydrogeology of the Lower Perch Lake Basin, in PJ Barry* Hydrological Studies on a Small Basin on the Canadian Shield, pages 625–680. Number AECL 5041/II. Atomic Energy of Canada, Ltd., Chalk River Nuclear Laboratories., Ontario, Canada, September 1975.

[2] K. H. Coats, C.H. Whitson, and L.K. Thomas. Modelling conformance as dispersion. SPE Annual Technical Conference and Exhibition, 26-29 September, Houston, Texas, September 2004. SPE 90390.

[3] Sverre G. Johnsen and Curtis H. Whitson. Analytical Treatment of a Push-Pull "Echo" Test, Part I - Development of a Single Layer Solution. Submitted to Transport in Porous Media, 2007.

[4] Sverre G. Johnsen and Curtis H. Whitson. Analytical Treatment of a Push-Pull "Echo" Test, Part II - Application of the Convection-Dispersion Equation. Submitted to Transport in Porous Media, 2007.

[5] G.P. Kruseman and N.A. de Ridder. *Analysis and Evaluation of Pumping Test Data, Bulletin 11*. International Institute for Land Reclamation and Improvement, Wageningen, The Netherlands, 1970.

[6] J.F. Pickens, J.A. Cherry, and R.W. Gillham. Field studies of dispersion in a shallow sandy aquifer. In *Invitational Well-Testing Symposium*, pages 55–62. Lawrence Berkely Lab., Berkely, California, October 1977.

[7] J.F. Pickens and G.E. Grisak. Scale-dependent dispersion in a stratified granular aquifer. *Water Resources Research*, 17(4):1191–1211, 1981.